

**Bioapplications of hyperbranched polymers**

Journal:	<i>Chemical Society Reviews</i>
Manuscript ID:	CS-REV-07-2014-000229.R1
Article Type:	Review Article
Date Submitted by the Author:	07-Jul-2014
Complete List of Authors:	Wang, Dali; Shanghai Jiao Tong University, School of Chemistry and Chemical Engineering Zhao, Tianyu; University College Dublin, School of Medicine and Medical Science Zhu, Xinyuan; Shanghai Jiao Tong University, School of Chemistry and Chemical Engineering Yan, Deyue; Shanghai Jiao Tong University, School of Chemistry and Chemical Engineering Wang, Wenxin; University College Dublin, School of Medicine and Medical Science

# Bioapplications of hyperbranched polymers

Dali Wang, Tianyu Zhao, Xinyuan Zhu\*, Deyue Yan and Wenxin Wang\*

<sup>1</sup> School of Chemistry and Chemical Engineering, State Key Laboratory of Metal Matrix Composites, Shanghai Jiao Tong University, 800 Dongchuan Road, 200240 Shanghai, P. R. China. E-mail: xyzhu@sjtu.edu.cn; Fax: +86-21-54741297

<sup>2</sup> Charles Institute of Dermatology, School of Medicine and Medical Science, University College Dublin, Belfield, Dublin 4, Ireland. E-mail: wenxin.wang@ucd.ie

## Abstract

Hyperbranched polymers (HBPs), one important subclass of dendritic macromolecules, are highly branched, three-dimensional globular nanopolymeric architectures. Attractive features like highly branched topological structures, adequate spatial cavities, numerous terminal functional groups and convenient synthetic procedures distinguish them from the available polymers (the linear, branched, and crosslinking polymers). Due to their unique physical/chemical properties, applications of HBPs have been explored in a large variety of fields. In particular, HBPs exhibit unique advantages in the biological and biomedical systems and devices. Firstly, the way to prepare HBPs usually only involves simple one-pot reactions and avoids the complicated synthesis and purification procedures, which makes the manufacturing process more convenient, thus reducing production costs. Secondly, the large number of end-groups of HBPs provide a platform for conjugation of the functional moieties and also can be employed to tailor-make the properties of HBPs, enhancing their versatility in biological applications. Thirdly, HBPs possess excellent biocompatibility and biodegradability, controlled responsive nature, and ability to incorporate a multiple array of guest molecules through covalent or noncovalent approaches. All of these features of HBPs are of great significant for designing and producing biomaterials. Up to now, significant progress has been made for the HBPs in solving some of the fundamental and technical questions toward their bioapplications. The present review highlights the contribution of HBPs in biological and biomedical fields with intent to aid the researchers in exploring HBPs for bioapplications.

## 1. Introduction

HBP are one important subclass of dendritic macromolecules following conventional linear, chain-branched and crosslinking polymers. They are highly branched macromolecules with three-dimensional dendritic architecture. Historically, highly branched polymers were first theoretically described by Flory in 1952 when he demonstrated the polycondensation of  $AB_x$  monomers to give polydisperse, highly branched architectures by statistical calculation.<sup>1</sup> The term “hyperbranched polymer” was first introduced to define dendritic macromolecules with random branch-on-branch topology by Kim and Webster in the late 1980s when they intentionally synthesized soluble hyperbranched polyphenylene.<sup>2,3</sup> Since then, HBPs have attracted tremendous interest of both scientists and engineers due to their unique properties and potential applications in diverse areas, and the field has experienced significant progress.

HBPs are in-between analogues of conventional linear polymers and dendrimers and show great superiority in structure and performances. Firstly, in comparison to linear polymers, HBPs exhibit the apparent advantages of non/low chain entanglements, low melt and solution viscosity, high solubility and a large number of terminal groups that are easy to be chemically modified.<sup>4-8</sup> Secondly, different from perfectly branched and monodisperse dendrimers consisting of dendritic units and terminal units, HBPs are composed of dendritic units, linear units and terminal units, and display a randomly branched structure with lesser degree of branching (DB, generally 0.4-0.6).<sup>9</sup> Besides, in contrast to the tedious and complicated synthetic procedure of dendrimers, the synthesis of HBPs is often based on one-pot reactions, requiring essentially no further purification.<sup>10-12</sup> Thus, HBPs not only retain some of the structural features and properties of dendrimers but also are accessible at lower cost than their dendrimer analogues. Actually, some HBPs are commercially available, such as Boltorn<sup>®</sup> (a hyperbranched aliphatic polyester), Hybrane<sup>®</sup> (a hyperbranched polyesteramide), polyethylenimine (a hyperbranched polyamine) and polyglycerol (a hyperbranched polyether). Taking these outstanding advantages into account, HBPs are one of the most promising materials from both academia and industry.

Up to now, a number of excellent reviews have been published on HBPs, covering synthesis, characterizations, properties, functionalization, supramolecular self-assembly and potential applications.<sup>13-18</sup> HBPs have been one of the most important research topics nowadays in polymer science, and are of great interest in materials science (mainly, in nanoscience and nanotechnology), as well as in biomedical science.<sup>19</sup> Many practical and potential applications have already been found for HBPs such as coatings, resins, polymer additives and crosslinkers, nanoreactors and nanocapsules, multifunctional platforms, etc.<sup>5,20</sup> Especially, the applications of HBPs in biological and biomedical field is arousing the tremendous interest of researchers in recent years.<sup>21-24</sup> HBPs are a type of important biomaterials

with attractive properties including excellent physicochemical properties, favorable biodegradability and biocompatibility, unusual self-assembly ability, versatile surface tailor-ability, improved multifunctionality, as well as their smart responsibility. These advantages pave the way for bioapplications of HBPs ranging from biology to biomedicine. In the past few years, a rapidly increasing amount of publications related to the bioapplications have been reported. However, a systematic review on the bioapplications of HBPs has not yet been published.

In this review article, we summarize recent research progress in bioapplications of HBPs, based partially on recent progress of our laboratories. Briefly, in the following sections, we first introduce the physicochemical and biological properties of HBPs, particularly paying attention to the properties associated with their bioapplications. Secondly, we summarize therapeutic applications of HBPs including drug delivery, gene transfection, and protein delivery. Thirdly, we describe in detail the bioimaging and diagnosis applications of HBPs as molecular probes, including optical imaging, magnetic resonance imaging (MRI), and nuclear imaging, respectively. Fourthly, we review the bioapplications of HBPs for biomineralization, tissue engineering, antimicrobial and antifouling. Finally, we discuss cytomimetic chemistry from HBPs. This review intends to outline these exciting achievements of HBPs for bioapplications and inspire continuous endeavors in this emerging research area.

## 2. Properties of HBPs

Besides chemical composition and functionality, topological structure plays a vital role in determining the materials properties. As compared to conventional linear polymers, HBPs exhibit unique physical and chemical properties. Generally, HBPs possess ellipsoid-like three-dimensional architecture, irregularly branched structure with  $DB < 1.0$  (normally, 0.4-0.6), high polydispersity of  $M_w$  (normally,  $PDI > 3.0$ ), and a high number of functional groups linked at both the linear and terminal units. Based on these characteristics, they exhibit low molecular entanglement, low melting/solution viscosity, weak mechanical strength, high solubility, highly reactive functional groups, excellent capacity of encapsulation for guest molecules, and unusual self-assembly behaviors. Moreover, the relative ease of synthesis and lower cost make them the preferred choice in various applications as compared with dendrimers. Salient properties of HBPs for bioapplications are listed below.

### 2.1 Physicochemical properties

#### 2.1.1 Functionalization of HBPs

HBPs are characterized by a high density of functional groups in combination with one-pot synthesis, which establishes the foundation for their functionalization.

Modification of HBPs is essential to control their solubility, compatibility, reactivity, adhesion to various surfaces, chemical recognition, self-assembly, as well as electrochemical and luminescence properties. The large number of functional groups allows customizing their thermal, mechanical, rheological, and solution properties, which provides a powerful tool to design HBPs for a large variety of applications. In general, the functionalization of HBPs includes terminal modification, backbone modification and hybrid modification.

Most of the applications of HBPs are based on the absence of chain entanglements, the globular shape, and/or the nature and the large number of functional groups within a molecule. Modification of the number and type of functional groups of HBPs is essential to control their physicochemical properties. Firstly, a remarkable feature of the dendritic structures is that they possess many functional groups in their periphery, which can be exploited to introduce a high density of functionalities via multiple derivatization reactions.<sup>25</sup> The common terminal groups at the periphery of HBPs contain hydroxyl, carboxyl, amine, thiol, and halide groups. Through these terminal groups, numerous functional components could be introduced into the periphery of HBPs, including different functional small molecules (drug, fluorescence probe, targeting ligand, etc.), oligomers or polymers, or the grafting polymerization of functional monomers can be directly initiated.<sup>26-28</sup> On the other hand, the non-covalent bonded strategy has also been employed to modify the HBPs, which provides a facile way to design functional HBPs.<sup>29</sup> The modification of the terminals of HBPs is capable, to some extent, of transforming the characteristics and functions of HBPs.

In addition to the functionalities that can be introduced onto the periphery of the hyperbranched structure via terminal modifications, the use of functional monomers also offers the opportunity to introduce functionalities into the backbone of the final HBPs. The backbone modification focuses on changing the intrinsic properties of HBPs by choosing the suitable monomers and appropriate polymerization methods.<sup>30</sup> In general, both the functional groups of monomers and their arrangement have a great influence on the functional behavior of HBPs.<sup>31</sup> Furthermore, by means of various effective synthetic methodologies, the functionality of HBPs could be controlled by adjusting the molecular structure and topology.<sup>32</sup> Correspondingly, the functions of HBPs depend on the resulting parameters, including the special distribution of different monomers, degree of branching, the molecular weight and polydispersity, etc.<sup>18</sup>

Different from the two modification approaches aforementioned, hybrid modification refers to introducing the exterior components into the HBPs systems.<sup>33</sup> The exterior components, such as metal nanoparticles, nanocrystals, carbon nanotubes, and quantum dots (QDs), can be bound with HBPs through the weak interactions

(electrostatic interaction, hydrogen bonding interaction, host-guest interaction, complexation interaction, or hydrophobic interaction), thus leading to the functionalization of HBPs.<sup>34-38</sup> The improved properties by hybrid modification facilitate processing and applications of HBPs. Up to now, various functional organic/inorganic nanoparticles, luminescent organic molecules, and novel functional polymers have been reported, and meanwhile the hybrid approaches of HBPs and other components are developing rapidly. In particular, hybrid modification of HBPs has been highlighted in the fields of biodetection, bioimaging and diagnosis. For example, QDs, silicon nanoparticles and magnetic particles have already been incorporated into the cavities of HBPs, achieving the functions of biodetection, bioimaging and magnetofection *in vitro* as magnetic nonviral gene vectors, respectively.<sup>14,23</sup>

### 2.1.2 Physical and chemical responsiveness of HBPs

Through the elaborate design or modification, HBPs could be endowed with responsive ability to external stimuli. For stimuli-responsive HBPs, the combination of the advantages of HBPs and the sensitive character can significantly expand the scope of these macromolecules in bioapplications such as drug/gene delivery, separation processes, and tissue engineering. The typical external stimuli can be mainly categorized into three groups: physical stimuli (temperature, light, magnetic or electrical field, ultrasound), chemical stimuli (pH, ionic strength, solvent, and chemical additives), and biological stimuli (enzymes and receptors). The sensitive property of responsive HBPs to these stimuli is always derived from the introduction of functionalized compartments into the backbone or the terminal groups of the HBPs. By changing the environmental factors, the architecture, volume, phase state, self-assemblies, or electrical, optical, mechanical and surface properties of HBPs can be affected accordingly. Therefore, the goal of preparing smart or controllable HBPs can be achieved. In this section, we mainly focus on stimuli-responsive HBPs which are sensitive to pH, temperature, light and redox, respectively.

Changing the pH is practical and useful for bioapplications due to the fact that numerous pH gradients exist in both normal and pathophysiological states of biological systems. For example, the pH at tumor sites as well as in intracellular compartments, such as the endosomes and lysosomes, is slightly more acidic than blood and normal tissues.<sup>39</sup> Therefore, the pH-sensitive HBPs or polymeric self-assemblies which can rapidly respond to the mild acidic pH trigger provide an opportunity for the achievement of programmable and controlled drug delivery. Up to now, a series of acid-cleavable HBPs have been designed and applied in biological and biomedical fields to obtain pH-sensitive materials.<sup>40-45</sup> Introducing pH-sensitive

moieties into HBPs endows them with responsive capacity. Current approaches toward the development of pH-responsive HBPs involve either the incorporation of “titratable” groups including amines or carboxylic acids into the terminal group of HBPs or the introduction of acid liable linkages such as acylhydrazone or oxime into the backbone of HBPs that degrade under acidic conditions. For instance, Zhu and coworkers prepared pH-responsive carboxyl-modified hyperbranched poly[3-methyl-3-(hydroxymethyl)oxetane] (HPMHO) and the pH-responsive range of these carboxyl-modified HPMHO (Suc-HPMHO) can be easily adjusted by changing the degree of carboxylation, involving the extracellular pH (pH = 6.5) (Fig. 1).<sup>43</sup> Benefiting from a large number of terminal carboxyl groups, Suc-HPMHO could form stable complex with the antitumor drug cis-dichlorodiammineplatinum (II) (cisplatin) to accomplish pH-targeting drug delivery. Also, the same authors reported pH-triggered backbone-cleavable hyperbranched polyacylhydrazone (HPAH) and hyperbranched polyoximes, which exhibited great potential for various bioapplications.<sup>44,45</sup>

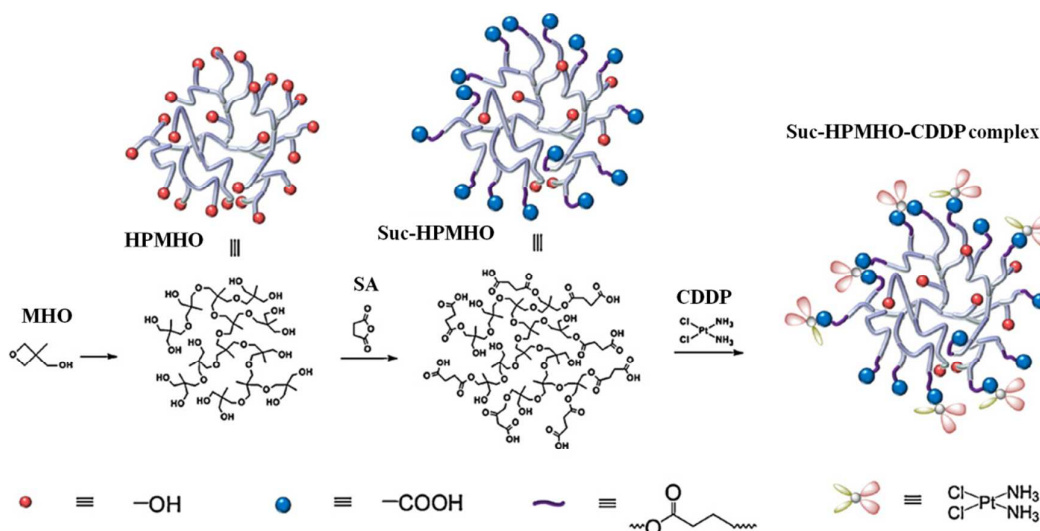


**Fig. 1** Synthesis and drug loading of Suc-HPMHO. Reproduced with permission from ref. 43.

Copyright 2011, Elsevier.

Among the external stimuli, heat could offer more opportunity for easy and safe medical applications, thus thermo-responsive HBPs have attracted considerable attention for various biomedical applications, especially in smart drug/gene delivery systems and tissue engineering. To date, two main strategies have been used to prepare thermo-responsive HBPs. One is to incorporate thermo-sensitive groups or oligomer/polymer segments, such as poly(*N*-isopropylacrylamide) (PNIPAM) or poly(2-(dimethylamino)ethyl methacrylate) (PDMAEMA), onto the surface of HBPs.<sup>46-48</sup> For example, Yan and coworkers successfully rendered hydrophobic

hyperbranched poly(3-ethyl-3-(hydroxymethyl)oxetane) (HBPO) temperature sensitive by peripheral modification with hydrophilic PDMAEMA.<sup>49</sup> The other strategy is to prepare backbone-thermoresponsive HBPs that possess the appropriate balance of hydrophilic and hydrophobic functionalities.<sup>32,50,51</sup> The backbone-thermoresponsive HBPs have a large number of functional groups at the chain ends; therefore they are potential intelligent matrixes for further modification. For example, functional molecules, such as drug molecules, target groups and fluorescent probes, can be easily introduced, allowing favorable bioapplications.

Photochemistry is particularly attractive for applications involving biological systems since it is always considered as a type of clean and instant energy and can provide a noninvasive pathway with spatial and temporal resolution. Light-responsive HBPs exhibit unique changes of chemical and physical properties and are promising materials for various bioapplications, especially in smart drug/gene delivery systems.<sup>52</sup> Light-responsive HBPs are usually prepared by introducing photosensitive molecules, such as azobenzene, spiropyran or o-nitrobenzyl groups, into the terminal or backbone of HBPs through covalent or non-covalent approaches. At present, several light-responsive HBPs have been synthesized successfully and showed great potential in bioapplications.<sup>53-55</sup> For example, recently, Zhu and coworkers reported a new kind of photo-responsive supramolecular HBP prepared by self-assembly of azobenzene dimer and  $\beta$ -cyclodextrin ( $\beta$ -CD) trimer, which can be switched reversibly by alternating ultraviolet/visible (UV/Vis) light irradiation through the reversible association and disassociation of the host-guest interaction in the backbone (Fig. 2).<sup>56</sup> These HBPs with excellent optical properties may be promising fluorescent materials as well as self-healing materials.

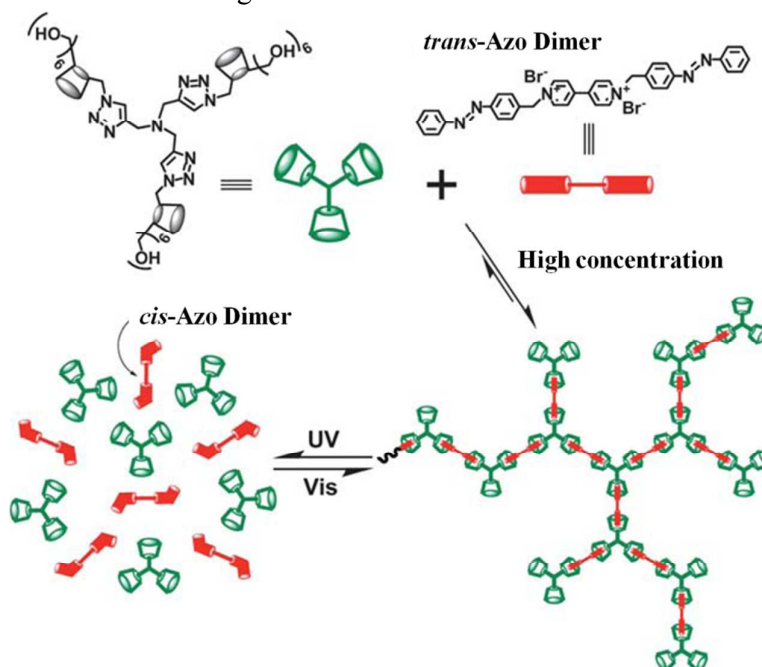


**Fig. 2** Schematic representation of the photo-controlled polymerization and depolymerization of supramolecular HBP based on  $\beta$ -CD trimer and azobenzene dimer based on host-guest interactions. Reproduced with permission from ref. 56. Copyright 2011, Royal Society of Chemistry.

Oxidation/reduction is a common biological phenomenon in living organisms, so it is interesting to develop redox-responsive HBPs for biological and biomedical applications. For example, redox-responsive HBPs have been designed for intracellular drug release because of the large difference in redox potential between cancer cells and normal cells.<sup>57</sup> Glutathione (GSH) is known as a substrate in both conjugation reactions and reduction reactions and exists in human blood plasma in micromolar concentrations.<sup>58</sup> However, the concentration of cytosolic GSH in some tumor cells has been found to be several-fold higher than that in normal cells. Materials incorporating disulfide bonds have been explored for this purpose, which can be cleaved in the presence of reducing agents such as GSH. Based on this concept, Liu et al. designed and synthesized a series of redox-responsive hyperbranched polyphosphates.<sup>58-60</sup> They prepared a redox-responsive hyperbranched homopolymer polyphosphate (HPHDP) by self-condensing ring-opening polymerization (SCROP) of 2-[(2-hydroxyethyl)-disulfanyl]ethoxy-2-oxo-1,3,2-dioxaphospholane, which was composed of alternating hydrophobic disulfide and hydrophilic polyphosphate segments (Fig. 3).<sup>60</sup> This novel homopolymer could self-assemble into micelles with a multi-core/shell structure and a narrow size distribution, which exhibited smart response in a reductive environment and could efficiently transport drugs into tumor cells. Very recently, the same authors synthesized another hydrogen peroxide-responsive HBP consisting of alternative hydrophobic selenide groups and hydrophilic phosphate segments.<sup>61</sup> Because the hydrophobic selenide groups could be easily oxidized into hydrophilic selenone groups under the exclusive oxidative microenvironment within cancer cells, the HBP became hydrophilic after oxidation, leading to the rapid disaggregation of the assemblies. This type of peroxide-responsive HBPs not only realizes rapid and selective intracellular drug release, but also possesses excellent intrinsic anticancer efficacy because of the existence of selenium-containing groups.

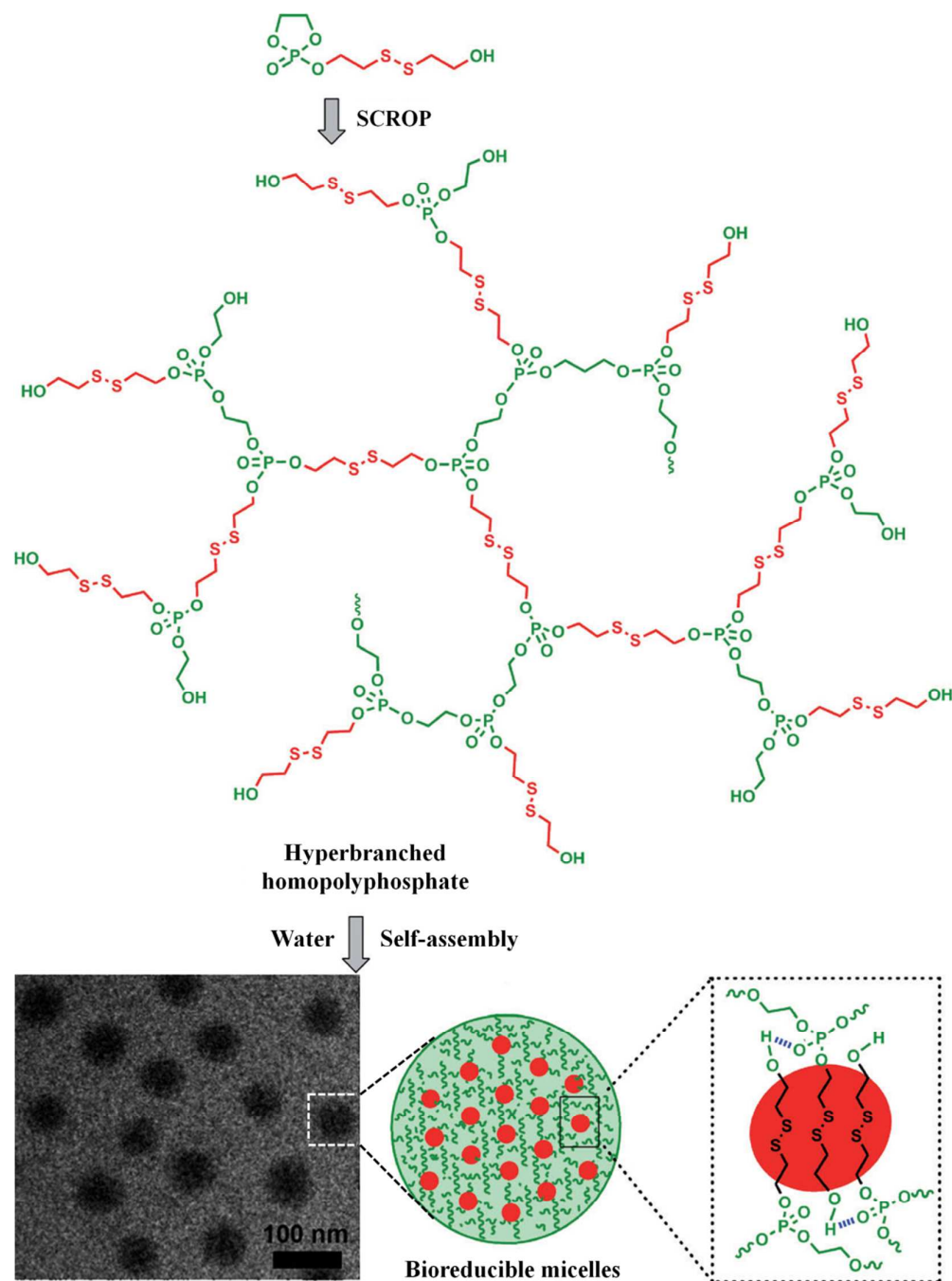


**Fig. 3** Synthesis of homopolyphosphates (HPHDP) and schematic representation of the self-assembled micelles. Reproduced with permission from ref. 60. Copyright 2011, Wiley.

### 2.1.3 Self-assembly of HBPs

Supramolecular self-assembly of HBPs is a newly emerging research area and the research progress has been highlighted recently by the review articles from Zhou and Yan.<sup>13,14</sup> It has received increasing attention due to their great advantages in biological and biomedical applications. Traditionally, the well-defined molecules including

surfactants, dendrimers and linear block copolymers could self-assemble into elaborate microscopic or mesoscopic supramolecular structures. In contrast, HBPs have irregular structures and randomly branched units, which make HBPs look difficult to perform supramolecular self-assembly. Nevertheless, HBPs have exhibited great potential to be excellent precursors for supramolecular self-assembly since the landmark work of Yan and coworkers in 2004 when they reported macroscopic multiwalled tubes through the self-assembly of amphiphilic HBPO-*star*-PEO with a hydrophobic hyperbranched poly(3-ethyl-3-oxetanemethanol) core (HBPO) and many hydrophilic poly(ethylene oxide) arms (PEO) in acetone.<sup>62</sup> Since then, the self-assembly of HBPs has experienced a rapid development and numerous delicate supramolecular structures with various morphologies and functions have been reported by primary self-assembly or hierarchical self-assembly of amphiphilic HBPs, such as spherical micelles, nano- or micro-scale vesicles, ribbons, honeycomb-patterned films, fibers, tubules, and so on (Fig. 4).<sup>63-70</sup> Compared with the self-assembly of conventional molecules, HBPs have displayed some unique characteristics in self-assembly behavior.<sup>13</sup> Firstly, the topologies of HBPs are easily controlled by tailoring the molecular weight and degree of branching (DB), and the type, number and length of the arms with a relatively simple synthesis. Thus, diverse supramolecular assemblies over all dimensions and scales can be obtained conveniently by adjusting the topology of the HBPs. Due to the globular structure, HBPs have the specific self-assembly mechanism which is greatly different from the linear block copolymers. The amphiphilic HBPs generally self-assemble into unimolecular micelles with the diameter of smaller than 10 nm in solution, whereas linear polymers can not form unimolecular micelles. The unimolecular micelles from HBPs could aggregate into large micelles above 100 nm without phase separation. However, the self-assembly process of linear polymers generally refer to phase separation or inverse phase separation. Additionally, HBPs can self-assemble into vesicles and tubes through the special phase separation process that is different from the one observed for the linear polymers. Thirdly, to a certain degree, the properties of supramolecular structures from HBPs are superior to assemblies of conventional molecules. For example, Yan and Zhou reported a new type of temperature-responsive polymer vesicles from HBPO-*star*-PEO with broadly adjustable and reversible lower critical solution temperature (LCST) transitions from 8 to 81 °C.<sup>71</sup> In addition, they also prepared pH-sensitive polymer vesicles self-assembled from carboxylated hyperbranched polyester, which possessed a controllable size in a broad range from 200 nm to 10 μm by simply changing the solution pH from 1.5 to 5.5.<sup>42</sup> Finally, the supramolecular assemblies of HBPs can easily be functionalized through covalent or non-covalent approaches because of their void-containing topology structure and a large population of functional groups. For

example, Yan and Gao reported fluorescent honeycomb-patterned films self-assembled from amphiphilic hyperbranched polyamidoamines (HPAMAMs).<sup>67</sup> In this work, the dye molecules were encapsulated into the cavity of HPAMAMs to form colorful host-guest supramolecular complexes, which further self-assembled into luminescent films on substrates. Taking these aforementioned characteristics into consideration, the supramolecular self-assembly of HBPs enlarges the diversity of structures, opens up a straightforward route to the functionalization of self-assembly structures, and paves a new way for the bioapplications of HBPs.

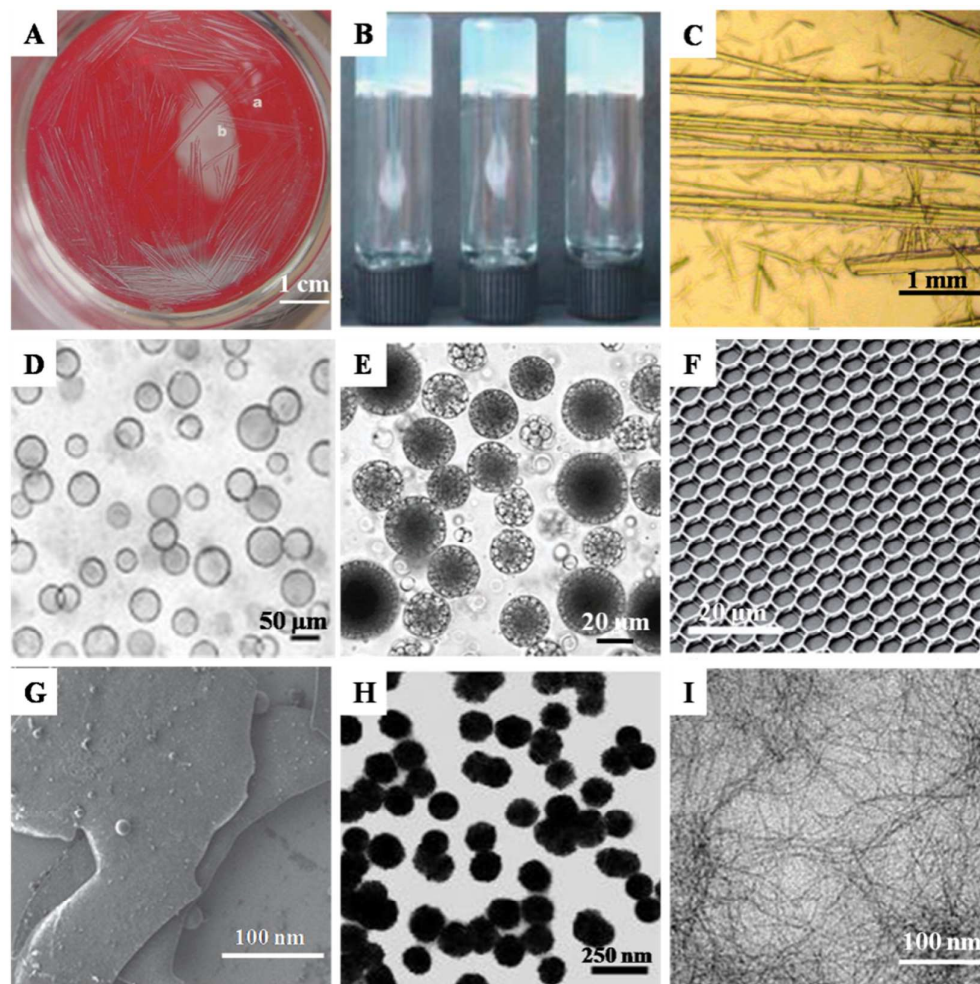


**Fig. 4** Self-assembled structures of amphiphilic HBPs: (A) macrotubes,<sup>62</sup> (B) physical hydrogel,<sup>63</sup> (C) mesoscopic tubes,<sup>64</sup> (D) giant vesicles,<sup>65</sup> (E) composed vesicles,<sup>66</sup> (F) honeycomb films,<sup>67</sup> (G) 2D sheets,<sup>68</sup> (H) spherical micelles,<sup>69</sup> (I) nanoscale fibers<sup>70</sup>.

## 2.2. Biological properties

### 2.2.1 Biodegradability and biocompatibility of HBPs

The rapid emergence of HBPs in biological and biomedical applications has been accompanied by a growth in the number of HBP backbones designed to be

biodegradable and biocompatible. The availability of biodegradable HBPs with defined structure, controlled degradation profiles, and excellent biocompatibility is significant for the development of *in vivo* drug delivery systems, scaffolds for tissue engineering, imaging agents, and other biomaterials associated with life. At present, a large amount of biocompatible HBPs such as hyperbranched polyglycerol (or polyglycidol), poly(ethylene oxide), and sugar derivatives together with biodegradable polymers like hyperbranched polyesters, polyphosphates, and polypeptides have been well-designed and widely used in biological fields (Fig. 5). Hyperbranched polyglycerol (HPG) was prepared in a controlled manner by Frey and coworkers through the anionic ring-opening multibranching polymerization (ROMBP) of AB<sub>2</sub>-type monomer glycidol.<sup>72</sup> The HPG possesses good hydrophilicity, high chemical stability, excellent biocompatibility and low/absent immunogenicity.<sup>16</sup> Therefore, HPG and its derivatives offer enormous potential for a variety of biological and medical applications in diagnostics and therapy, for example, bioconjugation with peptides, encapsulation of drugs and probes as well as surface attachment for protein-resistance.<sup>21</sup> Considering that a flexible aliphatic polyether backbone of HPG is not degradable, the long-term accumulation of these external objects is a great concern to the human body. Therefore, the development of HBPs that degrade under physiological conditions is of particular interest for the design of new biomedical polymeric materials. From this perspective, hyperbranched polyesters have received increased attention in the biomedical field due to their ease of metabolism of the degradation products. The most widely used hyperbranched polyester at present is a commercially available HBP known as Boltorns<sup>®</sup> Hx (x = 20, 30, 40). In addition, a new concept to produce sophisticated materials is to introduce biodegradable or bioresponsive compartments into polymeric structures. Biodegradable functionalities sensitive to proteases (peptides), to redox conditions (disulfide, diselenide) or to pH (esters, ketals, and acetals) have been incorporated within the backbone of HBPs.<sup>57,73-76</sup> For example, Kizhakkedathu and coworkers incorporated ketal groups into the backbone of hyperbranched polyether to endow biocompatible polyether with tunable biodegradability.<sup>77</sup> A range of poly(ketal hydroxyether)s (PKHEs) were synthesized by anionic ring-opening multibranching polymerization (ROMBP) of newly designed AB<sub>2</sub>-type ketal monomers containing structurally different ketal groups (both cyclic and acyclic). Due to the differences in ketal group structures, the pH-dependent degradability of PKHEs could be well-controlled at mild acidic pH values with the hydrolysis half-lives from a few minutes to a few hundred days (Fig. 6). Moreover, PKHEs and their degradation products exhibited high biocompatibility confirmed by the cell viability assay and blood compatibility assays including complement activation, platelet activation, and coagulation. These hyperbranched PKHEs have demonstrated great potential as multifunctional drug delivery vehicles

for efficient endosomal escape and cytosolic delivery.

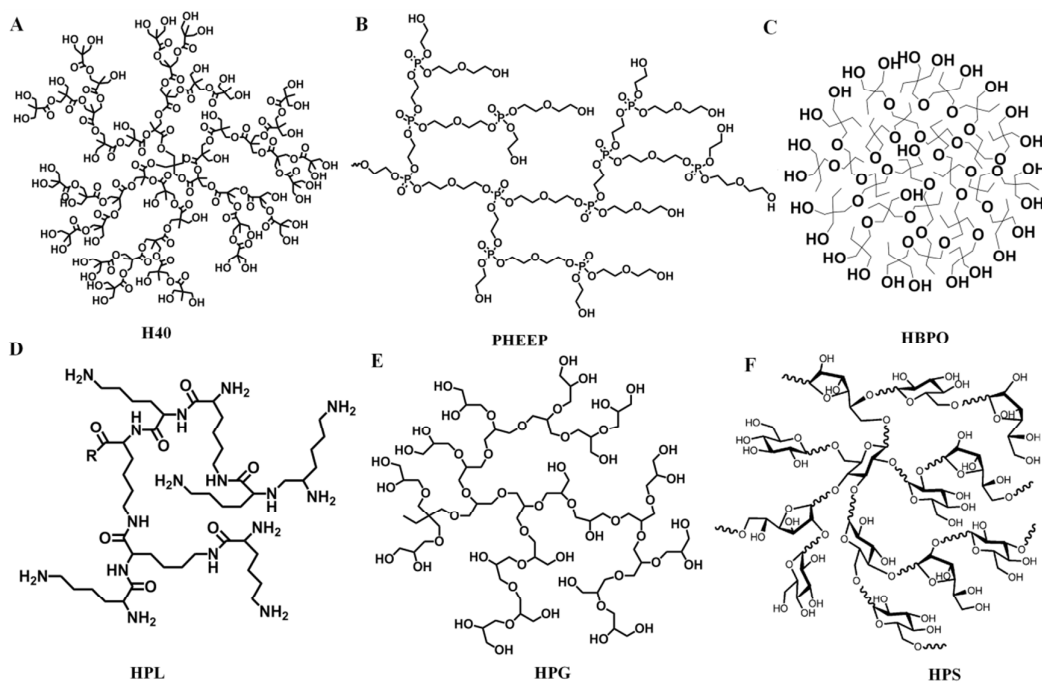


**Fig. 5** Schematic structures of biocompatible or biodegradable HBPs: (A) hyperbranched polyester (H40), (B) hyperbranched polyphosphate (PHEEP), (C) hyperbranched poly(3-ethyl-3-oxetanemethanol) (HBPO), (D) hyperbranched polylysine (HPL), (E) hyperbranched polyglycerol (HPG), (F) hyperbranched polysaccharide (HPS).

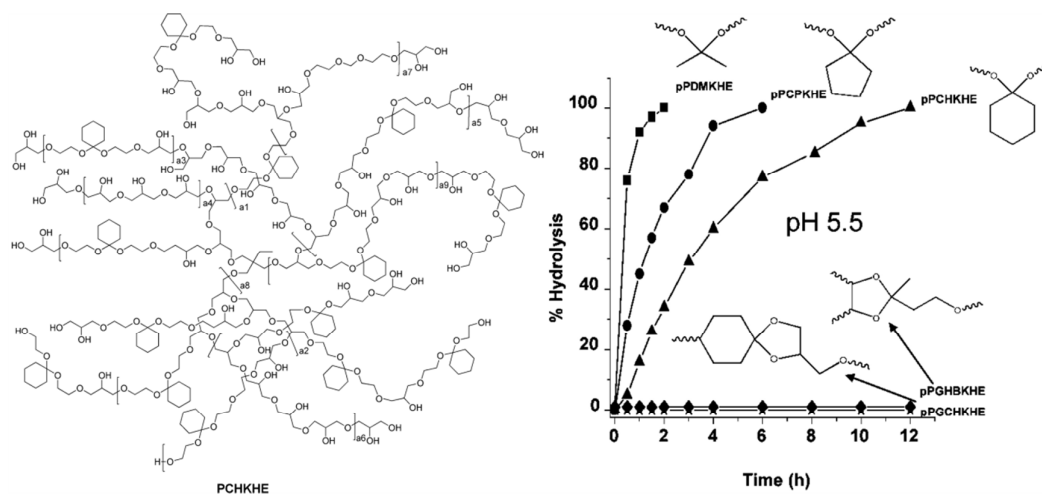


**Fig. 6** Schematic structures of hyperbranched PKHEs and comparison of hydrolysis kinetics plots of different PKHEs at pH 5.5. Reproduced with permission from ref. 77. Copyright 2012, American Chemical Society.

Since phosphates, peptides and saccharide units are the main elements in biomolecules of lipids, proteins and polysaccharides, the HBPs that were constructed from these units are inherently biodegradable and biocompatible. Hyperbranched

polyphosphates were reported by Huang and Yan through self-condensing ring-opening polymerization of hydroxyl-functionalized cyclic phosphate inimer 2-(2-hydroxyethoxy)ethoxy-2-oxo-1,3,2-dioxaphospholane (HEEP).<sup>78</sup> These polymers and their derivatives have demonstrated eminent biocompatibility, biodegradability, and flexibility in adjusting the pendant structures and are promising candidates in biomedical applications.<sup>79-81</sup> Compared to linear peptide analogues, the hyperbranched peptides generally displayed higher solubility, enhanced proteolytic stability and a lower toxicity. Hyperbranched polypeptides may be an interesting, cheap alternative for the peptide dendrimers that are widely used or are being explored for many medical applications.<sup>82-84</sup> Recent development of synthetic strategies for hyperbranched polypeptides is particularly interesting and many potential bioapplications are being investigated. For hyperbranched polysaccharides, although some HBPs based on sugar or its derivatives have been synthesized and explored for bioapplications, most of them are still isolated from natural materials and under exploration.<sup>85-87</sup> With the readily available feedstocks and rapidly developing chemistries, more and more biodegradable and biocompatible HBPs will be designed and used for biological and biomedical applications.

### 2.2.2 Biological responsiveness of HBPs

By means of various synthetic methodologies, HBPs can be endowed with biological responsiveness (enzyme, receptors, etc.). Among a variety of external stimuli, enzymes have emerged to be a promising triggering motif for the design of a new class of responsive HBPs in recent years. Enzymes are involved in all biological and metabolic processes of living organisms.<sup>88</sup> Compared to HBPs responding to physical and chemical stimuli, enzyme-responsive HBPs exhibit superior advantages such as high selectivity and substrate specificity. Furthermore, they respond under quite mild conditions (37 °C, aqueous media, typically neutral or slightly acidic and alkaline pH). The integration of enzyme responsiveness with dendritic structure can further broaden the design flexibility and scope of applications by endowing the HBPs with enhanced triggering specificity and selectivity. To some extent, among all of the stimuli, enzymes are the best candidates for triggering transformations and transitions of HBPs or polymeric assemblies. For example, Haag and coworkers synthesized enzyme-responsive drug-conjugated HPG for tumor tissue-targeted delivery and site-specific triggered release.<sup>89</sup> The doxorubicin (DOX) or methotrexate (MTX) was conjugated to the terminal groups of HPG by either a self-immolative para-aminobenzyloxycarbonyl spacer coupled to the dipeptide Phe-Lys or the tripeptide D-Ala-Phe-Lys as the protease substrate. They were cleaved in the presence of cathepsin B, an enzyme overexpressed by several solid tumors, thus leading to the release of DOX or a MTX lysine derivative and exhibiting superior antitumor efficacy

*in vivo* over the free drug.<sup>90,91</sup>

### 3. HBPs for therapeutic applications

#### 3.1 HBPs for drug delivery

An ideal drug carrier should have excellent biocompatibility, form a stable complex with the drug, transport the drug into the targeting site, and then release them efficiently, while keeping the pharmacological properties of the drug. HBPs are emerging as potentially ideal drug delivery vehicles because they can be tailored and carry plenty of functional end-groups. During the past few decades, the use of HBPs as drug carriers to achieve controlled and targeted delivery of drugs to the tissues and sites has been widely explored.

##### 3.1.1 Encapsulation and covalent attachment of drug

The encapsulation of a large amount of the hydrophilic and hydrophobic guest molecules using HBPs such as hyperbranched polyesters, polyglycerols, polyesteramides, and polyethylenimines has been widely investigated in the past few years.<sup>92-96</sup> Firstly, the simplest drug encapsulation pattern is that small-molecule drugs are directly entrapped within the inner nanocavities of HBPs via physical interactions.<sup>93,94</sup> Secondly, by design of special structures, HBPs can self-assemble into unimolecular micelles capable of encapsulating and solubilizing drugs into the void spaces within the HBPs' interior and exhibit higher stability than multimolecular micelles from conventional linear amphiphilic block copolymers under general conditions.<sup>95</sup> Usually, HBPs possess enhanced encapsulation ability when compared with their linear analogues. For example, Haag and coworkers investigated the loading capacity of hyperbranched PEI functionalized with different fatty acids (C18, C16, C11, C6).<sup>96</sup> The resulting amphiphilic HBPs based on hyperbranched PEI formed core-shell architectures and were suitable for encapsulation of guest molecules containing anionic groups such as carboxylate, sulfonate, phosphate, and acidic OH groups (Fig. 7). They found that the modification using different types of fatty acids increased the encapsulating capacity of hyperbranched PEI, allowing up to 150 guest molecules to be molecularly encapsulated and transported. The modified hyperbranched PEI exhibited a higher encapsulation capacity than the linear one. However, the unimolecular micelles of HBPs can only encapsulate a small amount of guest molecules due to the limited volume of the interior cavities. In contrast, multimolecular micelles possess larger hydrophobic cores, thus enhancing the encapsulating capacity and the controllability of drug delivery. Thus, multimolecular micelles from HBPs are very attractive in drug delivery. For the multimolecular micelles, the drugs are loaded in the micelle cores or shells through the non-covalent

interactions based on their hydrophilicity. In addition to loading single-guest molecules, HBPs have the ability of encapsulating double or multiple-guest molecules, which was reported by Gao and coworkers.<sup>97</sup> They discovered the synergistic encapsulation phenomenon of amphiphilic HBPs in the process of double-dye host-guest encapsulation. The loading capacity of one kind of guest molecule can be significantly increased in the presence of other kinds of guest molecules. All of these aforementioned results demonstrate three-dimensional hyperbranched topology of HBPs plays a crucial role on their encapsulation capacity.

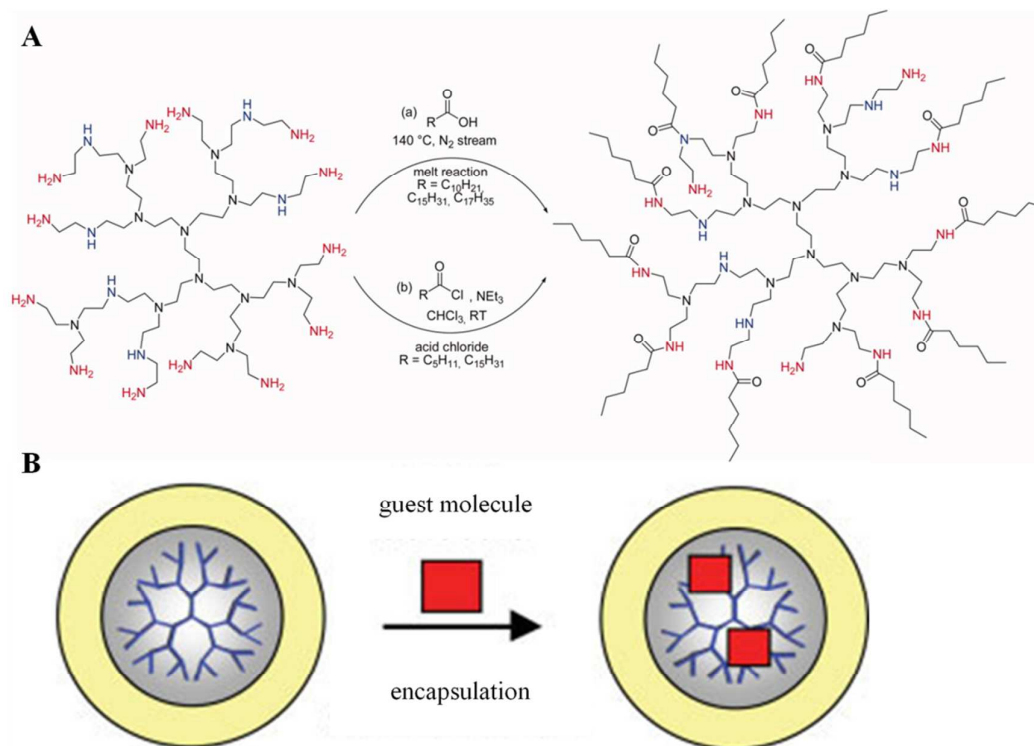
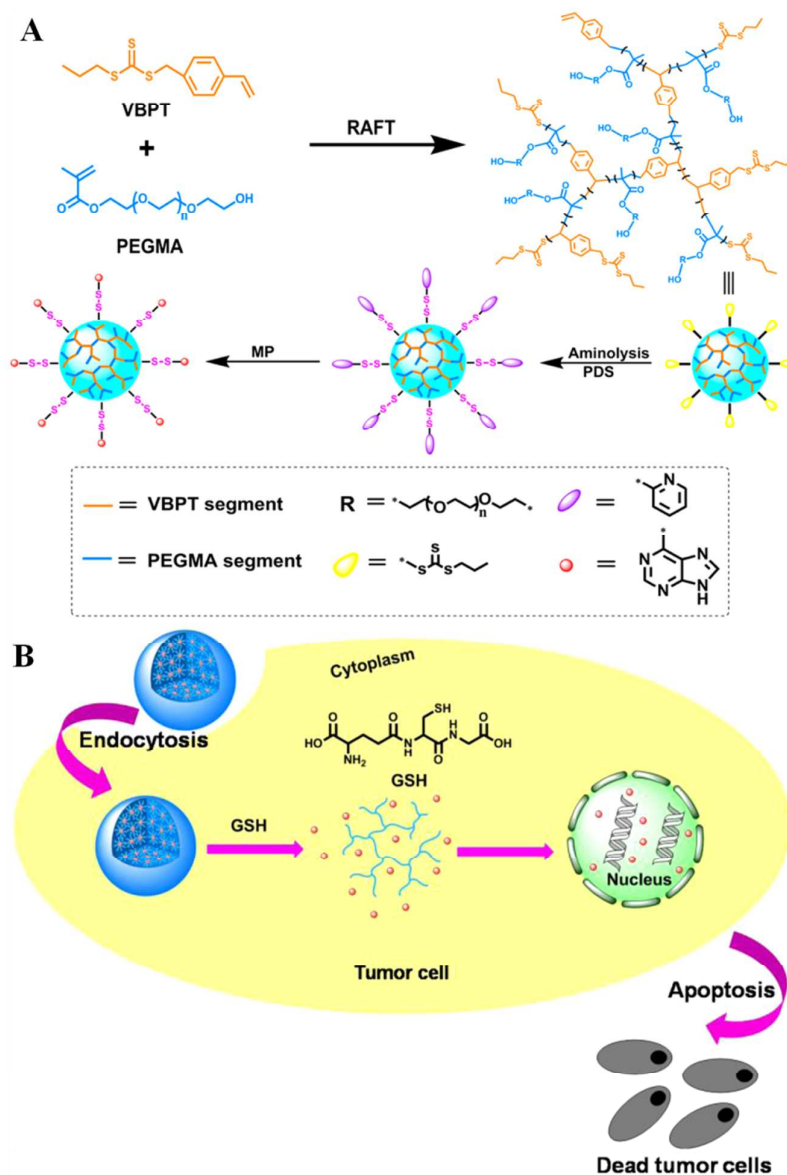


**Fig. 7** Functionalization of hyperbranched PEIs with hydrophobic alkyl chains leads to a core-shell type architecture that is able to encapsulate polar guest molecules. (A) Functionalization of hydrophilic hyperbranched PEIs ( $M_w = 800\text{--}25,000\text{ g mol}^{-1}$ ) with (a) an alkyl chain acid (melt reaction route) and (b) with an acid chloride to obtain core-shell type architectures suitable for encapsulation; PEI functionalized with C6 acid is shown as an example. (B) Schematic representation of encapsulating polar guest molecules with core-shell type architectures. Reproduced with permission from ref. 96. Copyright 2007, Wiley.

Although the drug encapsulation with HBPs for drug delivery has been proved successfully, some limitations still exist for efficient drug encapsulation and controlled release. The main limiting issue is the relatively rapid and uncontrollable release of drug molecules from the HBPs core. In contrast, the covalently bound HBP-drug conjugates remain stable in both water and buffered solutions and thus significant research has focused on covalent drug attachment. The types of linker

groups for the covalent attachment of drug molecules to the HBPs periphery have an important effect on the activity of the HBP-drug conjugates and can be used to control drug release.<sup>98,99</sup> Usually, the linker groups refer to (1) ester groups,<sup>100</sup> which can be readily broken by the esterase enzymes within the cell; (2) acid labile cis-aconityl or acylhydrazone groups,<sup>44,101</sup> which are easily cleaved under the mildly acidic conditions such as the intracellular endosome and lysosome; or (3) disulfide groups,<sup>102</sup> which can be reduced by GSH within the cytosol. For example, Zhu and coworkers reported that DOX was covalently conjugated through acylhydrazone bonds to HPAH.<sup>44</sup> Importantly, DOX-conjugated HPAH was stable at physiological conditions (pH = 7.4), but was cleaved after the acidic lysosomes (pH = 5-6) trigger, leading to the controlled release of DOX drugs. Very recently, they designed and prepared redox-responsive HBP-drug conjugates through the coupling of the multithiol HBPs and thiol-containing drugs.<sup>102</sup> The HBP poly((S-(4-vinyl) benzyl S'-propyltrithiocarbonate)-*co*-(poly(ethylene glycol) methacrylate)) (poly(VBPT-*co*-PEGMA)) with multiple thiol groups was synthesized via reversible addition-fragmentation chain transfer (RAFT) copolymerization, which could conjugate with the thiol-containing drugs via disulfide linkages to accomplish a redox-triggered release (Fig. 8A). Since the concentration of GSH in the tumor tissues is many-fold higher than that in normal tissues, the redox-responsive HBP-drug conjugates could selectively release the drug at tumor sites, thus resulting in a high anticancer efficiency (Fig. 8B). This redox-responsive HBP-drug conjugate may provide a novel platform for the delivery and controlled release of thiol-containing drugs or biological molecules.



### 3.1.2 HBPs for controlled drug release

The effect of drug therapy is closely related to the release behavior of the delivery system in the body. Slow and controlled release of drugs is of great importance in an effective drug delivery system because it allows the drug-encapsulated system to reach the site of action without significant loss of drug from the delivery system. HBPs can form unimolecular micelles or self-assemble into multimolecular micelles

with a very low critical micelle concentration (CMC) in aqueous solution, exhibiting high stability as drug carriers. Moreover, HBPs have many functional groups, customizable degree of substitution, and adjustable DB to allow the control over the drug release. For example, Burt and coworkers reported that two commercially available HBPs (HPG and H40) modified with carboxylic acid were used as macromolecular ligands for the controlled release of anticancer drug cisplatin.<sup>103</sup> It was found that the modified HPG formed strongly bound platinum complexes, which exhibited sustained release over 7 days in physiological saline with almost all of the cisplatin being released. Compared to the modified HPG, the modified H40 was found to form a higher proportion of weakly bound complexes with cisplatin. H40 demonstrated more rapid initial release of cisplatin than HPG, and only 60% of the total drug loading was released over 5 days in physiological saline, implying that 40% of cisplatin was strongly bound to H40 and released much slower. The release results showed that the complexes of HPG and cisplatin were a promising delivery system. Yan and coworkers prepared hyperbranched poly[methylenebis(acrylamide)-aminoethylpiperazine] containing various amounts of  $\beta$ -CD for controlled drug release.<sup>104</sup> The anticancer drug chlorambucil could be loaded in the cavities of HBP and  $\beta$ -CD. The *in vitro* release experiments showed that the release rate of chlorambucil could be well-controlled by adjusting the  $\beta$ -CD content and the presence of  $\beta$ -CD could appropriately slow drug release.

In many controlled-release applications, HBPs are always functionalized to respond to the target environment. Generally, a change in pH, temperature, light, redox conditions, or a bacterial, enzymatic activity disintegrates the HBPs carrier system, leading to the controlled release of the encapsulated drug at target site. For example, Zhu and coworkers constructed pH-responsive HPAH to release autophagy inhibitor LY294002 (LY) and anticancer drug DOX in a controlled programmable manner for oral squamous cell carcinoma therapy.<sup>105</sup> Firstly, the hydrophobic DOX was conjugated onto the terminal groups of hydrophilic HPAH via acylhydrazone linkages, forming amphiphilic DOX-conjugated HPAH (HPAH-DOX). Then the HPAH-DOX self-assembled into nanomicelles in an aqueous solution and the autophagy inhibitor LY was encapsulated into the core of HPAH-DOX micelles (Fig. 9A). The release of the encapsulated LY and conjugated DOX was well-controlled and pH-dependent, whereas LY was released significantly faster than DOX at a mildly acidic condition due to the physical encapsulation (Fig. 9B). *In vitro* evaluation demonstrated that the preferential release of LY induced early inhibition of protective autophagy of tumor cells and rendered them more sensitive to the subsequent liberation of DOX, thus leading to significantly high antitumor efficacy (Fig. 9C). This HBP-based system for controlled release of the chemotherapy drug and the autophagy inhibitor may open up new perspectives in clinically applicable combination therapy.

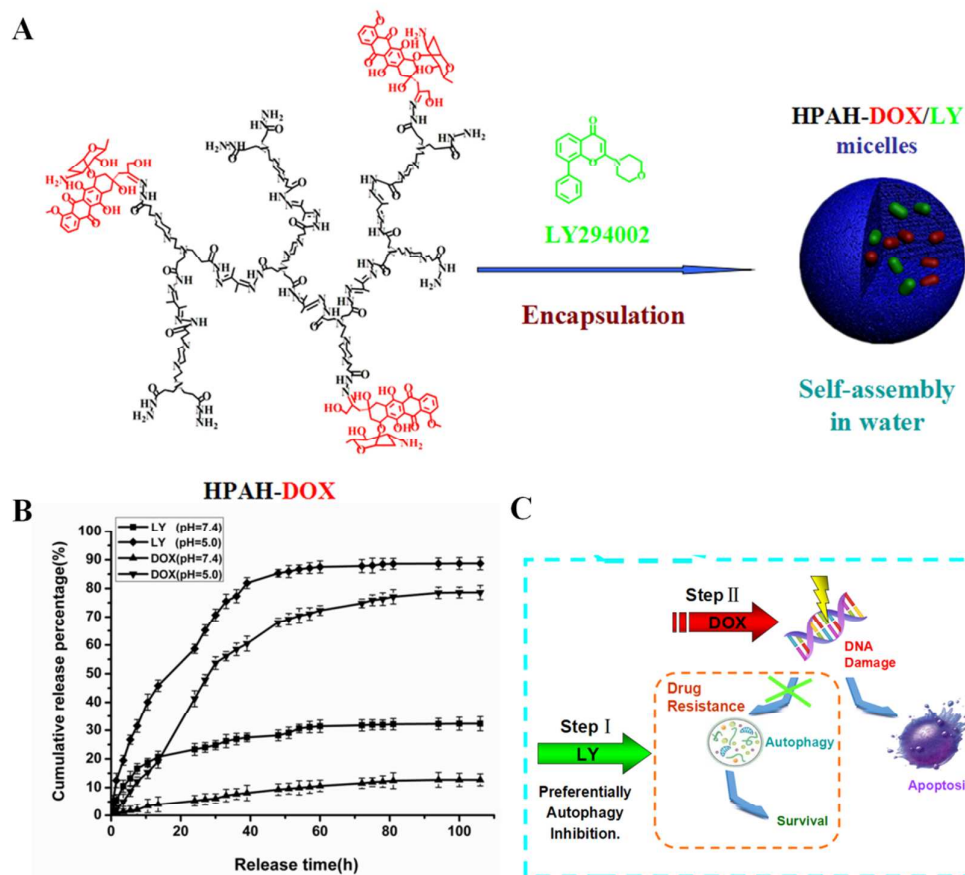


**Fig. 9** (A) Schematic representations of the structure of HPAH-DOX and the encapsulation of the LY with HPAH-DOX micelles. (B) *In vitro* release profiles of LY and DOX from the LY-loaded HPAH-DOX micelles at different pH values (7.4 and 5.0) at 37 °C. (C) Schematic representation of proposed mechanism of synergistic inhibition of tumor cell proliferation by sequential release of autophagy inhibitor and chemotherapeutic drug. Reproduced with permission from ref. 105. Copyright 2014, American Chemical Society.

### 3.1.3 HBPs for targeting therapy

Polymeric nanocarriers have been explored for tissue-specific drug delivery and enhanced endocytosis.<sup>106</sup> One of the most important advantages is that they can passively accumulate into the porous tissues, such as tumor tissues. It has been reported that pores in the tumor vasculature typically have a diameter from 40 to 80 nm; however they can be as large as 1  $\mu\text{m}$  across.<sup>107</sup> This phenomenon is called the enhanced permeation and retention (EPR) effect and refers to passive targeting. The use of macromolecules or their assemblies with suitable size as efficient carriers for the delivery of anticancer drugs has been strengthened by recent studies concerning the enhanced permeability of tumor blood vessels and their subsequent accumulation in solid tumors. From the structural perspective, HBPs can be easily adjusted due to

their three-dimensional topological architecture and numerous terminal groups. Therefore, passive targeting of HBPs or their assemblies can be well-controlled by rational design. As an example, Zhu and coworkers utilized a supramolecular strategy to construct supramolecular amphiphilic multiarm hyperbranched copolymer based on the molecular recognition between adenine and uracil moieties.<sup>108</sup> By adjusting the ratio of hydrophobic building block and hydrophilic arm, the size of the self-assembled micelles from hyperbranched copolymer could be tunable with the diameter ranging from 10 nm to 200 nm. This supramolecular HBP-based system could transport anticancer drugs for the preferential accumulation to tumor tissues.

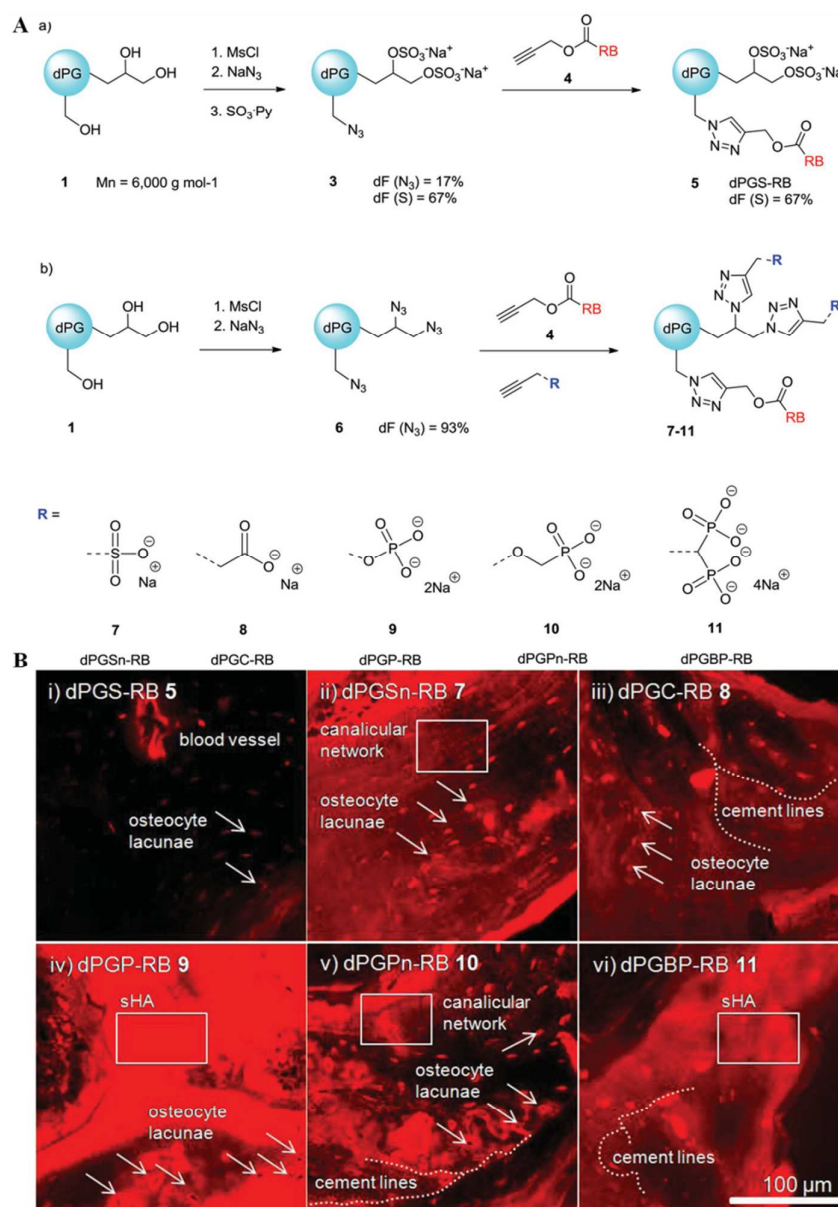


**Fig. 10** (A) a) Reaction pathway for the synthesis of  $dPGS\text{-}RB$  5 by partial mesylation, azidation, sulfation, and click coupling of propargylated  $RB$  4, b) Preparation of  $dPG$  anion  $RB$  conjugates

7-11 from dendritic polyglycerol (dPG) azide 6 by applying a sequential one-pot click reaction first with alkyne functionalized rhodamine 4 and then followed by the respective anionic alkynes; (B) Qualitative confocal laser scanning microscopy images of inner parts of native murine bone samples. Femur, cross-section, 40× magnification after incubation with dPG polyelectrolytes (red) in PBS at pH 7.4. Enhanced targeting of organic compartments, e.g., osteocyte lacunae (red dots) and blood vessels is found for nonphosphorous containing polymers (i-iii), whereas areas of high HA concentration, such as cement lines or surroundings of osteocyte lacunae (black dots) and cut surfaces (sHA), are mainly targeted by dPGP-RB 9, dPGPn-RB 10, and dPGBP-RB 11 (iv-vi). Reproduced with permission from ref. 112. Copyright 2014, Wiley.

One major limitation with size-related passive targeting is that it is difficult to achieve a sufficient drug concentration at the disease sites, which may lead to low therapeutic efficacy and elicit severe side effect. To further improve the drug delivery efficiency, strong attention has been paid on exploiting materials with active targeting ability. Compared to traditional linear polymers, HBPs have a large number of functional end-groups in their peripheries that can be easily modified to connect targeting groups, which make them more ideal for use as targeted drug-delivery agents. Generally, the targeting ligands include antibodies, lectin, peptides, other small molecules (e.g. folic acid, saccharide and lactose) and so on, which can recognize and bind to specific receptors. For example, Cheng and Gong have reported folate(FA)-conjugated amphiphilic hyperbranched block copolymer based on aliphatic polyester Boltorn H40 for tumor-targeted drug delivery.<sup>109,110</sup> As expected, *in vitro* experiments demonstrated that drug-loaded FA-functionalized HBP assemblies exhibited enhanced cellular uptake and increased tumor cell inhibition due to the FA-receptor-mediated endocytosis mechanism. Zhu and coworkers synthesized alendronate(ALE)-conjugated amphiphilic hyperbranched copolymer H40-*star*-PEG/ALE as a carrier for bone-targeted drug delivery.<sup>111</sup> The self-assembled H40-*star*-PEG/ALE micelles with bone-targeting bisphosphonate moieties showed strong affinity to the skeleton mineral hydroxyapatite (HA), which was proved by the HA binding assay. The H40-*star*-PEG/ALE could encapsulate the hydrophobic anticancer drug DOX, showing great potential as bone-targeted drug delivery for skeletal metastases. Recently, Haag and coworkers studied a series of HPG and polyanion dye conjugates, including sulfates, sulfonates, carboxylates, phosphates, phosphonates, and bisphosphonates, for selective bone-targeting applications (Fig. 10A).<sup>112</sup> As shown in Fig. 10B, the phosphate, phosphonate, and bisphosphonate-functionalized HPG expressed high affinity toward inorganic, highly carbonated HA compartments. In contrast, the sulfate, sulfonate, and carboxylate-functionalized HPG exhibited weaker affinity to HA but a more apparent affinity toward organic collagen. Interestingly, HPG carboxylate showed strong

binding to both compartments and the phosphate, and phosphonate-functionalized HPG polyelectrolytes displayed remarkable affinities to HA, which may be due to the multiple organizations of densely arranged anionic groups. Therefore, hyperbranched polyanions based on the biocompatible HPG scaffold may represent a promising class of polymers for therapeutic or diagnostic applications, for example, as drug delivery systems or for selective bone-targeting imaging.

### 3.1.4 Multifunctional HBPs for drug delivery

Consecutive functionalization of these basic HBPs by introducing various types of functional groups results in the formation of multifunctional HBPs, which exhibit the property of multivalency for drug delivery. For example, protective groups such as poly(ethylene glycol) (PEG) have been introduced on the surface of HBPs through suitable functionalization to improve the stability of drug carriers and prolong their *in vivo* circulation duration. The incorporation of translocating agents or molecular transporters at the periphery of HBPs can improve the drug transport efficiency through cell membranes. In addition, the imaging probes at the core or external surface of HBPs provide a powerful tool to study the *in vivo* behavior of drug or carrier materials and the integration of HBPs and imaging probes can achieve synergistic functions such as drug delivery, diagnosis, and imaging-guided therapy. Finally, the nanocavities of HBPs have been tailored in such a way that drug release can be controlled by changing external environment at the site of action.

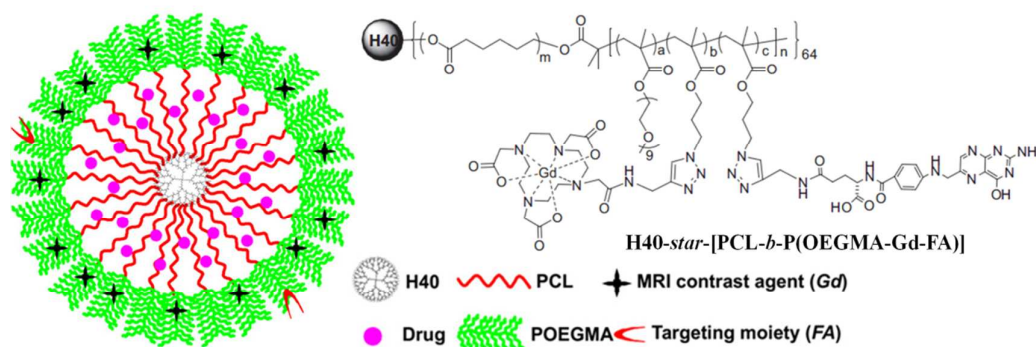


**Fig. 11** Schematic illustration of multifunctional unimolecular micelles based on amphiphilic multiarm star block copolymers H40-*star*-[PCL-*b*-P(OEGMA-Gd-FA)]. Reproduced with permission from ref. 115. Copyright 2011, Elsevier.

In recent years, some multifunctional HBPs systems have been developed by employing commercially available or custom-made HBPs in agreement with the above mentioned criteria and applied for drug delivery.<sup>113-116</sup> Paleos and coworkers prepared and investigated multifunctional HPG bearing protective PEG chains and the FA-targeting ligand at their end as prospective drug carrier systems.<sup>114</sup> It was found

that the introduction of the PEG chains not only provided stability and protection in biological milieu but also enhanced the encapsulation efficiency. Liu and coworkers reported on the fabrication of multifunctional amphiphilic multiarm hyperbranched copolymers, H40-*star*-[PCL-*b*-P(OEGMA-Gd-FA)], as an integrated platform for cancer cell-targeted drug delivery and MRI contrast enhancement.<sup>115</sup> The hyperbranched copolymers were composed of hydrophobic hyperbranched polyester H40 core, a hydrophobic poly( $\epsilon$ -caprolactone) (PCL) inner layer, and a hydrophilic polyoligo(ethylene glycol) monomethyl ether methacrylate (POEGMA) outer corona covalently bonded with targeting FA moieties and MRI contrast agents DOTAEgD (DOTA is 1,4,7,10-tetraazacyclododecane-1,4,7,10-tetrakisacetic acid), which further self-assembled into structurally stable unimolecular micelles in aqueous solution (Fig. 11). The hydrophobic anticancer drug, paclitaxel, was encapsulated into the inner hydrophobic core of unimolecular micelles efficiently and could be released in a controlled manner. Paclitaxel-loaded unimolecular micelles showed significantly higher cytotoxicity compared to non-targeting ones because of the FA receptor-mediated endocytosis. Meanwhile, *in vitro* evaluation demonstrated that the  $T_1$  relaxivity of unimolecular micelles enhanced  $\sim 6$  times compared to that of small molecular DOTAEgD complexes. Furthermore, *in vivo* MR imaging experiments in rats demonstrated good accumulation of unimolecular micelles within liver and kidney, excellent positive contrast enhancement, and relatively long blood circulation time. The multifunctional HBPs synergistically integrated with cancer-targeted drug delivery and enhanced MR imaging functions showed great potential for theranostic applications. Dong and coworkers reported two-photon-sensitive and sugar-targeted carriers from degradable amphiphilic HBPs for controlled drug release and targeted drug delivery.<sup>116</sup> The dendritic amphiphiles self-assembled into the near-infrared (NIR) light sensitive micelles, which would target the diseased sites by sugar-induced active targeting, and then light-triggered drug release could be achieved in a controlled manner.

### 3.2 HBPs for gene transfection

Gene therapy represents a promising approach for the treatment of various human diseases by transmission of exogenous nucleic acids into the nucleus of the specific cells of the patient. Considering the fact that genetic materials (free oligonucleotides, DNA and RNA) are easily to be degraded by serum nucleases in the blood when injected intravenously, it is of great significant to develop effective gene vectors to protect genetic materials from degradation. Comparing to the viruses and cationic liposomes, cationic polymers show several favorable characteristics such as enhanced bio-safety and biocompatibility, favorable biodegradability, high flexibility of

tans-gene size, high stability, low cost of synthesis and applicable scale-up to production. Therefore, nonviral polycationic vectors are receiving considerable attention as gene delivery systems. Among various cationic polymers, cationic HBPs that integrate a high density of amino groups with a three-dimensional branched structure and high molecular design flexibility, which greatly facilitates the therapeutic genes to arrive at the target tissues with high efficiency and specificity, would be very attractive for successful gene transfection. The specific advantages and disadvantages of several important classes of cationic HBPs, with emphasis on recently designed gene-delivery materials, will be described in more detail below.

### 3.2.1 Hyperbranched polyamines based gene vectors

Cationic polymeric vectors interact with negatively charged DNA in aqueous solution through electrostatic interactions to generate polyplexes, which can enhance cellular uptake efficiency and transfection efficiency of DNA or RNA. In the field of cationic HBP vectors, hyperbranched polyamines including hyperbranched polyethylenimine (HPEI) and hyperbranched polypropylenimine (HPPI) are very promising for effective gene transfection because of their high positive charge density. Especially, HPEI displays superior transfection efficiency in various cell lines and tissues and has been known as the gold standard among nonviral polymeric gene delivery systems. HPEI-based gene vectors have several attractive characteristics that are beneficial to gene delivery. Firstly, due to the existence of numerous terminal primary amines, they can condense nucleic acids sufficiently into nanosized compactable particles through electrostatic interaction at physiological pH, which facilitates cellular uptake. Furthermore, the plenty of tertiary amine groups present in the HPEI structure endow them with a strong proton buffer capacity, which can prevent polyplexes from lysosomal degradation and enable them to escape into the cytoplasm. This process is called as “proton-sponge effect”. While HPEI offers these advantages, there are still several obstacles associated with gene delivery, especially high cytotoxicity and a lack of cell specificity, all of which seriously limit its further application.

In the past decade, with an aim to reduce the cytotoxicity and improve the *in vivo* gene delivery efficiency of HPEI-based delivery system, the design of biocompatible and biodegradable HPEI vectors presents two main trends. Firstly, the surface of HPEI is modified with functional small molecules, hydrophilic or biodegradable polymers through covalent or noncovalent approaches in order to shield some positive charges and improve serum stability.<sup>117-119</sup> Various biocompatible polymers have been employed to modify HPEI, such as PEG, natural glucose polymers, proteins, peptides, etc. In addition, the functional small molecules such as aliphatic lipids, targeting groups have been conjugated to the surface of hyperbranched polyamines in order to

increase the specific uptake efficiency and transfection efficiency. Correspondingly, the transfection efficiencies are enhanced to different degrees over the unmodified hyperbranched polyamines, depending on types of functional groups and degree of substitution. In a few cases, the transfection efficiencies of these modified hyperbranched polyamines approximated or exceeded those of 25 kDa HPEI standard control. For instance, peptide-modified HPEIs show great advantages because they improve the biocompatibility and are easily metabolized, making various combinations possible.<sup>120</sup> Wu and coworkers designed a series of histidine-based peptide modified HPEI (25 kDa) for gene transfection studies (Fig. 12A).<sup>121</sup> Compared with HPEI, these polymers showed high transfection efficiency and enhanced cell survival to the human embryonic kidney cell line (HEK 293FT). More importantly, transfection of human adipose stromal cells (ASCs), dermal fibroblasts, and cardiac progenitor cells (CPCs), which are known to be highly resistant to gene transfection, with the modified HPEI demonstrated high transfection efficiency. Another important advantage of using these polymers is that all transfections are convenient as they are carried out in the same medium where cells are grown in the presence of serum and antibiotics, avoiding frequent changes of the medium before, during, or post transfection. The results demonstrated that L-Carnosine-HPEI and Boc-L-Carnosine-HPEI displayed great potential as gene delivery agents based on their reduced production of reactive oxygen species (ROS) and consistently high transfection efficiency in all cell types among six complexes tested.

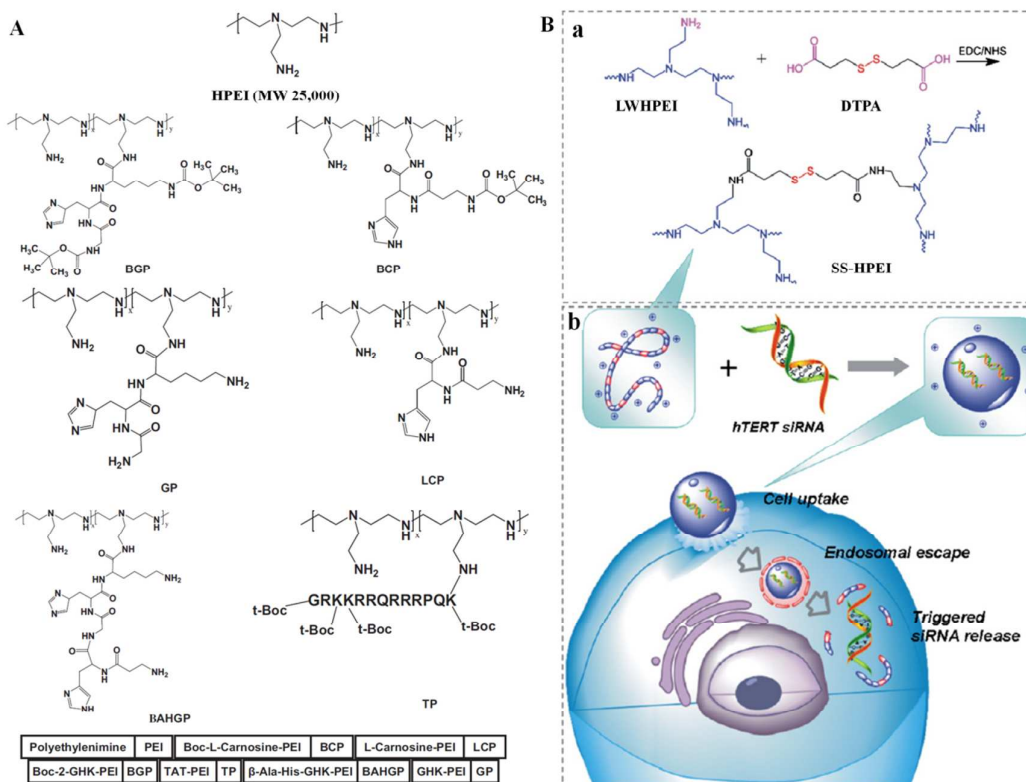


**Fig. 12** (A) Schematic diagram of the structures of the basic polymer HPEI (top) and the peptide-modified HPEI. The peptide groups were linked to the primary amine group of HPEI; (B) Schematic representation of bioreducible HPEI: (a) synthesis of bioreducible HPEI (SS-HPEI), (b) schematic illustration of SS-HPEI-mediated intracellular siRNA delivery. Reproduced with permission from ref. 121 and 127. Copyright 2011 and 2012, Elsevier.

Secondly, the biodegradable linkages such as reducible disulfide bonds or ester conjugation are incorporated into the backbone of hyperbranched polyamine.<sup>122</sup> The introduction of biodegradable linkages in the backbone of hyperbranched polyamines not only facilitates the controlled release of DNA in cytoplasm, but also helps to reduce cytotoxicity by avoiding accumulation of high molecular weight cationic polymers inside the cells. Take reduction type for an example, biodegradable HPEIs containing the disulfide bond can be polymerized by monomers containing disulfide bonds or by crosslinking low molecular weight HPEI segments with reducible disulfide crosslinkers. Some groups have reported that cross-linking of low molecular weight HPEI (e.g., 800 and 1800 Da) with different disulfide-containing cross-linking agents (e.g., 3'-dithiobispropanoic acid (DTPA), dithiobis(succinimidylpropionate) (DSP), and dimethyl-3,30-dithiobispropionimide-2HCl (DTBP)) resulted in considerably enhanced *in vitro* transfection efficiency as compared with the parent low molecular weight HPEI, with transfection activity approaching or in some cases

over that of 25 kDa HPEI control.<sup>123-127</sup> As an example, Wang and coworkers prepared bioreducible disulfide bond-containing HPEI (SS-HPEI) by chemical coupling of the DTPA and the low molecular weight HPEI (800 Da) via an EDC/NHS activation reaction (Fig. 12B-a), which was employed as siRNA carrier for intracellular delivery of the human telomerase reverse transcriptase (hTERT) siRNA *in vitro* and *in vivo*.<sup>127</sup> It was found that the SS-HPEI could strongly condense siRNA into nano-sized and positively-charged complexes, but it was able to release siRNA sufficiently in a reducing environment. *In vitro* transfection experiments demonstrated that the complexes of SS-PEI/siRNA were able to transfect HepG2 cells efficiently and revealed relatively low cytotoxicity. This might be due to the fact the SS-HPEI was cleaved under intracellular reducing environment, which further facilitated intracellular siRNA release (Fig. 12B-b). Importantly, *in vivo* results showed that the complexes of SS-PEI/siRNA could inhibit HepG2 tumor growth in a xenograft mouse model and exhibited almost no adverse effect on liver and kidney functions.

### 3.2.2 Hyperbranched polyamidoamine (HPAMAM) based gene vectors

Among various types of HBP systems explored for gene delivery, HPAMAMs have been shown to be a versatile class of polymers for gene delivery owing to their properties including biocompatibility, biodegradability, generally low hemolytic activity and peptide-mimicking properties. They have very similar unit structure to the classic hyperbranched polyamines but possess much lower cytotoxicity. As an alternative to hyperbranched polyamines, various HPAMAM-based HBPs have been synthesized and investigated for gene transfer. In general, three kinds of strategies have been employed to construct safe and efficient HPAMAM-based gene vectors.

First of all, the branching architecture of HPAMAM has been investigated and optimized to improve gene transfection efficiency.<sup>128-131</sup> The HPAMAM possesses compact and globular structures with plenty of various amino groups, which influence the ability to complex plasmid DNA (pDNA) and cationic polymer. The DB of the highly branched cationic polymers determines the ratio of primary, secondary and tertiary amines, which have a remarkable influence on the condensation ability, the escape of polyplexes from lysosome, the cytotoxicity and the transfection efficiency. PAMAM dendrimers have lower transfection efficiency than their degraded derivatives with a lower DB, however, Engbersen and coworkers showed that polyplexes from HPAMAM yielded higher transfection efficiency in comparison with that from their linear analogs.<sup>130</sup> The results also demonstrated that HPAMAM with disulfide linkages in the main chain could be enhanced by the presence of serum. Interestingly, this kind of HPAMAM displayed significantly lower cytotoxicity and higher gene expression in DNA transfection tests with COS-7 cells than that of linear PEI (22 kDa). Considering the important effects of the topological structures on the

gene transfection efficiency, Zhu and coworkers prepared a series of cationic PAMAMs with similar compositions and molecular weights but different branched architecture (DBs from 0.4 to 0.44) for gene delivery (Fig. 13A).<sup>131</sup> It was found that the DNA condensation capabilities of HPAMAMs could be readily adjusted by only altering the branched architecture of polycations as shown in Fig. 13B. With the increase in branched architecture, the cytotoxicity of PAMAMs reduced because of the small hydrodynamic size and compact spatial structure. In contrast, the complexing capabilities of PAMAMs and DNA were strengthened, which could be attributed to the more and more compact structure and the enhancement of primary and tertiary amino groups. Correspondingly, the gene transfection efficiency was improved by more than three orders of magnitude. The results of this study indicate that the gene delivery can be readily regulated by only changing the branched architecture of polycations. This study demonstrates the importance of branched architecture of cationic HBPs in regulating gene expression and cell toxicity, which provides a new strategy to promote cationic HBPs as nonviral gene vectors with good transfection efficiency. Although great progress has been achieved, the relationship between DB of cationic polymers and transfection efficiency is still not very clear because the synthesis of cationic HBPs with the similar chemical composition and molecular weights but different DBs is difficult.

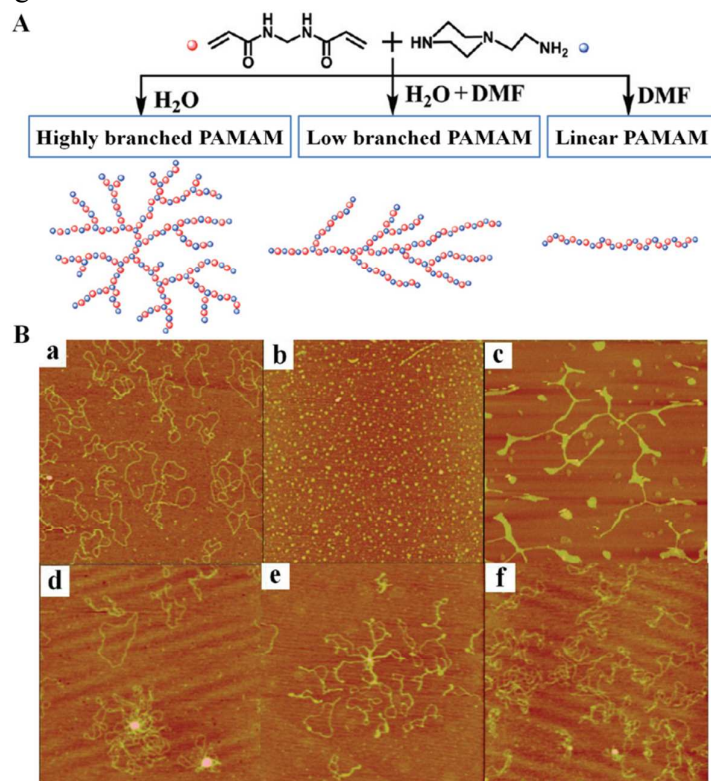


**Fig. 13** (A) Synthesis route of different branched PAMAMs. Highly branched PAMAM was obtained in pure water, low branched PAMAM was obtained in mixture solvent of water and

DMF and linear PAMAM was obtained in pure DMF. (B) AFM images of DNA condensation by various branched PAMAMs. DNA was binding by polymers at  $N/P = 2$ . Each image represents a  $2 \times 2 \mu\text{m}$  scan. (a) Pure plasmid DNA in Hepes buffer. (b-f) DNA is binding by various PAAs with different branched architecture ( $DB = 0.44, 0.31, 0.21, 0.11, \text{ and } 0.04$ , respectively). Reproduced with permission from ref. 131. Copyright 2010, American Chemical Society.

Secondly, various chemical functionalities have been introduced into the periphery of HPAMAMs in order to lower the cytotoxicity and improve the gene transfection activity. The effects of terminal groups on transfection efficiency have been investigated by Gao and co-workers recently.<sup>132</sup> They synthesized phenylalanine-modified HPAMAM by conjugating phenylalanine to the terminal amino groups to improve its bioactivity. Interestingly, *in vitro* transfection showed that the resulting transgene expression of phenylalanine-modified HPAMAM was almost one order of magnitude higher than HPEI. Zhu and coworkers reported a series of  $\beta$ -CD-functionalized HPAMAMs, which show lower cytotoxicity and significantly enhanced photoluminescence in comparison with HPAMAMs.<sup>133</sup> Very recently, Liu and coworkers investigated the performance of HPAMAMs with the same tertiary amino cores and different terminal groups for gene delivery.<sup>134</sup> They found that the difference in the terminal structures resulted in a definite distinction in terms of biophysical properties and transfection efficiency *in vitro*.

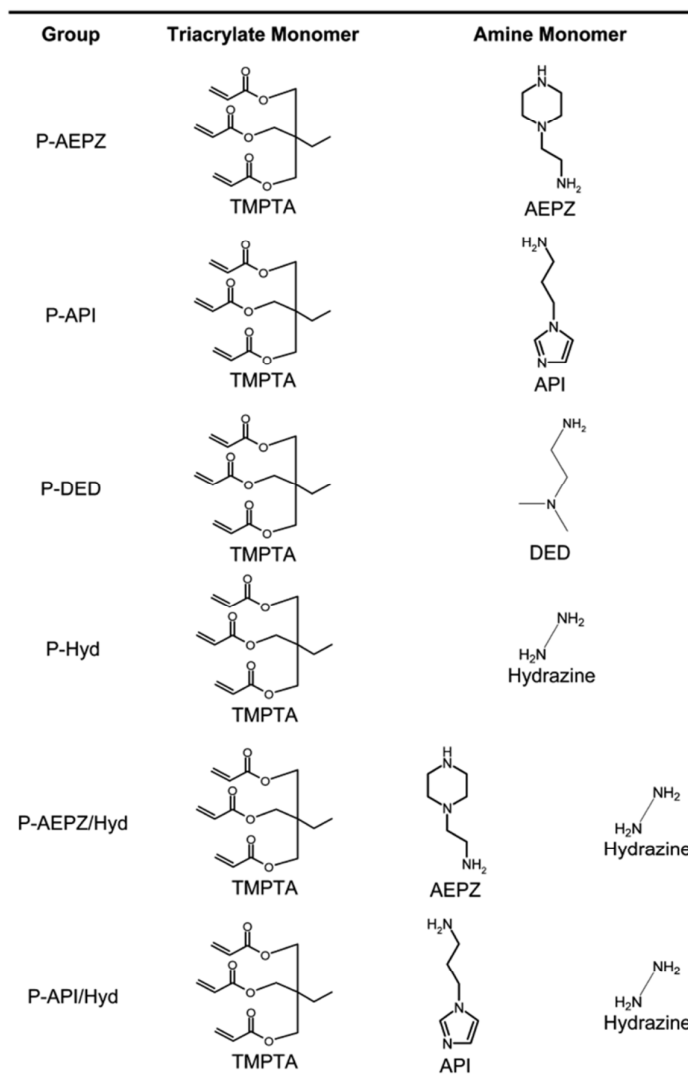
Thirdly, introducing biodegradable linkages such as reducible disulfide bonds or ester groups in HPAMAM backbone facilitates enhancing transfection efficiency and reducing cytotoxicity.<sup>135,136</sup> As an example, Oupický and coworkers designed and synthesized a series of reducible HPAMAMs with *N,N*-dimethylaminodipropylenetriamine and two bisacrylamide monomers *N,N'*-hexamethylene bisacrylamide and *N,N'*-cystamine bisacrylamide through Michael addition copolymerization as nonviral gene delivery vectors.<sup>136</sup> The results demonstrated that disulfide content in HPAMAMs was well-tuned by varying the feed molar ratio of the monomers, which determined ease of DNA release. These reducible HPAMAMs with optimized formulations showed lower cytotoxicity and significantly increased transfection activity, almost 200-fold higher than that of control HPEI polyplexes, which represent a promising class of gene delivery vectors.

### 3.2.3 Hyperbranched poly(ester-amine) based gene vectors

An important drawback of hyperbranched polyamines and HPAMAMs as gene delivery carriers is their relatively high cytotoxicity. Even upon modification, their toxicity is still problematic. In order to reduce cytotoxicity, while preserving sufficient transfection efficiency, hyperbranched poly(ester-amine)s (HPEAs) have been

developed as hyperbranched polyamine analogues which are readily biodegradable. Similar to HPAMAMs, HPEAs possess high density of primary amines for DNA condensation and tertiary amines for the proton-sponge effect. Meanwhile, they exhibit excellent biodegradability due to the hydrolytically degradable ester groups. Thus, HPEAs are promising for effective gene delivery because of their reduced cytotoxicity, their ability for controlled DNA release within the cells and great potential for structural diversity. Park and coworkers reported a cationic HPEA with biodegradable ester backbone, primary amine at the periphery, and tertiary amine groups in the interior.<sup>137</sup> This biodegradable cationic polymer was minimally toxic and could condense negatively charged DNA. Its transfection efficiency was relatively lower than those of HPAMAM or HPEI, but was increased over 10-fold compared with that of poly[ $\alpha$ -(4-aminobutyl)-L-glycolic acid].<sup>138</sup> Subsequently, Liu and coworkers prepared a kind of biodegradable HPEA containing primary, secondary and tertiary amines simultaneously through the Michael addition polymerization of trifunctional amine monomers 1-(2-aminoethyl)piperazine with 1,4-butanediol diacrylate.<sup>139</sup> The different types of amine groups may play various roles such as the condensation of DNA and improving the pH-buffering ability to facilitate escape of vectors from lysosomes. This kind of HPEA displayed low cytotoxicity and high transfection efficiency at a polymer/DNA weight ratio of 30:1 comparable to those of HPEI. Feijen and coworkers also reported a series of water-soluble and degradable gene carriers based on HPEAs containing primary, secondary and tertiary amino groups, which exhibited high buffering capacities between pH 5.1 and 7.4 and effectively condensed plasmid DNA into positively charged complexes with the diameters of 94-135 nm.<sup>140</sup> More importantly, their transfection efficiency was higher than or comparable to that of PEI and PDMAEMA. Furthermore, these HPEAs revealed no or low cytotoxicity. These results demonstrated that HPEAs could be applied as safe and efficient gene delivery carriers.

**Table 1** HPEA composition and structures of the triacrylate and amine monomer building blocks. Reproduced with permission from ref. 143. Copyright 2010, American Chemical Society.



To maximize the gene transfection efficiency and lower cytotoxicity, optimized HPEA structures have been reported by changing the terminal groups, the amine type and the ester monomer. Liu and coworkers designed and synthesized three kinds of HPEAs with the same core containing tertiary amines and different types of amines at the periphery to investigate the effects of the terminal amine type on the gene transfection properties of HPEAs.<sup>141</sup> The results demonstrated that the terminal group of the HPEAs had a negligible effect on the hydrolysis rate, and the internal spatial structure determined the hydrolysis rate. Compared with HPEI 25 kDa, these HPEAs exhibited much lower cytotoxicity. It should be noted that all the HPEAs showed high DNA transfection efficiency similar to HPEI 25 kDa in HEK293, HepG2, and COS7 cells regardless of the terminal amine type. It was clearly revealed that the terminal amine type showed insignificant effects on the hydrolysis, cytotoxicity and *in vitro* DNA transfection efficiency of HPEAs. Mikos and coworkers prepared a series of

HPEAs with the same amine monomer, 1-(2-aminoethyl)piperazine, and different types of triacrylate monomers to evaluate the effects of hydrophilic spacer lengths on HPEAs properties relevant for the gene delivery process.<sup>142</sup> It was found that the introduction of hydrophilic spacers into the backbone of HPEAs decreased polymer cytotoxicity and increased hydrolytic degradation rate. These alterations of the triacrylate monomer chemistry, however, reduced charge density of HPEAs, which affected DNA condensation, endosomal escape, and polymer degradation. In addition, variations of the hydrophilicity of the triacrylate monomers did not have a considerable effect on the dissociation properties of the HPEAs. In the following work, the same group synthesized different HPEAs with a single triacrylate monomer, trimethylolpropane triacrylate (TMPTA), and different amine monomers by Michael addition polymerization to study the effects of amine basicities on gene delivery parameters of HPEAs (Table 1).<sup>143</sup> By altering the amine monomers for HPEA synthesis, the amine group density, the basicity and buffering capacity of the HPEAs could be changed and controlled, which significantly influenced the gene delivery process of the polymers. The results revealed that HPEAs with amines that dissociated above pH 7.4 were capable of complexing pDNA. The HPEA with the most amines dissociating above physiological pH, formed stable polyplexes with high potential and decreased hydrodynamic size which showed higher transfection efficiency than HPEI. In addition, the unprotonated amines could autocatalyze degradation of the HPEAs but did not predetermine the polymer degradation rate. All synthesized HPEAs exhibited low cytotoxicity, which could be applied at high N/P ratios (where N and P are the number of polymer nitrogen and DNA phosphorus atoms, respectively) for effective pDNA complexation and cellular transfection.

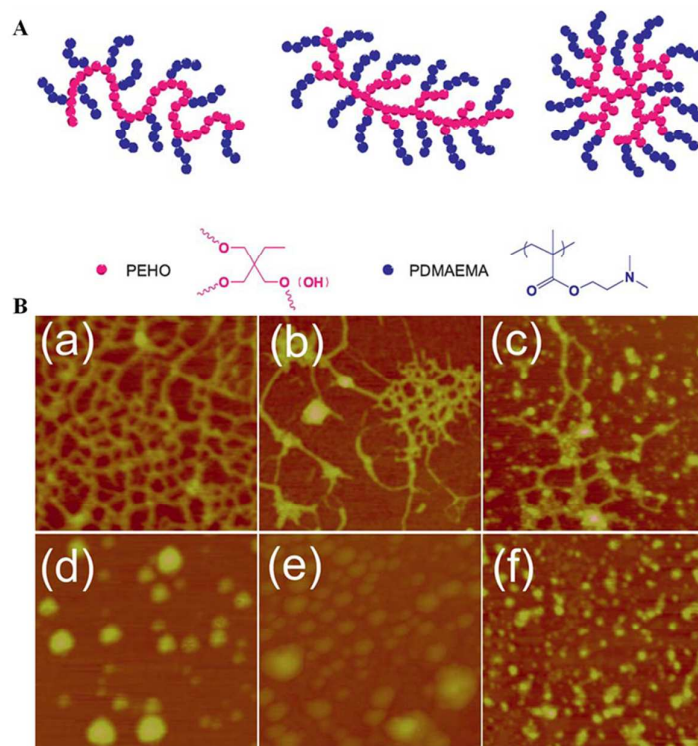


**Fig. 14** (A) Schematic representation of the different topological architectures of PEHO-*g*-PDMAEMA copolymers. (B) AFM images of copolymer/pDNA complexes by D<sub>0.07-4</sub> (a and d), D<sub>0.35-4</sub> (b and e) and D<sub>0.48-4</sub> (c and f) at N/P = 1 (a-c) and 10 (d-f). All images were obtained with complexes deposited onto fresh mica surface. Each image represents a 1 × 1 mm scan. Reproduced with permission from ref. 150. Copyright 2012, Royal Society of Chemistry.

Another important kind of poly(ester-amine)s is PDMAEMA-based polymers containing protonated tertiary amine groups at physiological pH, which have exhibited excellent transfection efficiency. Hennink and coworkers have performed the pioneering work on PDMAEMA-based polymers and reported that these polymers displayed high gene transfection efficiency, which might be attributed to their endosomal destabilizing property and ability to release DNA into cytosol.<sup>144,145</sup> Nevertheless, their high cytotoxicity had hindered further application. Up to now, several hyperbranched PDMAEMAs have been reported to reduce their cytotoxicity while trying to retain their high gene transfer efficiency. Davis and coworkers prepared biodegradable disulfide-based hyperbranched PDMAEMA through reverse addition-fragmentation chain transfer (RAFT) polymerization.<sup>146</sup> The hyperbranched PDMAEMA could package DNA efficiently to yield DNA polyplexes via multivalent electrostatic interactions. Under cellular reducing conditions, inherently biodegradable polyplexes could be cleaved, thus enhancing gene release and subsequent generating small molecular weight oligomer chains with low cytotoxicity.

Freitag and coworkers studied PDMAEMAs with three different structures (linear, highly branched, and star-shaped) for gene delivery, and linear and branched PEI were used as the control.<sup>147</sup> They found that highly branched PDMAEMA only had a slight increase in transfection efficiency in comparison with its linear counterpart but efficiency was considerably lower than branched PEI standard. In contrast, Wang and coworkers synthesized the hyperbranched DMAEMA/ethylene glycol dimethacrylate (EGDMA) copolymer which showed higher transfection ability than linear PDMAEMA and was comparable to the HPEI and the SuperFect<sup>®</sup> dendrimer but with lower cytotoxicity.<sup>148</sup> The much greater comparative transfection ability shown by hyperbranched DMAEMA/EGDMA copolymer over previous report may be due to the optimizing molecular weight and DB. Recently, Thurecht and coworkers incorporated poly(ethyleneglycol monomethylether methacrylate) (PEGMA) into the surface of the hyperbranched PDMAEMA in order to reduce the cytotoxicity by shielding partially the positive charges.<sup>149</sup> However, the polymer became less effective at the cell uptake and DNA condensation presumably owing to the so-called “stealth” properties of PEG. When the polycation was functionalized with folic acid, the DNA/polycation complex showed enhanced cell uptake at the higher N/P ratios due to the interaction between folic acid ligands and overexpressed folic acid receptors on the cell surface of tumor cells. To investigate structure-transfection property relationships, Zhou and coworkers prepared a series of amphiphilic hyperbranched copolymer PEHO-g-PDMAEMAs with the hydrophobic DB-variable PEHO (PEHO means poly(3-ethyl-3-(hydroxymethyl)-oxetane)) cores and length-variable PDMAEMA arms for gene transfection.<sup>150</sup> Compared with HPEI and PDMAEMA homopolymers, this copolymer exhibited lower cytotoxicity, higher buffering ability and transfection efficiency. The results demonstrated that the gene transfection efficiency of the copolymers was enhanced with the increase of the DB of PEHO cores and such a DB-dependence may be explained by the self-assembly ability of the polymers with pDNA (Fig. 14).

#### 3.2.4 Hyperbranched poly(ether-amine) based gene vectors

The interest in the potential of hyperbranched poly(ether-amine)s for use in gene delivery is motivated by their improved water solubility and biocompatibility. For example, low toxicity and biocompatibility of HPG are promising matrixes for developing novel functional derivatives through proper functionalization of their surface groups, which could be employed as gene delivery systems.<sup>29,151-153</sup> Kizhakkedathu and coworkers incorporated quaternary or tertiary amino groups onto the surface of PEG-functionalized HPG to form cationic poly(ether-amine)s, which combined the biocompatibility of polyglycerol and transfection capacity of HPEI.<sup>151</sup>

These poly(ether-amine)s exhibited good biocompatibility as confirmed by its negligent effects on hemolysis, erythrocyte aggregation, platelet activation, complement activation and coagulation. Moreover, they showed much lower cytotoxicity than HPEI and higher degrees of quaternization resulted in higher cytotoxicity. The ethidium bromide displacement assay revealed that these poly(ether-amine)s had high affinity to DNA and was able to condense DNA to highly compact, stable, water soluble nanoparticles with the size of 60-80 nm. Interestingly, the results showed that quaternization of amines had insignificant influence on DNA binding and should be avoided because of the increased cytotoxicity. Tziveleka and coworkers also prepared a series of HPG partially functionalized with quaternary or tertiary amino groups to evaluate the effects of amino type and numbers to gene transfection.<sup>153</sup> It was found that all the investigated polymers had low cytotoxicity to mammalian cells. In contrast to the above results, only the selected quaternized polymers exhibited high transfection efficiency comparable to that of HPEI. The introduction of tertiary amino groups on HPG did not improve the transfection of the ineffective parent polymer. Furthermore, altering the degree of quaternization of the HPG would affect the transfection efficiency. Therefore, the feasibility of application of these polymers for gene delivery still remains to be investigated. Recently, Zhu and coworkers reported one kind of charge-tunable supramolecular poly(ether-amine)s based on host-guest interactions between primary- or tertiary amine-modified  $\beta$ -CD derivatives (per-6-amino- $\beta$ -CD with seven primary amines and per-6-dimethylaminoethyl- $\beta$ -CD with seven tertiary amines) and an AD-modified HPG for gene delivery (Fig. 15A).<sup>29</sup> Through altering the molar ratios of these two cationic  $\beta$ -CD derivatives, the surface charge of the resulting poly(ether-amine)s could be efficiently regulated and optimized. *In vitro* transfection showed that these poly(ether-amine)s had comparable transfection efficiency and lower cytotoxicity in comparison with 25 kDa HPEI. Meanwhile, the gene transfection efficiency of these supramolecular poly(ether-amine)s generally improved with increased charge density of poly(ether-amine)s due to the enhanced buffer capacity (Fig. 15B). Interestingly, the transfection efficiency of the poly(ether-amine) polyplexes is almost independent of the N/P ratio, whereas that of the HPEI polyplexes is apparently determined by the N/P ratio probably because of its high cytotoxicity.

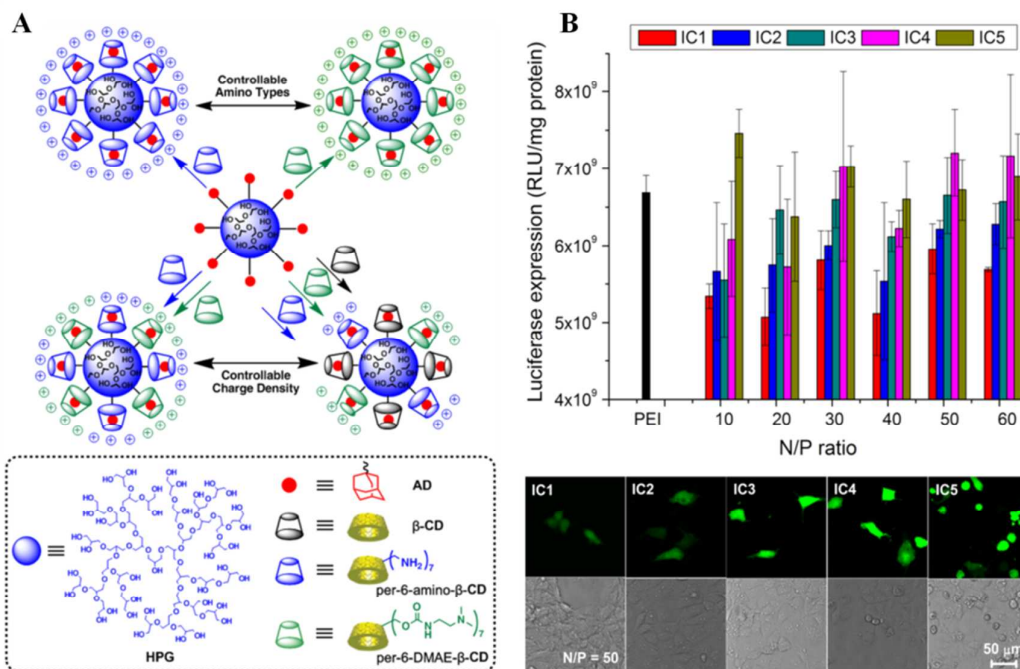


**Fig. 15.** (A) Preparation of charge-tunable supramolecular poly(ether-amine)s via host-guest interactions. (B) Luciferase expression (top) and green fluorescent protein expression (bottom) of these supramolecular poly(ether-amine)s in COS-7 cells. Reproduced with permission from ref. 29. Copyright 2011, Royal Society of Chemistry.

Besides the HPG-based cationic polymers, the poly(ether-amine)s based on hyperbranched polysiloxysilane (HBPS) have also been reported as gene delivery carriers. Lee and coworkers prepared the amphiphilic HBPS containing terminal carboxylic acid and quaternary amino groups, which was used to investigate nonviral gene delivery.<sup>154</sup> The results suggested that the cationic HBPS nanoparticles possessed excellent ability to complex pDNA, which offered an important pre-requisite for their use as gene delivery vector. The ability of HBPS to form complexes was improved with increasing amounts of quaternary amine groups on the nanoparticles. For gene transfection, it is worth noting that the HBPS-CN30:70 nanoparticles (prepared from a mixture of 70 mol% HBPS-N<sup>+</sup>(CH<sub>3</sub>)<sub>3</sub>I<sup>-</sup> and 30 mol% HBPS-COOH) exhibited the highest transfection efficiency compared with pure HBPS-N<sup>+</sup>(CH<sub>3</sub>)<sub>3</sub>I<sup>-</sup> and HBPS-COOH, which might be due to the sufficient stability, suitable size, and high uptake efficiency of HBPS-CN30:70 nanoparticles.

### 3.2.5 Hyperbranched polycation and metallic/inorganic nanoparticles as gene vectors

During the past years, the hybrids of hyperbranched polycation and metallic/inorganic nanoparticles have been developed and employed as nonviral gene vectors.<sup>155</sup> The

hybrids integrate the characteristic properties of metallic/inorganic nanoparticles and HBPs. Compared to cationic HBPs carriers, hybrid nanoparticles are more stable with respect to physical stresses and not subject to microbial attack. Various surface modifications have been used to improve the transfection efficiency of nanoparticles. Some inorganic nanoparticles, such as gold nanoparticles, silica nanoparticles, carbon nanotubes, QDs, and magnetic nanoparticles, have been modified with HBPs in different ways to develop effective gene delivery systems.<sup>156,157</sup> Kim and coworkers grafted low molecular weight HPEI ( $M_w$  1.8 kDa) on the outer surface of the silica nanotubes (SNT) and found this hybrid material could easily condense pDNA into polyplexes and transport the cargo into the cells efficiently.<sup>158</sup> The results demonstrated that conjugation of the low molecular weight HPEI to SNT increased its effective molecular weight, enhanced DNA binding and condensation, and therefore improved transfection efficiency. More interestingly, the hybrid material of HPEI and SNT exhibited comparable efficiency to HPEI 25 kDa but had considerably low cytotoxicity. Klivanov and coworkers reported gold nanoparticles (GNPs) conjugated with HPEI (2 kDa) as gene vectors for the delivery of pDNA into COS-7 cells in the presence of serum *in vitro*.<sup>159</sup> It was found that the hybrid nanoparticles showed six times higher transfection efficiency compared with HPEI 25 kDa. Importantly, the efficiency of these nanoparticles could be enhanced further by complex formation with hydrophobic N-dodecyl-HPEI 2 kDa, which revealed the synergetic action of two modified low molecular weight HPEIs. Zhu and coworkers fabricated a series of size-controlled magnetic iron oxide nanocrystals in the presence of ferrous salts and HPEI as magnetic nonviral gene vectors (Fig. 16A).<sup>160</sup> Various magnetic iron oxide nanocrystals with different sizes were prepared using HPEI as the nanoreactors and stabilizers. Interestingly, as shown in the Fig. 16B, the resulting iron oxide/HPEI nanocomposites showed significantly higher transfection efficiency compared with that for standard HPEI transfection. Moreover, the transfection efficiency of these nanocomposites was enhanced with the increasing mean size of magnetic iron oxide. When a pure HPEI transfection enhancer was added into these nanocomposites, the magnetofection efficiency of all prepared nanocomposites with various sizes in COS-7 cells under a magnetic gradient field increased greatly, and the size of magnetic iron oxide displayed an insignificant effect on the transfection properties.

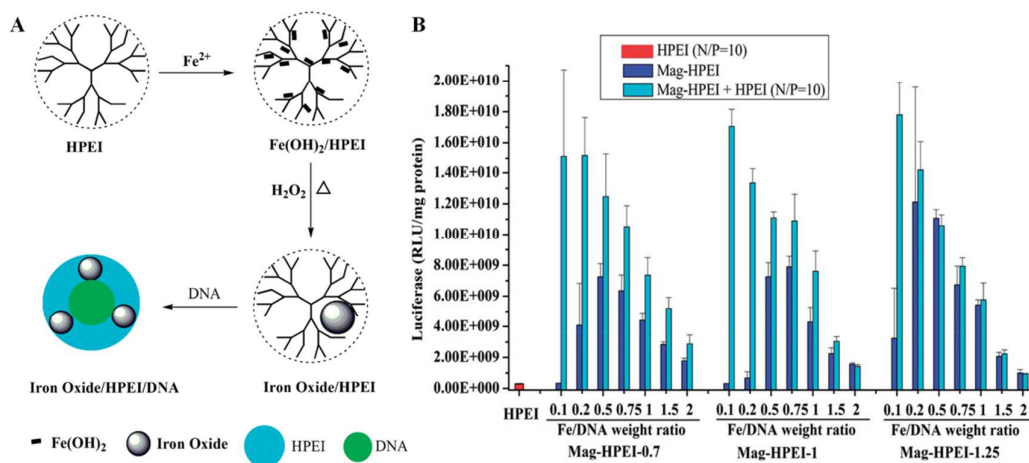


**Fig. 16** (A) Schematic representation of size-controlled preparation of iron oxide nanocrystals within HPEI and condensation of DNA by the resulting iron oxide/HPEI nanocomposites; (B) Magnetofection efficiency of HPEI, Mag-HPEI-0.7, Mag-HPEI-1, and Mag-HPEI-1.25 in COS-7 cells in the absence (blue bars) and in the presence (cyan bars) of pure HPEI compared with that of HPEI standard transfection (red bars). The luciferase activity was reported as relative light units (RLU) normalized by the mass of total protein in the cell lysate. Each value represents the mean  $\pm$  SD of three determinations. (The average mass contents of iron oxide NCs in samples Mag-HPEI-0.7, Mag-HPEI-1 and Mag-HPEI-1.25 estimated by TGA are about 20.5%, 21.4%, and 22.6%, respectively.) Reproduced with permission from ref. 160. Copyright 2012, Royal Society of Chemistry.

### 3.3 HBPs for protein delivery

In recent years, the application of pharmaceutically active peptides and proteins for the treatment of various disorders, including cancer, hormone deficiency, anaemia and metabolic diseases, is developing rapidly.<sup>161</sup> A great challenge in the administration of protein drugs is their often poor hydrolytic stability and low bioavailability.<sup>162</sup> They can easily undergo inactivation by physical and chemical denaturation or enzymatic degradation during the process of formulation, storage or delivery. To combat these limitations in the protein administration, various systems have been developed. Polymeric systems have been explored for protein delivery and showed great potential because they can increase the protein stability, improve the bioavailability, enhance the absorption across the biological barriers, and prolong the protein residence in the bloodstream. Furthermore, some polymers have been found to facilitate the protein internalization into cells or improve their immunogenic potential as immune adjuvant in vaccination protocols. In particular, HBPs show several advantages compared to corresponding linear polymers, such as chemical stability, good solubility, plenty of functional end-groups and controllable surface functionality, which are powerful tools for the construction of protein carriers.

Zhang and coworkers prepared copolymer nanoparticles formed by self-assembly of polylactic acid functionalized HPG (HPG-*star*-PLA) for bovine serum albumin (BSA) delivery.<sup>163</sup> The results revealed that the loading capacity and association efficiency of HPG-*star*-PLA were up to 23% and 86%, respectively, and the protein release was well-controlled by accurately adjusting the characteristics of HBPs. Importantly, the physicochemical integrity of released BSA was well preserved over 4 days. Very recently, the same group reported  $\beta$ -CD functionalized HPG (HPG-g-CD) for enhancing the nasal transport of insulin in rats.<sup>164</sup> The insulin was encapsulated into the HPG-g-CD nanoparticles efficiently with the size ranging from 198 to 340 nm with a positive charge. The *in vivo* evaluation demonstrated that insulin-loaded HPG-g-CD nanoparticles could cross the nasal mucosal epithelia and significantly decrease the blood glucose concentrations, which suggested that HPG-g-CD nanoparticles showed a promising potential for nasal insulin delivery. Wu and coworkers fabricated the self-assembled micelles from hyperbranched poly[(ester-amine)-*co*-(D,L-lactide)] (HPEA-*co*-PLA) copolymers as protein carriers for BSA delivery.<sup>165</sup> The BSA-loaded micelles displayed enhanced encapsulation efficiency and the structure of BSA was retained during the release process.

In addition to micro- and nanoparticles, biocompatible HBPs have been evaluated as a way to form colloidal formulations for protein delivery. These HBPs can be chemically or physically associated with proteins under physiological conditions to generate supramolecular nanocomposites with suitable physicochemical and biopharmaceutical properties. HPG shows excellent solubility and stability, good biocompatibility and low toxicity and immunogenicity, which is an outstanding choice for preparing protein-polymer bioconjugates. Frey and coworkers reported hyperbranched-linear HPG-PEG heterotelechelic consisting of a linear PEG block and a HPG block for noncovalent bioconjugation of biotin.<sup>166</sup> This kind of HBPs has remarkable advantages for introduction of a variety of functional groups and also covalent bioconjugation with other proteins and peptides. Recently, Klok and coworkers attached BSA and lysozyme into the HPG and hyperbranched-linear polymer HPG-PEG with the squaric acid mediated coupling strategy, and subsequently used for protein delivery.<sup>167</sup>

#### 4. HBPs for bioimaging and diagnosis

Bioimaging has become a hot topical research area to reveal the specific molecular pathways *in vivo* by combining sophisticated bioimaging probes with modern advanced modalities.<sup>168</sup> Over the past decades, a wide range of bioimaging probes have been developed in order to enhance detection sensitivity and selectivity. Compared to small-molecule probes, polymer-based bioimaging probes for the

diagnosis and treatment of disease are attracting more and more interest of researchers due to their enhanced stability, prolonged plasma half-lives, reduced cytotoxicity and improved targeting ability. Especially, hyperbranched polymeric probes have exhibited unique advantages in the diagnostic applications owing to their convenient synthesis, highly branched architectures and versatile functionalization. Until now, different kinds of bioimaging techniques, such as optical imaging, MRI, single photon emission computed tomography (SPECT), positron emission tomography (PET) and others have been successfully developed and are widely applied in medicine.<sup>23</sup> These techniques are of vital significance for locating tumors and investigating various biological processes. They each exhibit different characteristics regarding spatial resolution, tissue contrast, depth penetration, time requirements for imaging, and cost. Herein, we highlight the remarkable advances in hyperbranched polymeric probes for bioimaging and diagnosis.

#### 4.1. HBPs as fluorescent probes

Optical imaging is a powerful modality of biomedical imaging in preclinical research. In comparison with other modalities such as MRI or PET, optical imaging exhibits attractive features including high sensitivity, low cost, the possibilities to use multiplexed or activatable signals to assess biological activities, and selectable parameters (wavelength, intensity and lifetime).<sup>168</sup> Despite these unique advantages, its application in clinic is hindered due to light scattering, autofluorescence and absorption by tissues occurring in biological systems.<sup>169</sup> The combination of HBPs and optical bioimaging has resulted in the generation of HBP-based fluorescent probes, which provide unique advantages for physiological utilities and clinical implementations. In general, the HBP-based fluorescent probes can be divided into two classes. The first group is composed of complexes of HBPs and fluorescent materials such as small fluorophores, fluorescent proteins, inorganic fluorescent agents, and the other class is composed of fluorescent HBPs.

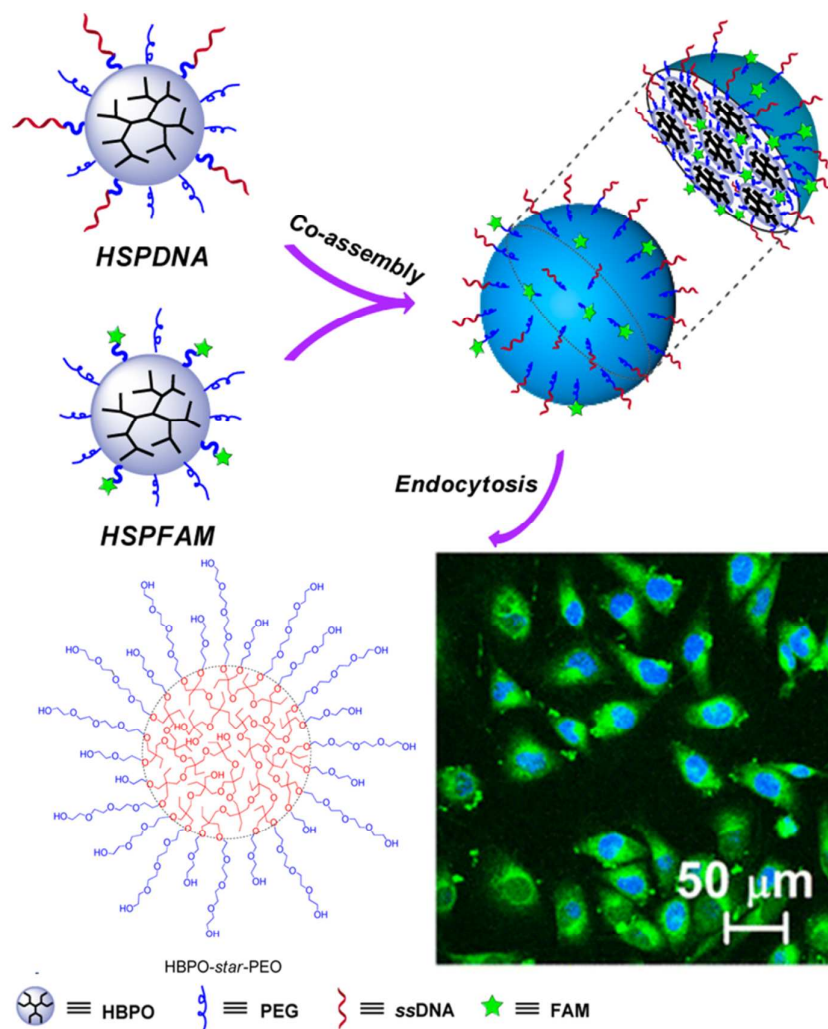


**Fig. 17.** Representation of the co-assembly of aptamer-functionalized and fluorescently functionalized hyperbranched copolymers and their cell imaging. Reproduced with permission from ref. 173. Copyright 2014, American Chemical Society

Organic fluorescent dyes have been widely used as fluorescent component of bioimaging probes. However, they suffer from some intrinsic disadvantages, such as low photobleaching thresholds, short half-life in blood, and poor membrane permeability to live cells, lack of specificity for their target cells, tissues, or organs.<sup>170</sup> Hyperbranched polymeric fluorescent probes, which consist of HBP-conjugated or HBP-encapsulated organic fluorescent agents, have been developed to overcome these problems. Benefiting from their multiple functional terminal groups, HBPs have been widely used for fluorescent bioimaging by fluorescent labeling with conventional dyes. Fluorescein isothiocyanate (FITC) is one of the most used fluorescent dyes. FITC was easily covalently linked to HBPs for bioimaging. Hyperbranched poly(sulfone-amine) (HPSA) was prepared and labeled with FITC by our group.<sup>171,172</sup>

Owing to its low cytotoxicity and good serum-compatibility, FITC-labeled HPSA has been used to study the cell entry mechanism and the subcellular distribution of HPSA. Recently, Zhou and coworkers reported that carboxyfluorescein(FAM)-functionalized HBP (HSPFAM) and aptamer-functionalized HBP (HSPDNA) were used for targeted cancer imaging (Fig. 17).<sup>173</sup> With a large amount of hydroxyl groups, HBP was covalently linked with FITC for imaging and DNA aptamer for targeting, respectively. By co-assembly of HSPFAM and HSPDNA, HSPFAM/HSPDNA mixed micelles with both imaging and targeting ability were obtained and applied for MCF-7 cells. Bright green fluorescence was observed in MCF-7 cells after cultured with the mixed micelles, while no significant fluorescence could be seen from cells treated with the control micelles, confirming the targeting and imaging ability of mixed micelles. Except FITC, other organic dyes have also been used to construct hyperbranched star copolymers and evaluate the cell internalization of HBPs in tumor cells through flow cytometry and confocal laser scanning microscope.<sup>174-176</sup> For example, DOX, one of the mostly utilized chemotherapy drugs, has been widely studied not only for its good pesticide effect, but also for its autofluorescence, which makes it a good candidate for bioimaging. DOX can be conjugated to HBPs to form an imaging probe. The fluorescence of DOX was used directly to measure the cellular uptake without additional markers. Except for the covalent conjugation, DOX can also be encapsulated into HBPs, forming imaging nanoparticles through non-covalent or host-guest interactions.<sup>57,104,177,178</sup>

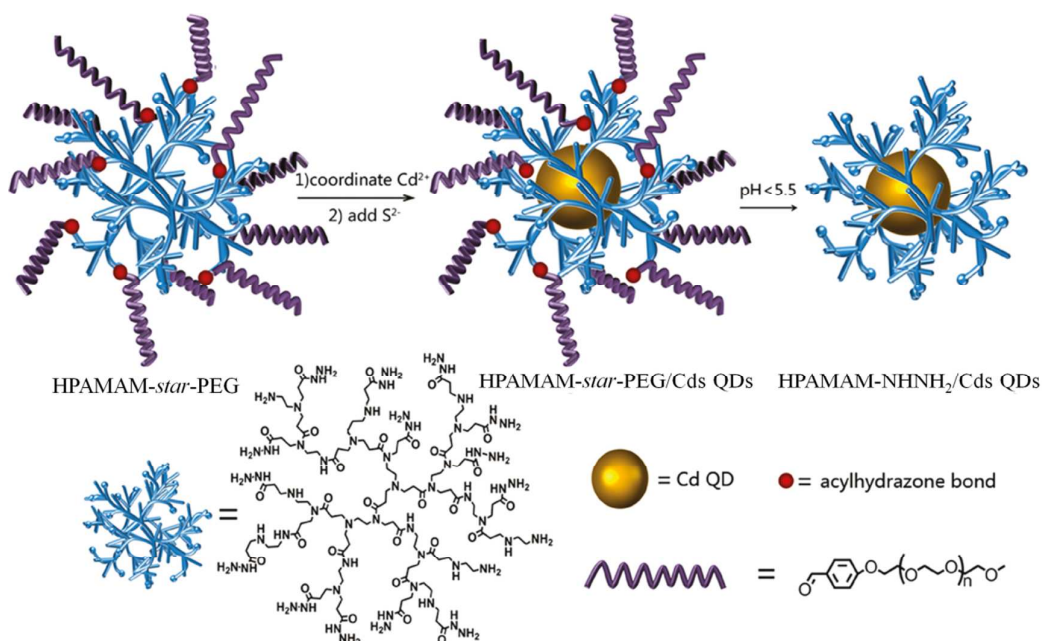


**Fig. 18** Preparation of HPAMAM-*star*-PEG/CdS QD nanocomposites with pH-sensitive properties. Reproduced with permission from ref. 180. Copyright 2010, American Chemical Society.

Inorganic fluorescent agents such as QDs, silicon nanoparticles and upconversion nanoparticles have also great potential for bioimaging and targeting biomarkers. Compared to organic dyes, inorganic fluorescent agents possess some distinguished features as they show resistant to photobleaching, permit attachment of numerous targeting ligands, and have much higher quantum yields.<sup>179</sup> HBPs can be used as nanoreactors to prepare QDs due to their internal nanocavities. Zhu and coworkers designed and synthesized double-hydrophilic multiarm hyperbranched polymer HPAMAM-*star*-PEG with dendritic HPAMAM core and many linear PEG arms connected by pH-sensitive acylhydrazone bonds, which was used as a nanoreactor for CdS QD synthesis in aqueous solution (Fig. 18).<sup>180</sup> The obtained HPAMAM-*star*-PEG and HPAMAM-*star*-PEG/CdS QD nanocomposites combined the excellent optical properties of CdS QDs with high stability, low cytotoxicity and pH-responsive characteristics of HBPs. The fluorescence intensity of HPAMAM-*star*-PEG/CdS QD nanocomposites was controlled by adjusting the pH value. When these nanocomposites were added into the culture medium of COS-7 cells (a cell line derived from kidney cells of the African green monkey), the fluorescence intensity in COS-7 cells increased greatly with increasing culture time, which might be attributed to the cleavage of acylhydrazone bonds and the subsequent departure of linear PEG chains from the HPAMAM core at the acidic environment in lysosomes. Therefore, these pH-responsive HPAMAM-*star*-PEG/CdS QD nanocomposites hold great potential as a novel fluorescent probe in cells. Besides, fluorescent silicon nanoparticles and upconversion nanoparticles can be modified with hydrophilic HBPs to form water-soluble nanoparticles of high colloidal stability, giving the ability for bioimaging *in vitro/in vivo*.<sup>181,182</sup>

Fluorescent HBPs including hyperbranched conjugated polymers (HCPs) and hyperbranched polyamines are also widely studied and used for optical imaging in biological systems, due to their unique properties.<sup>183-186</sup> For instance, amphiphilic conjugated HBPs have been prepared after grafting hydrophilic functional units. Zhu and coworkers reported that a multiarm HCP (HCP-*star*-PEG) containing a HCP core and many PEG arms could form unimolecular micelles, which further self-assembled into multimolecular micelles to enhance the emission greatly by preventing intermolecular aggregation and phase separation.<sup>187</sup> The emission-enhanced HCP-*star*-PEG micelles could be used to evaluate the cellular uptake of MCF-7 cell. The strong fluorescence was observed mainly in the cytoplasm of the cells when the cells were cultured in HCP-*star*-PEG for 2 h, illustrating the successful cellular imaging of multiarm HCPs. By incorporation ionic side chains onto the conjugated backbone, the conjugated HBPs form water-soluble conjugated polyelectrolytes, and the corresponding optical properties in aqueous media are comparable with the

organosoluble conjugated polymers, which allows them to interact with the various biological substances for pathophysiological diagnosis and enlarges the application fields of HCPs.<sup>188-190</sup> For example, by combining the benzothiadiazole unit, the uniform core-shell nanospheres based on hyperbranched conjugated polyelectrolytes showed blue to green fluorescence, which were readily used for bioconjugation and bioimaging.<sup>188,189</sup> Compared with HCPs, the fluorescence intensity of hyperbranched polyamines is relatively weak. To improve the fluorescence intensity of these hyperbranched polyamines for bioimaging, some strategies are being explored further.<sup>25,191</sup>

#### 4.2. HBPs as MRI contrast agents

MRI has been one of the most promising *in vivo* medical diagnostic techniques, since it possesses several attractive features such as noninvasiveness, no exposure to radiation, high spatial and temporal resolution, excellent penetration depths towards soft tissue, and the ability to extract physiological and anatomical information of soft tissue.<sup>192</sup> However, one major drawback of MRI is its inherent low sensitivity. To increase the sensitivity of MRI, a variety of contrast agents have been developed to shorten the spin-lattice relaxation time ( $T_1$ ) and spin-spin relaxation time ( $T_2$ ) of water protons over the last few decades.<sup>23</sup> Generally, the contrast agents can be divided into three categories:  $T_1$  contrast agents that mainly shorten  $T_1$  and lead to image brightening, using mostly paramagnetic gadolinium based contrast agent;  $T_2$  contrast agents that largely decrease  $T_2$  and result in image darkening with superparamagnetic iron oxide nanoparticles being the most important example; molecular imaging agents, where a unique molecular character is directly detected (e.g.  $^{19}\text{F}$  MRI). Nowadays, the low molecular weight contrast agents suffer from low contrast efficiency, nonspecificity, and fast renal excretion, which severely limit the application of these materials for molecular MRI. One important approach to increase the contrast and reduce the required dosage is to attach MRI contrast agents into a polymer scaffold.<sup>193</sup> The combination of MR imaging contrast agent with polymer-based nanocarrier platform is fairly appealing since the polymer can endow the MRI system with aqueous dispersibility and low/no cytotoxicity for *in vivo* applications, preservation or even enhanced MRI performances in most cases, and improved accumulation in tumor tissues via EPR effect. Among the available polymeric contrast agents, HBPs are especially appealing. Their branched structure imparts rigidity and a large number of functional groups for the multivalent display of contrast agents and other synergistically integrated agents for effective therapy and diagnosis. In addition, the tunable branched architecture and size allow their selection for specific applications. Correspondingly, the pharmacokinetics, pharmacodynamics, excretion routes,

permeability of HBP-based contrast agents may be well-controlled. Up to now, a wide range of contrast agents based on HBPs have been widely studied.<sup>194-200</sup>

To enhance the MRI sensitivity based on  $T_1$  contrast agent, Sideratou and coworkers reported multifunctional gadolinium complexes based on hyperbranched aliphatic polyester H40 bearing the gadolinium chelates ethylenediaminetetracetic acid (EDTA) or diethylenetriaminepentaacetic acid (DTPA), a FA targeting ligand and protective PEG chains, which was used as prospective contrast agents for targeted MRI.<sup>201</sup> It was found that the  $Gd^{3+}$  complexes attached into HBPs displayed an increased rotational correlation lifetime when their rotation was slowed down due to the macromolecular nature of the compounds. Therefore, the relaxivity value of H40-EDTA-PEG-Folate and H40-DTPA-PEG-Folate gadolinium complexes was 2- to 3-fold higher than that of the clinically used [Gd(DTPA)] complex. Furthermore, the hyperbranched complexes showed low cytotoxicity and FA receptor specificity, which made them promising candidates for MRI applications.

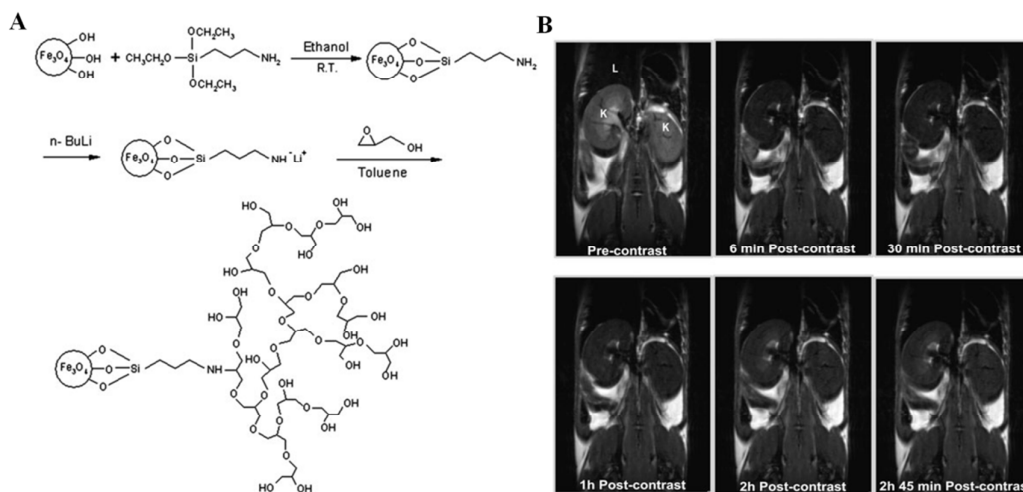


**Fig. 19** (A) Surface modification of  $Fe_3O_4$  nanoparticles with 3-aminopropyl triethoxysilane, and anionic polymerization of glycidol on the surface; (B) MRI images of a live mouse with a  $T_2$ -weighted spin-echo sequence (L, liver; K, kidney). Images were acquired before (pre-contrast) and 6 min, 30 min, 1 h, 2 h and 2 h 45 min after intravenous injection of HPG-grafted nanoparticles. Reproduced with permission from ref. 202. Copyright 2012, Wiley.

Muller and coworkers grafted a water-soluble and biocompatible HPG onto the surface of superparamagnetic iron oxide nanoparticles by ring-opening anionic polymerization as a negative  $T_2$  contrast agent (Fig. 19A).<sup>202</sup> Since superparamagnetic  $Fe_3O_4$  nanoparticles are excellent  $T_2$ -type contrast agents in MRI, and HPG is a water-soluble and biocompatible macromolecule, the effect of HPG-grafted magnetic nanoparticles can be expected in terms of MR signal-enhancing property. The results demonstrated that the HPG-grafted magnetic nanoparticles could be easily dispersed

in aqueous solution to form a uniform suspension and exhibited sufficient stability for several months. The spin-echo abdomen images of a living mouse were obtained before and after intravenous injection of HPG-grafted magnetic nanoparticles solution at different time (Fig. 19B). The *in vivo* MRI studies showed that a strong negative contrast was found in the liver and kidneys in T<sub>2</sub>-weighted images after intravenous injection for 6 min. More importantly, the negative contrast persisted in liver for 80 min and in kidneys for 110 min, and then weakened over time, suggesting that HPG coating endowed the nanoparticles with stealth ability and sensitivity to renal excretion.

Compared with T<sub>1</sub>- and T<sub>2</sub>-type contrast agents, the organic molecular imaging agent may possess broader MRI applications in the future due to their relatively excellent biocompatibility. Wooley and coworkers designed hyperbranched fluoropolymers as <sup>19</sup>F MRI agent assemblies.<sup>203</sup> With the aim of improving the solvation and mobility of the fluorinated groups, the fluorinated component was incorporated in the shell domain of hyperbranched copolymers. These HBPs were then self-assembled into micelles with the hydrodynamic diameters of about 20 nm. The results suggested that these self-assembled micelles had a narrow, single resonance <sup>19</sup>F NMR signal and good T<sub>1</sub>/T<sub>2</sub> relaxation time. These hyperbranched fluoropolymer micelles with good signal-to-noise (S/N) ratios could be used as imaging agents for <sup>19</sup>F MRI in various biomedical studies.

#### 4.3. HBPs for nuclear tomographic imaging

Nuclear tomographic imaging techniques are widely used for pre-clinical research and clinical applications due to their higher detection efficiency, non-invasiveness, excellent tissue penetration, and superb quantitative accuracy.<sup>23</sup> At present, the two most widely used modalities are PET and SPECT.<sup>204</sup> Polymers facilitate the implementation of nuclear tomographic imaging due to their reduced toxicity, ease of modification, prolonged circulation time, amplified signals and improved specificity. Especially, HBPs with highly branching architecture and plenty of functional end-groups provide excellent platform for radioisotope.

SPECT provides three-dimensional images of the complex anatomic structure of the organs using the radionuclides as planar gamma scintigraphy. It is a very popular technique in the clinic and research owing to the affordable instrumentation and radioisotopes and long half-lives of the isotopes.<sup>168</sup> For instance, Zhu and coworkers designed hyperbranched poly(sulfone-amine) (HPSA) functionalized with the human-mouse chimeric monoclonal antibody CH12 and *N*-hydroxy succinimidyl *S*-acetylmercaptoacetyltriglycinate (NHS-MAG3) for labeling <sup>188</sup>Re, forming the <sup>188</sup>Re-labeled and CH12-tethered HPSA (CH12-HPSA-<sup>188</sup>Re), which was used to the

tumor detection and targeted radioimmunotherapy.<sup>205</sup> The *in vivo* distribution of CH12-HPSA-<sup>188</sup>Re was acquired by SPECT, and the results demonstrated that CH12-HPSA-<sup>188</sup>Re could escape from recognition by the reticular endothelial system and effectively target at the hepatocarcinoma tumor tissues with overexpressed epidermal growth factor receptor vIII (EGFRvIII). In comparison with free radionuclide <sup>188</sup>Re, CH12-HPSA-<sup>188</sup>Re exhibited longer circulation time in blood. The SPECT images successfully revealed the gradual accumulation of CH12-tethered HPSA-based radiopharmaceutical via passive and active targeting at the tumor site of tumor-bearing mice.

Compared with SPECT, PET offers the more accurate images and is often used to study *in vivo* biodistribution due to the high sensitivity of the technique.<sup>204</sup> Nevertheless, sometimes the short half-lives of PET radionuclides (e.g., <sup>11</sup>C, <sup>18</sup>F and <sup>64</sup>Cu) limit its further applications. To solve this problem, the radionuclide-labeled HBPs are developed in recent years.<sup>206,207</sup> For example, Gong and co-workers reported a multifunctional unimolecular micelle self-assembled from a hyperbranched amphiphilic block copolymer H40-*star*-[poly(L-glutamate hydrazone-doxorubicin)-*b*-poly(ethylene glycol)] (H40-*star*-P(LG-Hyd-DOX)-*b*-PEG) conjugated with cyclo(Arg-Gly-Asp-D-Phe-Cys) peptide (cRGD, for integrin  $\alpha_v\beta_3$  targeting) and macrocyclic chelator (1,4,7-triazacyclononane-*N,N',N''*-triacetic acid [NOTA]) for cancer-targeted PET/CT imaging and drug delivery in tumor-bearing mice.<sup>208</sup> Complexation of <sup>64</sup>Cu onto the resulting HBP via NOTA was beneficial to reducing the copper binding with plasma proteins which minimized its non-specific background activity and its accumulation, correspondingly lowering the toxicity in the liver and kidney.<sup>209</sup> The representative microPET/CT images of tumor-bearing mice are shown in Fig. 20. PET scans were conducted after intravenous injection of H40-DOX-<sup>64</sup>Cu, H40-DOX-cRGD-<sup>64</sup>Cu, or H40-DOX-cRGD-<sup>64</sup>Cu with a blocking dose of cRGD peptide (10 mg/kg of mouse body weight) at the time points of 0.5, 4, 16, and 24 h. As shown in Fig. 20A, H40-DOX-cRGD-<sup>64</sup>Cu mainly located in the tumor, liver, lung, kidney and intestines, but not in most of the normal tissues (e.g. muscle, bone, brain, etc.), suggesting good tumor-targeting capacity and excellent tumor contrast. The microPET/CT fused images of the mouse at 4 h post-injection of H40-DOX-cRGD-<sup>64</sup>Cu further demonstrated the tumor-targeting efficacy (Fig. 20B). By contrast, the tumor accumulation of H40-DOX-<sup>64</sup>Cu and H40-DOX-cRGD-<sup>64</sup>Cu with a blocking dose of cRGD peptide was relatively low. Moreover, the biodistribution data obtained from region-of-interest (ROI) analysis of non-invasive microPET/CT scans were in line with the quantification results from *ex vivo* fluorescence imaging, further confirming that quantitative ROI analysis truly reflected the *in vivo* distribution of H40-DOX-<sup>64</sup>Cu and H40-DOX-cRGD-<sup>64</sup>Cu.

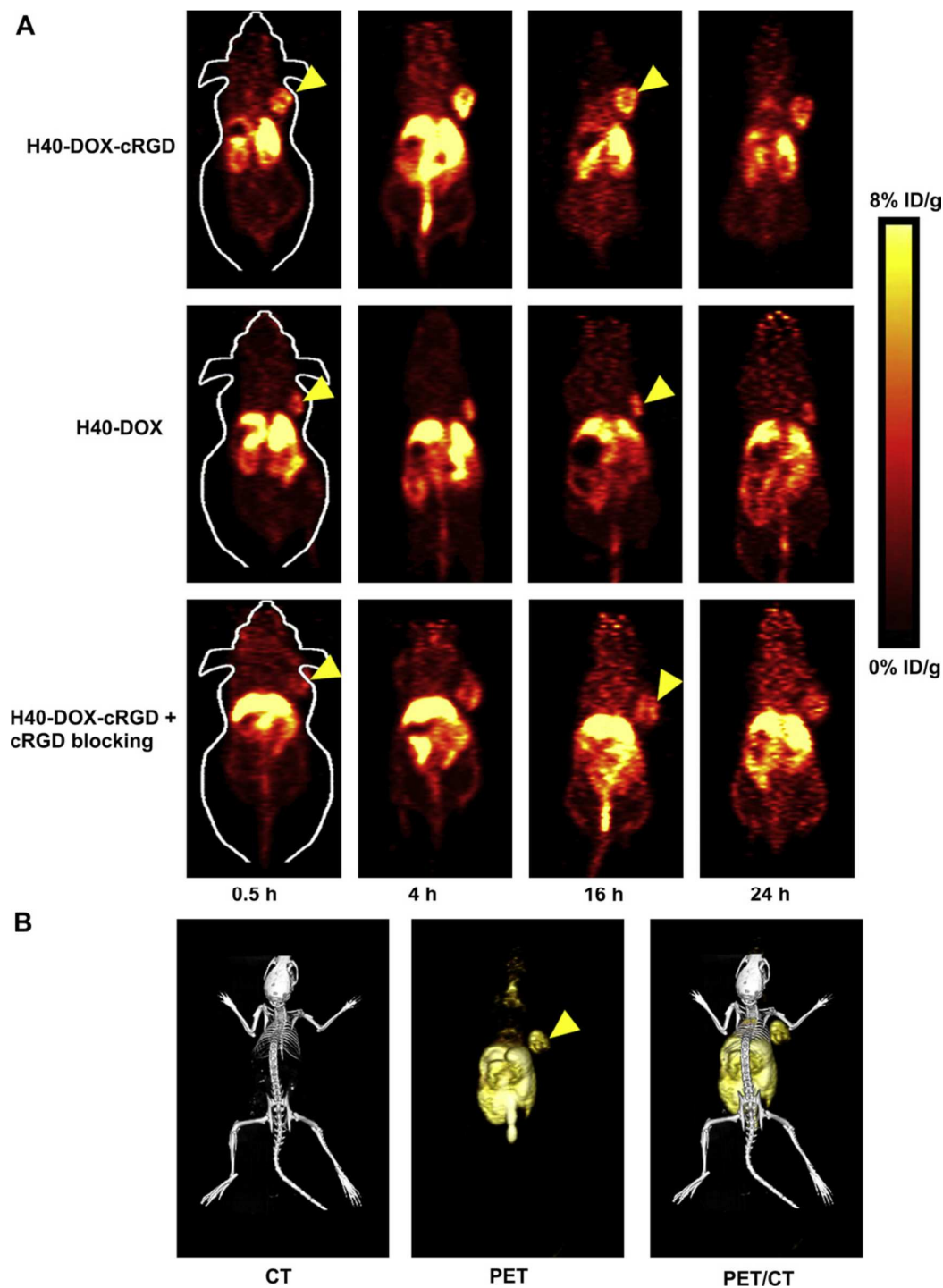


**Fig. 20** PET/CT imaging of  $^{64}\text{Cu}$ -labeled nanocarriers in U87MG tumor-bearing mice. (A) Serial coronal PET images of U87MG tumor-bearing mice at various time points post-injection of H40-DOX- $^{64}\text{Cu}$ , H40-DOX-cRGD- $^{64}\text{Cu}$ , or H40-DOX-cRGD- $^{64}\text{Cu}$  with a blocking dose of cRGD. (B) Representative PET/CT images of a U87MG tumor-bearing mouse at 4 h post-injection of H40-DOX-cRGD- $^{64}\text{Cu}$ . Reproduced from ref. 208 with permission from Elsevier.

#### 4.4 HBPs for multimodal imaging

Multimodal imaging technologies provide unique opportunities to visualize disease states *in vivo* and have received increasing attention recently owing to the distinct advantages of combination of two or more individual imaging modalities.<sup>210</sup> In order to fulfill the multifaceted requirements of such molecular imaging devices, HBPs with elegant architectures have been developed to facilitate incorporation of the various combinations of imaging modalities as well as targeting ligands and therapies, which is beneficial for diagnosis and treatment of various human diseases. For example, optical imaging is safe, highly sensitive and inexpensive but suffers from tissue absorption in the mid-visible range, making the technique inadequate for most deep tissue analyses. MRI has high spatial resolution, a nonionizing radiation source, and is available to extract physiological and anatomical information of soft tissue. However, it often generates ambiguous assignments due to poor sensitivity. Therefore, combination of highly sensitive optical imaging modality with MRI which exhibits exceptional spatial and anatomical resolution is a potential means by which the step-change in bioimaging can be achieved. Some groups have reported the combination of the fluorescent tag with MRI on the hyperbranched polymeric construct.<sup>211,212</sup> For instance, Whittaker and coworkers developed multimodal hyperbranched polymeric nanoparticles with combination of high resolution  $^{19}\text{F}$  MRI and sensitive fluorescence imaging for tunable, targeted, multimodal imaging *in vivo*.<sup>212</sup> The HBPs with controlled molecular structure and size were synthesized by RAFT polymerization (Fig. 21A). Then the end-groups of HBPs were modified with the targeting ligand folic acid and fluorescent label rhodamine B isothiocyanate using standard coupling chemistries. The fluoro-segments were incorporated within a hydrophilic PEG-based macrostructure and remained extensive segmental mobility in solution, both in serum and in intracellular fluid. Thus, imaging of the  $^{19}\text{F}$  nuclei could be achieved, even in an aqueous environment with up to 20 mol% of fluoro-monomer. They employed a mouse subcutaneous tumor model to investigate the effectiveness of the HBP nanoparticles for molecular imaging. The results demonstrated that fluorescence imaging provided whole animal images, allowing tracking of nanoparticles, while  $^{19}\text{F}$  MRI provided high-resolution images for analyzing the *in vivo* distribution of nanoparticles within single organs. As shown in Fig. 21B, the non-targeted nanoparticles are mainly distributed in the bladder and kidney, suggesting that the nanoparticles are excreted by the kidneys, whereas the FA-targeted polymeric nanoparticles are localized in the tumor and liver besides the kidney and bladder. Similar to the  $^{19}\text{F}$  MR images, the fluorescence imaging shows that the signal from the FA-conjugated nanoparticles is observed in the liver, bladder, kidney, and tumor, while that from the unconjugated nanoparticles is seen only in the

kidney. This dual-modal system integrates the sensitivity and relatively low-cost advantages of optical imaging with the high-resolution capabilities of MRI.

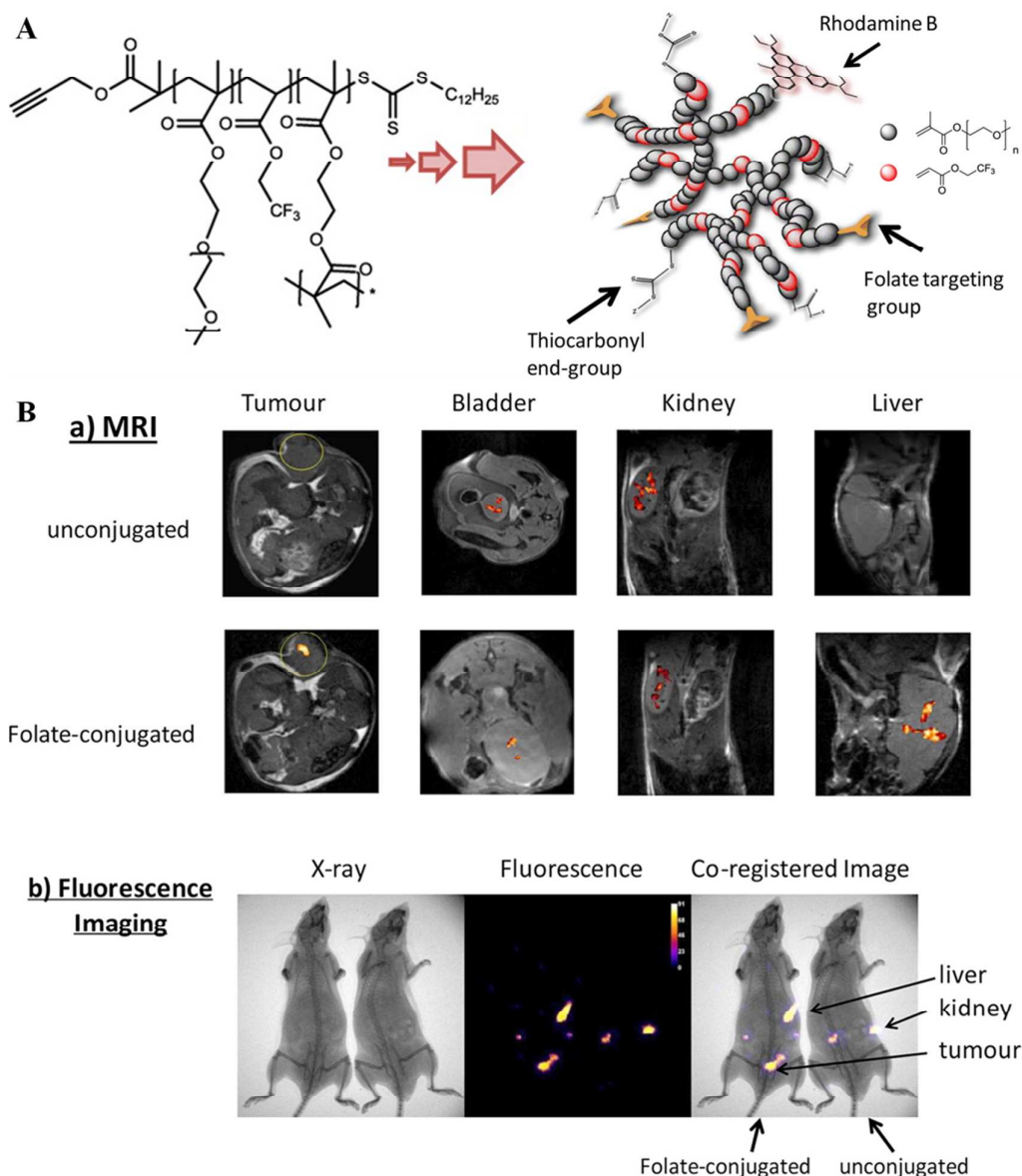


**Fig. 21** (A) Schematic representations of the molecular structure of HBPs. (B) Molecular images of HBP nanoparticles using the mouse subcutaneous B16 melanoma model : (a) MRI images of bladder, kidney, liver, or tumor (circled in image) in the tumor-bearing mice 1 h following intravenous injection of 100  $\mu$ L of FA-conjugated or unconjugated (control) HBP (20 mg/mL in PBS). The high-resolution  $^1\text{H}$  MR image is overlaid with the  $^{19}\text{F}$  image. (b) Fluorescence images of mice following injection of the same two compounds at the same concentration. The fluorescence images are co-registered with X-ray images of the mice 1 h following subcutaneous injection. Reproduced with permission from ref. 212. Copyright 2014, American Chemical Society.

The combination of optical imaging and PET facilitates high throughput scanning

and *ex vivo* analysis associated with fluorescent probe with the exceptional sensitivity of the PET probe. HBPs play an important role in constructing PET/SPECT-optical imaging agents since their simple synthesis and functionalization. Thurecht and coworkers developed multimodal molecular imaging agents based on HBPs, which integrated the complementary capabilities of optical fluorescence imaging and PET/CT.<sup>213</sup> Firstly, two hydrophilic HBPs with different size and level of branching were synthesized through RAFT polymerization, and then conjugated with the near infrared dyes for optical imaging and a copper chelator capable of binding of <sup>64</sup>Cu as a PET radio nuclei. *In vivo* multimodal imaging of mice was used to evaluate the biodistribution of the polymeric materials and it was demonstrated that the larger HBP with high DB had a considerably longer circulation time and showed enhanced accumulation in solid tumors in a murine B16 melanoma model. Importantly, it was shown that the PET modality resulted in high sensitivity immediately after injection of the imaging agent, whereas the optical modality facilitated extended longitudinal studies, thus highlighting the complementary advantages of the multimodal molecular imaging agents.

The incorporation of three kinds of imaging modalities on a single imaging probe allows the development of more advanced systems, in which the synergistic advantages of imaging modalities can be exploited. Recently, Häfeli and coworkers reported that high molecular weight HPG were functionalized with a suitable ligand for <sup>111</sup>In radiolabeling and Gd coordination, and additionally labeled with a fluorescent dye, thus became a trimodal bioprobe for detection with SPECT, MRI, and fluorescent imaging.<sup>214</sup> It was found that *in vivo* MR imaging of the HPG labeled with Gd could provide physiologically relevant data regarding vascular function, while <sup>111</sup>In-labeled HPG was able to quantitatively analyze the probe's biodistribution over time. The microregional location of the probe within the tumor microenvironment, including for how long the probe stayed in intravascular, could be evaluated at the microscopic level using the HPG tagged with fluorescent dye imaged using fluorescence microscopy. The combination of three imaging modalities possesses great potential in preclinical investigations to provide highly specific and quantitative data regarding the physiological function of tumor blood vessels.

## 5. HBPs for biomineralization

Biomaterials have attracted increasing attention in recent years due to their unique optical and mechanical properties as well as spectacular morphologies.<sup>215,216</sup> Much effort has been devoted to understanding the growth mechanism of biomaterials and to mimicking the biomineralization processes in past decades. HBPs are widely used as a soluble or functional matrix to study and to control the biomineralization processes

including nucleation, growth, polymorph and orientation of the inorganic compounds. Besides, HBPs can act as a structural or insoluble matrix to supply a high level of spatial control as the mineralization usually takes place in a confined reaction environment.

### 5.1 HBPs for calcium carbonate mineralization

Calcium carbonate ( $\text{CaCO}_3$ ), which has three crystalline phases (vaterite, aragonite, and calcite) and an unstable amorphous phase, is one of the most studied systems for its important role in understanding the natural mechanism of biomineralization and designing new composite materials.<sup>217-221</sup>  $\text{CaCO}_3$  has been of considerable interest because it is one of the most abundant biominerals and used industrially in vast quantities. Hydrophilic polymers, including proteins, polysaccharides and glycoproteins, exist in  $\text{CaCO}_3$  biominerals and guide the development of the mineral phase. Acidic groups (carboxylate, sulfate, phosphate, etc.) in these copolymers could bind  $\text{Ca}^{2+}$  and crystal faces to control the nucleation and growth of  $\text{CaCO}_3$ .<sup>222-226</sup> The HPG is perhaps the most studied HBP for controlling  $\text{CaCO}_3$  crystal growth. The first HPG was reported by Vandenberg in the 1980s. Anionic polymerization of glycidol was used for the synthesis of HPG, resulting in relatively monodisperse, highly branched products with a controlled molecular weight in the range of a few thousand daltons.<sup>72,227</sup> The earliest example applied HPG to  $\text{CaCO}_3$  crystallization derived from 1,1,1-tris(hydroxymethyl)propane without further functionalization, which is adsorbed to self-assembled monolayers (SAMs) with different surface polarities to result in the formation of aragonite.<sup>228</sup> The morphology (calcite, aragonite, vaterite) of the crystals formed was subsequently investigated by scanning electron microscopy (SEM). HPGs of different molecular weight were adsorbed on nonpolar surfaces due to their intrinsic amphiphilic character. For alkyl-terminated SAMs, the crystallization was fully controlled and only aragonite crystals were observed. As expected, the thermodynamically most stable polymorph calcite was formed in solution. The latter observation shows that the cooperative interaction between the surface and the highly branched macromolecules plays a key role during the biomineralization process.

Inspired by carboxylate functionalized PAMAM dendrimers<sup>229,230</sup> and the concept of the double hydrophilic block copolymers, which typically consist of one hydrophilic block that interacts with the appropriate inorganic minerals and another hydrophilic block that provides stabilization in water, You and coworkers synthesized new types of sulfate or carboxylate-functionalized HPG arising from pentaerythritol and, for the first time, HPG was used as additive for biomimetic crystallization of  $\text{CaCO}_3$ .<sup>226</sup> The crystallization process of  $\text{CaCO}_3$  was carried out using a slow  $\text{CO}_2$

gas-diffusion method described by Addadi and co-workers.<sup>231</sup> One of the HPG candidates functionalized with sodium carboxylate (HPG-CH<sub>2</sub>COONa) was found to be capable of mediating the formation of uniform spherules with stacked multilayers. Interestingly, the morphology evolution of rod–dumbbell–sphere transition process was observed directly, providing considerable insight into the mechanism of formation of calcite microspheres. (Fig. 22) The authors also showed a morphological transition in the product particles from truncated rhombohedra to rounded rhombohedra and to spherules while the cations of sulfate-based polyglycerols (HPG-SO<sub>3</sub>H) were changed from H<sup>+</sup> and Na<sup>+</sup> to imidazolium. HPG-SO<sub>3</sub>H derived from a three-armed initiator (1,1,1-tris(hydroxymethyl)propane) showed less effective control over the morphologies of CaCO<sub>3</sub> particles than HPG-SO<sub>3</sub>H derived from a four-armed initiator (pentaerythritol), which suggested that the secondary structures of HPG could dramatically influence the control of growth of inorganic particles.

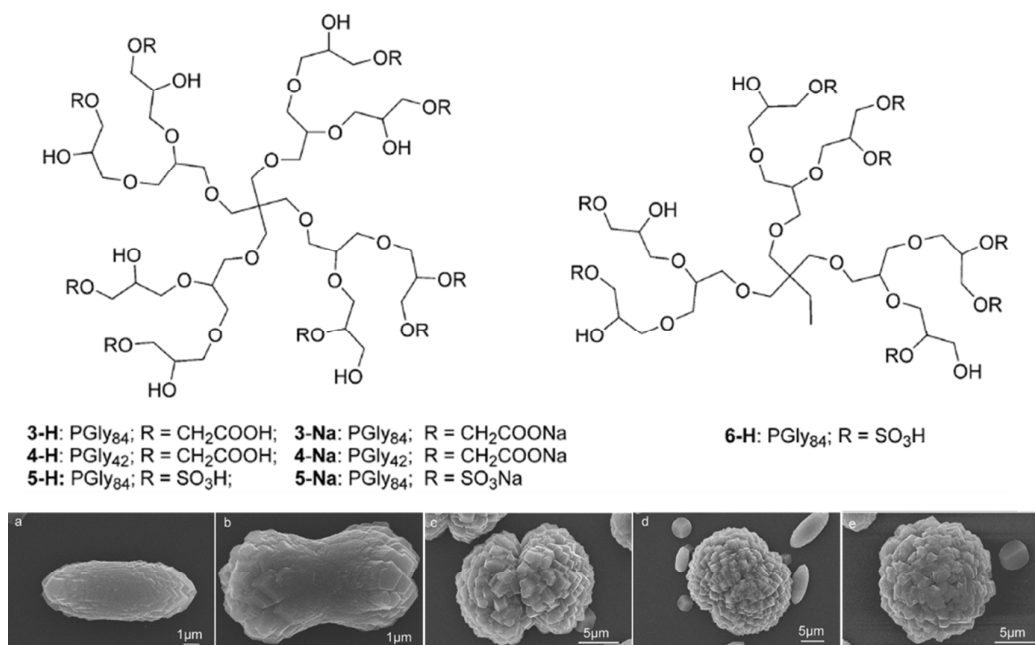


**Fig. 22** Chemical structure of HPGs and SEM images of progressive stages of the self-assembled growth of the calcite aggregates in the presence of 3-Na (5 gL<sup>-1</sup>) and Ca<sup>2+</sup> (10 mM): (a) rods; (b) peanuts; (c) dumbbells; (d) twinned superstructures; (e) spherules. Reprinted with permission from ref. 226. Copyright 2008, Royal Society of Chemistry.

By a different synthesis and functionalization method, Yan et al. synthesized a similar carboxyl-terminated HPG (HPG-COOH) with ~90% surface carboxyl functionalization efficiency.<sup>232</sup> Compared with its linear analogue, this functional polymer had a core-shell structure in which the carboxyl shell and the water-soluble

core acted as the interacting and stabilizing portions, respectively, and the 3D branched structure significantly increased the density of the carboxyl groups in the macromolecules.<sup>72,233</sup> The novel 3D modifier could efficiently control the crystallization of  $\text{CaCO}_3$  from amorphous nanoparticles to vaterite hollow spheres. The obtained vaterite hollow spheres had a special puffy dandelion-like appearance, constructed by platelet-like vaterite mesocrystals, perpendicular to the globe surface. When a controlled experiment without the additive HPG-COOH was performed, and only rhombohedral crystal characteristic of calcite was obtained. The starting pH value influenced the morphology of  $\text{CaCO}_3$  and disks with rough surfaces were obtained when the starting pH was set at 10. The authors inferred that the HBPs rearranged themselves to interact tightly with the faces of vaterite and help the transformation from amorphous phase to vaterite.

With a different mineralization method by directly mixing of  $\text{CaCl}_2$  solution with  $\text{Na}_2\text{CO}_3$  solution, the same group investigated the influence of the mole ratio of the interacting to the stabilizing portion ( $R_{I/S}$ ) in HPG-COOH on the morphology and the polymorph evolution of  $\text{CaCO}_3$ .<sup>234</sup> Upon increase of the  $R_{I/S}$  from 0.1 to 0.9, the morphology changed from pinecone-like to olive-like and finally to highly monodisperse spherical morphology when the  $R_{I/S}$  exceeded 0.5. (Fig. 23) The morphology evolution of  $\text{CaCO}_3$  was accompanied by the polymorph changing from pure calcite through mixed calcite and vaterite, and finally to pure vaterite. The size distribution of the monodisperse  $\text{CaCO}_3$  microspheres was less than 5%, which had rarely been accomplished. This uniformity in size was ascribed to strong inhibition of HPG-COOH on nucleation of  $\text{CaCO}_3$ . The morphology evolution of  $\text{CaCO}_3$  was explained using a flexible globular HBP model that at low  $R_{I/S}$  values, the HBPs adopt a prolate shape with loose packing and randomly oriented carboxyl groups; while at high  $R_{I/S}$  values, the higher number of carboxyl groups force the HBPs to flatten and the carboxyl groups pack more orderly and densely. Their work further confirmed the topology effect of the HBPs on biomineralization.

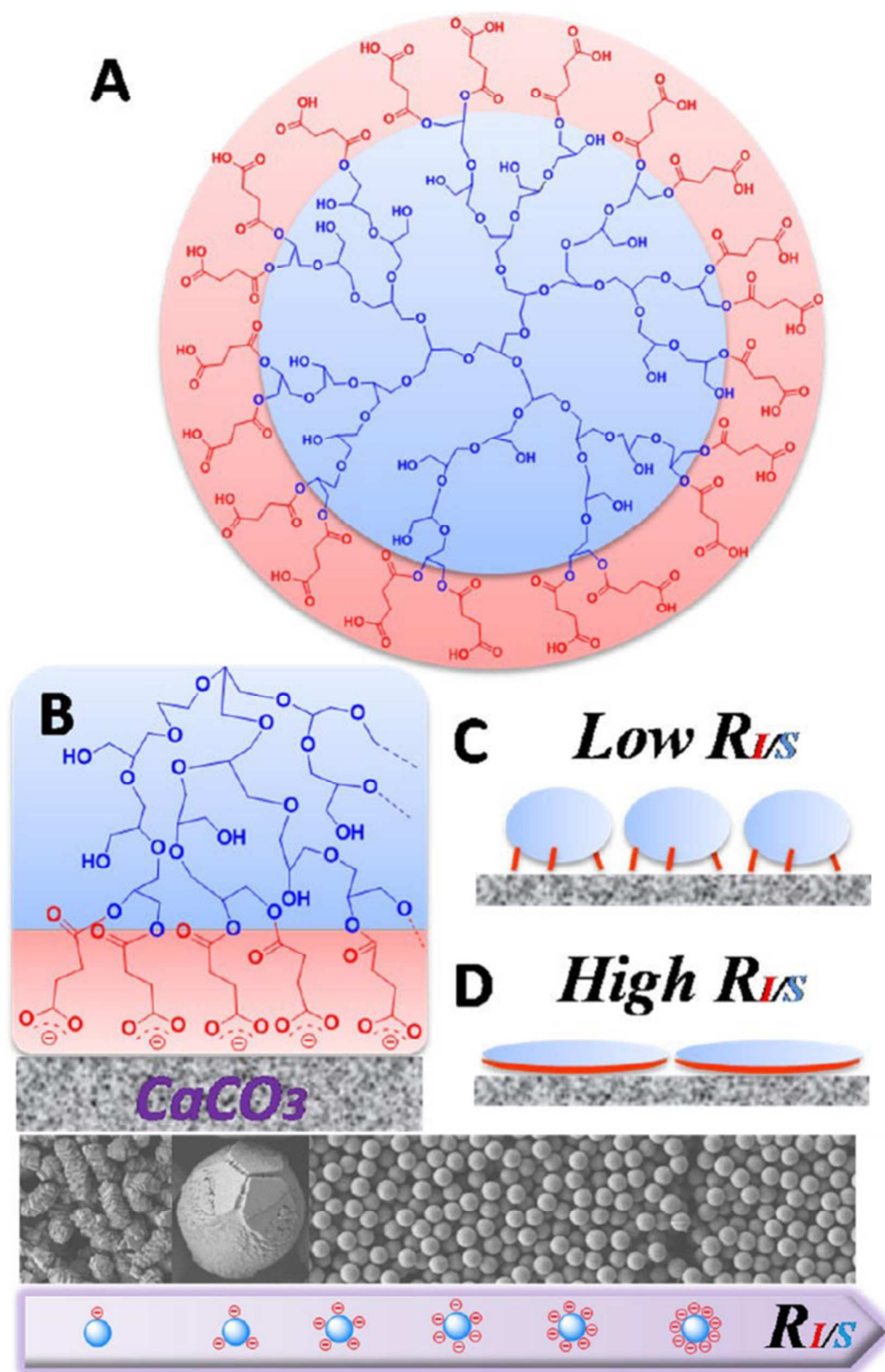


**Fig. 23** Models of HPG-COOH (A and B) with low (C) and high (D)  $R_{IS}$  interacting with  $\text{CaCO}_3$ . Reprinted with permission from ref. 234. Copyright 2012, American Chemical Society.

Another example using branched polymers to control  $\text{CaCO}_3$  growth is the study of branched polysaccharides.<sup>235</sup> The group chose five commercially available

polysaccharides: amylose, amylopectin,  $\beta$ -limit dextrin, polygalacturonate, and alginate to test the inhibitory effects of branched, linear, neutral, and acidic polysaccharides on calcite growth. The degree of branching was found to play a large role in determining inhibitor effectiveness. The highly branched, neutral polysaccharide, amylopectin, is as active an inhibitor of crystal growth as polygalacturonate. Inhibition decreases with a decrease in the extent of branching by comparing the effects of amylopectin and amylose.

## 5.2 HBPs for silica mineralization

The current industrial capacity for silica production is  $\sim 10^6$  tonnes per annum, while silica-based materials form a  $\sim$ £2 billion industry.<sup>236</sup> However, the scale of natural biological silica deposition is orders of magnitude greater than the industrial capacity, and it all takes place under mild conditions and achieves superior control over materials produced.<sup>237,238</sup> It is believed that an understanding of the secrets of biological silica formation could lead to materials with novel applications and/or new technologies for nanomaterials production. Thus, studies on bioinspired approach have become popular for controlling the morphology of silica materials with a high level of precision. Dendritic polymers, including dendrimers and HBPs, with excellent and promising architecture-dependent behavior have been frequently used as soft templates to synthesize silica particles.<sup>230,239,240</sup> However, the high cost and limited availability of dendrimers obviously favor the use of HBPs over their structurally perfect analogs.<sup>241</sup> Compared with the linear polymers, the advantages of HBPs include their tailor-made properties, well defined secondary structures, high functionality, and good solubility in directing biomineralisation.

It is highlighted that amines actively catalyze the condensation of silica precursors. Therefore, numerous amine-containing molecules, including polypeptides, synthesized polymers/oligomers, and small molecules, have been explored for the biomimetic deposition of silicas. Although many synthetic polyamines are utilizable for rapid silica deposition, they are not effective in silica architecture, because the polyamines do not show special conformations in aqueous media. Different from the many synthetic polyamines, including randomly hyperbranched PEI, linear PEI possessing only secondary amine residues in the backbone has specific all-trans zigzag conformation in aqueous media and thus easily forms ordered aggregates.<sup>242</sup> It is found that the organized aggregates of linear PEI are capable of directing silicas into multiple morphologies with hierarchical structures, in which the hydrolytic condensation of alkoxy silane occurred exclusively and rapidly around the PEI aggregates under ambient conditions.<sup>243-247</sup> It was found that various parameters,

including polymer architectures, concentrations, media, additives, and physical fields, could be facilely used for the shape and structure control of silica. One of the fascinating results is that star-architecture PEI could direct remarkably different silica compared with the linear counterparts.<sup>243,244</sup> The silica shapes are strongly dependent on the parameters of star architectures, such as the number of arms and core size. Four-armed porphyrin-core PEI produces aster-like silica, while six-armed benzene-core PEI gives silica with fiber-sponge morphology.<sup>243,244</sup> Another four-armed benzene-core PEI could shape the silicas into the nanofiber-based bundles, flowers, films or plates, and continuous films by varying the polymer concentration.<sup>247</sup> The comparative examination of silica shapes and structures between linear and star PEI indicates that the silica formation remarkably exhibits the star-specific character. The star architecture dramatically enhances the parallel aggregation of unit fibers and also promotes the fiber aggregation ability as compared with the linear architecture. When using linear PEI as mediator for silica deposition, the photo functional additive such as tetrakis(4-sulfophenyl)porphyrin (TSPP) can effectively switch the resulting silica morphology via association between PEI and TSPP to give particularly shaped silica with fluorescence.<sup>244</sup>

Although the randomly hyperbranched PEI is not a good candidate for controlling the deposition of silicas (the product is less homogeneous compared to the linear PEI,<sup>248,249</sup>) a star shaped poly(L-lysine) (PLL) based on a hyperbranched PEI core have shown good control over the silica morphology.<sup>250</sup> The group synthesized a star-shaped copolymer HPEI10000-*star*-PLL20, with a hyperbranched PEI core and multiple linear PLL peripheral chains. It was found that the mole ratio of tetraethoxysilane (TEOS) to lysine residue ( $\delta$ ) played a pivotal role in determining the silica morphology. As the  $\delta$  increased, various biosilica morphologies, such as spherical ( $\delta < 10$ ), clubbed ( $\delta = 11$ ), and hexagonal ( $\delta = 18$ ) shapes, were formed. (Fig. 24)

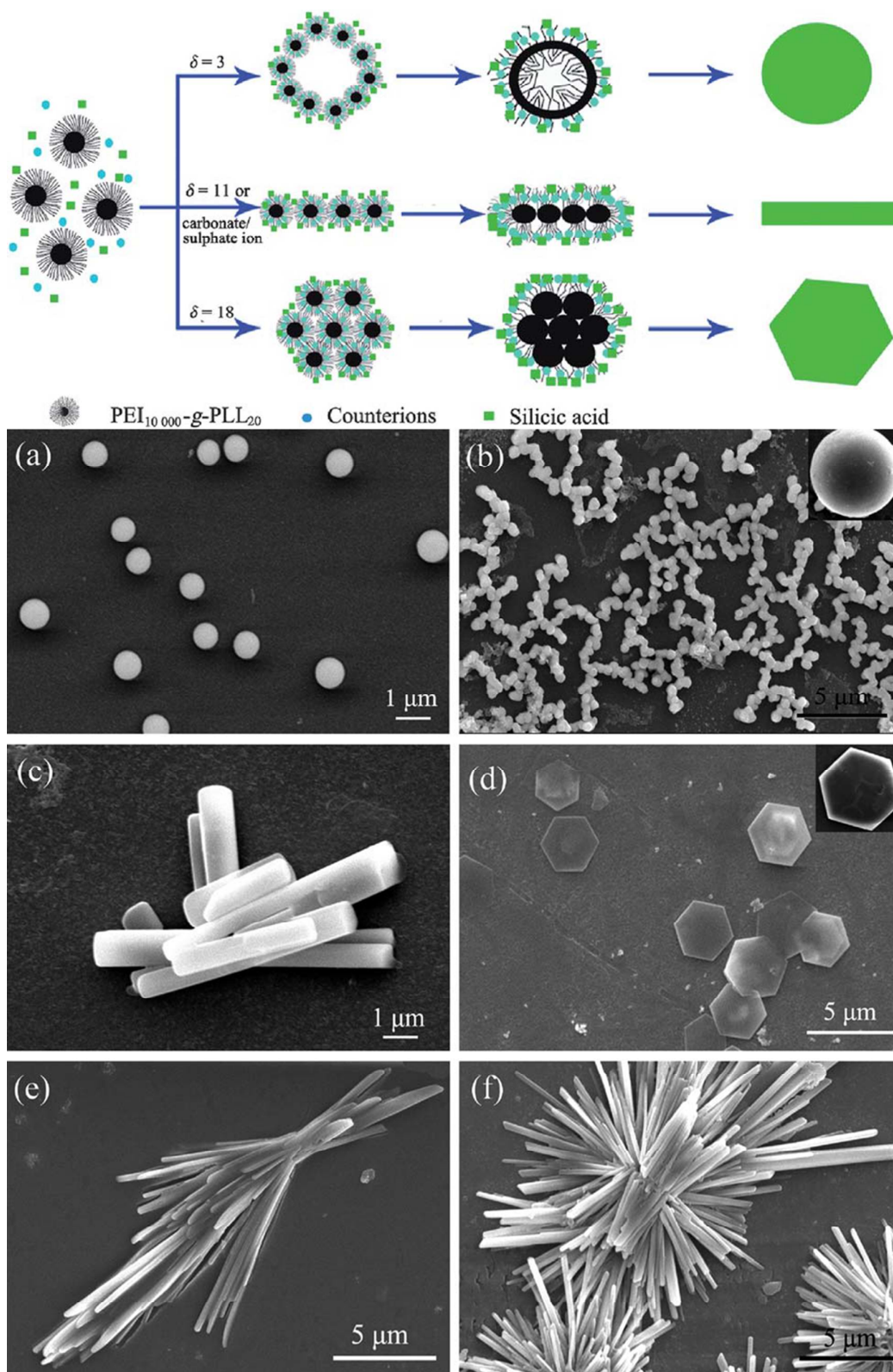


**Fig. 24** Proposed model for the morphological evolution and SEM spectra of the P<sub>2</sub>/phosphate/silicic acid system at different  $\delta$  values: (a) 3, (b) 5, (c) 11, and (d) 18; (e)

P<sub>2</sub>/carbonate/silicic acid; (f) P<sub>2</sub>/sulfate/silicic acid. Reprinted with permission from ref. 250. Copyright 2012, Royal Society of Chemistry.

## 6. HBPs for tissue engineering

HBPs with a three-dimensional architecture exhibit high surface functionality, high reactivity due to the presence of a large number of exposed free surface groups, and they may alter the absorption profile of biomolecules/proteins on a polymeric biomaterial in a positive way. One can introduce structural variations to tailor degradation kinetics as well as incorporation of appropriate functional groups for improved cell attachment. Besides, HBPs are capable to form porous hydrogels or films as scaffolds, and are promising to promote adhesion and proliferation of cells. Thus, HBPs, due to their special topological structures, have found various applications in tissue engineering fields.

### 6.1 HBPs as tissue scaffold components

The ideal synthetic scaffolds should (1) form an appropriate porous, three dimensional network that is resorbable *in vivo*, (2) mimic the mechanical properties of the native cartilage, (3) allow for the growth of necessary cells in the surrounding joint area, (4) be biocompatible and avoid eliciting an immune response *in vivo*, and (5) integrate with the remaining cartilage in the joint area and withstand the physiological loads until the tissue repair is complete. HBPs offer an advantage because their increased number of end groups can provide a more densely crosslinked matrix that resists excess swelling.<sup>251</sup>

A variety of HBPs, including hyperbranched poly(lactic acid) (PLA),<sup>252,253</sup> poly(lactic-glycolic acid) (PLGA),<sup>254</sup> polycaprolactone (PCL),<sup>255,256</sup> polyurethane,<sup>257-259</sup> PEG,<sup>260-270</sup> polyglycerol (PG),<sup>112,271-274</sup> poly(NIPAM)<sup>275,276</sup> have been extensively characterized and widely used to fabricate tissue-engineering scaffolds.

#### 6.1.1 Biodegradable hyperbranched polyesters

Aliphatic biodegradable polyesters are good candidates as a temporary tissue support material because of their simple hydrolysis of the ester backbone that supplies proper spaces for newly developing tissues. Being able to degrade into innocuous glycolic and lactic acid, PLA, PGA and their random block copolymers poly(lactic-*co*-glycolic acid) (PLGA) are widely used as medical implants and scaffolds. Song and his

coworkers developed an amorphous shape memory polymers (SMP) network crosslinked from a star-branched macromer containing polyhedral oligomeric silsesquioxane (POSS) nanoparticle core and eight PLA arms.<sup>277</sup> The rigid POSS nanoparticle core facilitated maximal participation of the urethane-tethered PLA arms in the elastic deformation and recoiling process with reduced excessive chain-chain entanglement below and above  $T_{\text{trans}}$ , respectively. Consequently, the resulting POSS-SMP nanocomposites, with cortical bone-like modulus ( $\sim 2$  GPa) at body temperature, could stably hold their temporary shape for  $>1$  year at room and body temperatures and achieve full shape recovery with a  $T_{\text{trans}} < 50$  °C in a matter of seconds. The group further examines the degradation profiles and immunogenicity of POSS-SMPs as a function of the PLA arm lengths using a rat subcutaneous implantation model. The degradation rates of POSS-SMPs, both *in vitro* and *in vivo*, inversely correlated with the length of the PLA chains within the crosslinked amorphous network. One year after the implantation of POSS-SMPs, no pathologic abnormalities were detected from the vital/scavenger organs examined. Kayaman-Apohan's group synthesized a FAME-terminated hyperbranched poly(lactide-*co*-glycolide) (PLGAFAME) by ring opening polymerization and used it as one of the components of the photo-crosslinked hydrogels. The degradation rate was increased by the introduction of PLGAFAME copolymer and all the hydrogels were cellularly compatible.

Due to their small size, spherical structure and limited interaction between molecules, HBPs have different properties compared to the linear polymers with equivalent molecular weight. They are less crystalline and have lower melting and solution viscosity but are easier to process and degrade faster. Chiellini etc. produced 3D meshes by wet-spinning method using a three-arm branched PCL.<sup>255,256,278</sup> They evaluated these meshes as scaffolds for the regeneration of bone tissue in the presence of infections. Both the enrofloxacin-loaded and Levofloxacin-loaded meshes, after a fast release at the early stages, provided sustained release for up to five weeks. The cytocompatibility of the branched PCL and the influence of the scaffold architecture on cell behavior were performed with MC-3T3 pre-osteoblast cells. After 14 days of culture, the cell adhesion and proliferation analyses showed that all of the fibers were covered by a cellular layer.

#### 6.1.2 PEG-based HBPs

Hyperbranched PEG-based polymers are another example of a synthetic material that has been investigated to form hydrogel scaffolds for the encapsulation and culture of stem cells. The techniques of controlled/living radical polymerization (CRP) have

given birth to a number of hyperbranched PEG-based copolymers with controlled molecular weights, well-defined chain ends, and different degree of branching. Poly(MEO<sub>2</sub>MA-*co*-OEGMA) was firstly reported by Lutz and his colleagues.<sup>279</sup> This linear copolymer with LCST around 37 °C was prepared via atom transfer radical polymerization (ATRP). In Lutz's later study, they attempted to introduce the multifunctional vinyl monomer of ethylene glycol dimethacrylate (EGDMA) to achieve HBP structures; however, only one percent of EGDMA caused the polymer macrogelation.<sup>280</sup> In contrast, a higher degree of EGDMA (up to 30% molar ratio of total feed monomers) was introduced as a multifunctional vinyl monomer by Tai's group.<sup>268,269</sup> Instead of causing macro gelation, they successfully achieved hyperbranched copolymers of PEGMEMA-PPGMA-EGDMA via a one-step deactivation enhanced ATRP approach. The introduction of the multi-vinyl crosslinker EGDMA enables the copolymer the capability of easy tailoring and photo-crosslinkable properties. Meanwhile, by adjusting the hydrophilic PEGMEMA and hydrophobic PPGMA composition, they can sensitively alter the polymer hydrophilicity and control the LCST value of the copolymers around body temperature. The combination of physical interaction (*in situ* thermal gelation) and covalent crosslinking (*in situ* photopolymerization) endows the gels with significantly enhanced mechanical properties compared to non-photocrosslinked thermoresponsive hydrogels. The thermally phase-separated gels have attractive advantages over non-thermoresponsive gels because thermal gelation upon injection allows easy handling and holds the shape of the gels prior to photopolymerization. Furthermore, due to the thermoresponsive property, the gels were releasing the carmoisine red dye at a faster rate in warm water (37 °C) compared to a slow release in cold water (25 °C). These gels were found to have low toxicity for mouse C2C12 myoblast cells as assessed with lactate dehydrogenase, Alamar Blue, and a Live/Dead assay at concentrations less than 1 mg/mL. Similar thermoresponsive polymers were synthesized by Wang's group.<sup>281</sup> By adjusting the "long" and "short" PEG chain monomer composition, the LCST value of the copolymers was controlled around 37 °C. 3T3 mouse fibroblast cell line was encapsulated in the hydrogel and no significant difference of cell viability was found between the control (cells alone) and polymer samples after four days' incubation. Despite the promising results *in vitro*, the authors discussed the need of structure modifications by introducing cell-adhesion functionality to improve cytocompatibility and the cell proliferation. Since the applications of UV photo-crosslinking systems are limited by extra equipment requirement and clinical safety concerns, Wang and coworkers developed a new class of thermoresponsive hyperbranched copolymer system PEGMEMA-MEO<sub>2</sub>MA-PEGDA and chemically crosslinked the HBP with a thiol-modified hyaluronan biopolymer which is considered to plays vital role in cell

proliferation and differentiation (Fig. 25).<sup>263,264</sup> After crosslinking, a semi interpenetrated polymer networks with porous structure is formed. Pore sizes and porosity increased with a decreased polymer concentration, which could offer advantage to optimize the hydrogel system for different tissue engineering applications. 3D cell culture of 3T3 fibroblast cells and rabbit adipose-derived stem cells (ADSCs) demonstrated the good cell viability after the cells were embedded inside the hydrogel. The Live/Dead assay showed after 1 week culture, both cell types survived well in 3D hydrogels. The group further studied the behavior of encapsulated ADSCs and identified the secretion profile of suitable growth factors for wound healing.<sup>265</sup> They found that the proliferation of mammalian cells was suppressed because of the slow hydrogel degradation, but viability could be maintained. Although cellular proliferation was inhibited, cellular secretion of growth factors such as vascular endothelial growth factor and placental-derived growth factor production increased over 7 days, whereas IL-2 and IFN $\gamma$  release was unaffected.

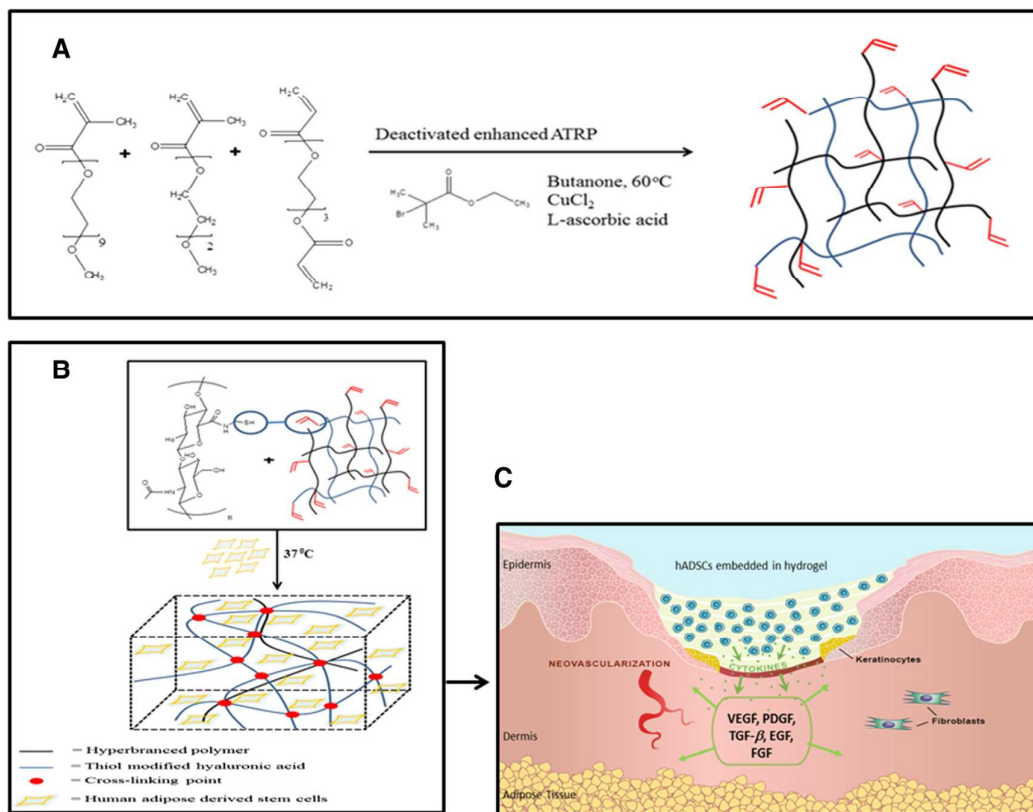


**Fig. 25** Schematic illustration of PEGMEMA<sub>475</sub>-MEO<sub>2</sub>MA-PEGDA<sub>258</sub> copolymer synthesis (A) and encapsulation of hADSCs in the crosslinked P-SH-HA hydrogel (B) and cartoon picture of application of P-SH-HA hydrogel on a skin wound (C) for secretion of growth factors to accelerate wound healing. Reprinted with permission from ref. 265. Copyright 2013, BioMed Central.

Although PEG-based hydrogels provide tissue engineers with large flexibility in material design, they do not have an intrinsic mechanism for interacting with cells, and cell adhesion is typically mediated by non-specific cell adhesion.<sup>282</sup> Thus, PEG hydrogels are often modified with tethered groups, such as adhesion peptides<sup>283,284</sup> or phosphates<sup>285</sup> to alter cellular interactions. PEG-based hydrogels have been used for the culture and differentiation of stem cells toward the engineering of numerous tissues.

Cooper-White et al. have generated hydroxy phenol functionalized hyperbranched PEG hydrogels, cross-linked via an enzyme mediated, oxidative process.<sup>286</sup> Göpferich et al. modified hyperbranched PEG-amines with collagenase sensitive peptides and cross-linked with hyperbranched PEG-succinimidyl propionates without the use of free-radical initiators (enzymatically degradable hydrogels).<sup>261</sup> Enzyme mediated gel degradation occurred within 10, 16, and 19 days. The hydrogels were functionalized with the laminin-derived adhesion peptide YIGSR, and seeded with 3T3-L1 preadipocytes. Compared to a standard two-dimensional cell culture model, the developed hydrogels significantly enhanced the intracellular triglyceride accumulation of encapsulated adipocytes. Functionalization with YIGSR further enhanced lipid synthesis within differentiating adipocytes. Long-term studies suggested that enzymatically degradable hydrogels promoted the formation of coherent tissue-like structures.

### 6.1.3 Hyperbranched polyglycerols (HPGs)

HPGs consist of an inert polyether backbone with functional hydroxyl-groups at every branch end. This structural feature resembles the well-known PEG that is accepted for various biomedical applications. The highly hydrophilic nature of HPG in combination with its hydroxyl functionalities makes HPG very suitable for the design of hydrogels. Frey and coworkers were pioneers in the synthesis of structured HPG hydrogels based on PEO multi-arm stars with a hyperbranched dendritic core.<sup>287</sup> The hydrogel products showed excellent stability with high compression module. Substantial suitability of these hydrogels as substrates for cell growth has been demonstrated. The biocompatibility of HPGs was presented by Brooks et al. in 2006.<sup>288</sup> The *in vitro* assays showed remarkably low cytotoxicity of HPG against fibroblast and endothelial cells. Investigations were later expanded to high molecular weight HPGs.<sup>289</sup> Huge potential of HPG as tissue scaffolds was confirmed by evaluations both *in vitro*<sup>290</sup> and *in vivo*.<sup>291</sup> Hennink and coworkers functionalized the end hydroxyl group of HPG into the photo-crosslinkable acrylate with different degree of substitution (DS) and fabricate hydrogels with both chemical and photo

initiation methods.<sup>272</sup> Rheological analysis showed that the storage modulus of these gels could be tailored by varying the concentration of HPG-MA in the aqueous solution as well as by the DS. Moreover, the obtained hydrogels had a limited swelling capacity indicating that rather dimensionally stable networks were obtained. Alblas and coworkers encapsulated bone marrow derived multipotent stromal cells (MSC) in the same photo-polymerized hydrogel for the development of printed bone grafts.<sup>274</sup> They demonstrated the adverse effects of photo-polymerization on the viability and cell cycle progression of exposed MSC monolayers, but their differentiation potential remained intact. The hydrogel with incorporated MSC supported survival and osteogenic differentiation of the embedded cells to a variable degree.

Another example indicating the tremendous practical capabilities of specifically derivative HPG is based on the sequential attachment of hydrophobic C18 alkyl chains as well as PEG-350 chains to a certain fraction of the polyether polyol OH groups.<sup>292</sup> Since the resulting materials exhibited low intrinsic viscosities coupled with high water solubility and facile synthetic accessibility, they are considered as extremely promising candidates for use as human serum albumin (HSA) substitutes. Plasma half-lives as high as 34 h clearly hint at the suitability for application as synthetic plasma expanders, avoiding the risk of disease transmission, which is inherent to native HSA. Recently, Frey and coworkers presented the attachment of singularly amino-functionalized  $\alpha,\omega_n$ -linear-hyperbranched heterotelechelic to biotin and explored these materials with respect to noncovalent bioconjugation.<sup>166</sup> This approach offers intriguing possibilities for the introduction of functional groups and bioconjugation with a variety of proteins and peptides.

HPG that contained nanoparticles of HA was also used to prepare novel bone scaffolding material by Queiroz and coworkers via electrospinning approach.<sup>293</sup> The potential use of the electrospun fibrous HPG-HA scaffolds for bone regeneration was evaluated *in vitro* with human osteoblasts (SaSO<sub>2</sub>) in terms of alkaline phosphatase (ALP) activity of the cells and cytotoxicity. The biocompatibility evaluation of the HPG-HA provided encouraging indications for long-term safety. The electrospun fibers exhibited highest ALP activity and appeared to promote both proliferation and differentiation of human osteoblasts.

#### 6.1.4 Hyperbranched polyurethanes (HPUs)

The PUs composed of linear aliphatic polyesters and their copolymers with high molecular weight usually have high glass transition temperature and modulus, thus

they are often utilized in biomedical applications varying from cardiovascular repair, cartilage implant, ligament regeneration, and bone replacement to controlled drug/gene delivery and mainly as hard-tissue scaffolds.<sup>294,295</sup> HPU-based biomaterials can meet diversified needs for different biomedical applications according to their required mechanical strength, flexibility, and chemical and biological properties.

Luo and coworkers prepared a THTPBA/PEG-derived HPU-based scaffold. The tensile stress-strain investigations showed that the hyperbranched architecture offered high elastic modulus and mechanical strength.<sup>258</sup> They stated that a hydrophobic reactive prepolymer with multifunctional groups inserted in the PEG-based PU backbone could constitute a scaffold with high mechanical properties and this combination was anticipated to influence or alter surface properties and haemocompatibility of the PEG-derived PU biomaterials. They also found that the incorporation of THTPBA could mediate the degradation rate, which took place at the urethane or ester bonds in polymer chains.

Karak and coworkers synthesized sunflower oil based HPUs with different weight percentages of pentaerythritol (a branch generating moiety) and this could be the first time that vegetable oil-based HBPs was used as a promising scaffold material for tissue engineering.<sup>257</sup> The MTT/hemolytic assay and subcutaneous implantation in Wistar rats followed by cytokine/ALP assay and histopathology studies confirmed a better biocompatibility of HPU with monoglyceride than without monoglyceride. HPU supported the proliferation of dermatocytes with no toxic effect in major organs. The group further prepared HPU/functionalized multi-walled carbon nanotube (f-MWCNT) nanocomposites (NCs) by an in situ polymerization technique with different wt% of f-MWCNTs. The tensile strength of the NCs was enhanced to 36.98–47.6 MPa from 23.93 MPa (HPU) and toughness from 12767 to 18427–19440 due to the addition and efficient dispersion of the f-MWCNTs in the HPU matrix. The NC with interconnected pores size (200–330 nm) showed better proliferation and adherence of osteoblast (MG63) cells compared to the HPU and the results were comparable with the control. The response of an animal model on their post-implantation suggested the safety potential of the prepared systems within the tested animal model.

## 6.2 HBPs as cell and tissue adhesives

The potential for cell and tissue adhesives from multivalent HBP scaffolds is enormous. Taking advantage of the multiple functionalization of HBPs, Brooks, Kizhakkedathu and colleagues synthesized HPGs decorated with multiple choline phosphate (CP) groups, which possessed the inverse orientation of phosphatidyl choline (PC), the end group of the major lipid presented in eukaryotic cell membranes

(Fig. 26).<sup>296</sup> These functionalized HPGs displayed a strong affinity for biological membranes, and thereby exhibited great potential for a number of biomedical applications, such as tissue sealing and drug delivery. In particular, the researchers systematically varied the concentration of CPs attached to two HPG samples of different molecular weights (23 and 65 kDa). They observed that these multivalent dendritic structures strongly bound to human red blood cells — in particular, as many as  $2.5 \times 10^5$  molecules of 65 kDa polyglycerol terminated with 80 CP groups bound to each cell in a solution of  $\sim 10 \text{ mg ml}^{-1}$  of the polymer — and that the cells formed aggregates when they were exposed to a saline-buffer solution with CP-terminated polymers. Instead, PC-decorated polyglycerols bound to the cells only weakly ( $1.8 \times 10^4$  molecules under roughly the same conditions). Also, a comparison of molecular weights revealed stronger binding for the 23 kDa constructs, which was at odds with what was expected from polymers adhering to surfaces, and was likely to be an entropy effect. From fluorescence labelling and tritiation results, the authors suggested a mechanism for the strong interaction between the CP-decorated dendritic polymers and the PC-terminated phospholipids: the formation of multiple CP–PC heterodimers driven by electrostatic interactions. Furthermore, the authors demonstrated that the strong binding of the CP-containing polyglycerols to cells also took place in blood plasma. Support for the generality of the membrane-binding capacity of HBPs was provided with experiments using Chinese hamster ovary cells. When they used fluorescently labelled polymers to monitor membrane binding, the authors found that the CP-substituted polyglycerols were rapidly taken up by the cells, hinting at the potential of the material for use as a drug-delivery vehicle. Also, no cell uptake was detected for the PC-containing polymers, thus confirming the authors' previous observations.

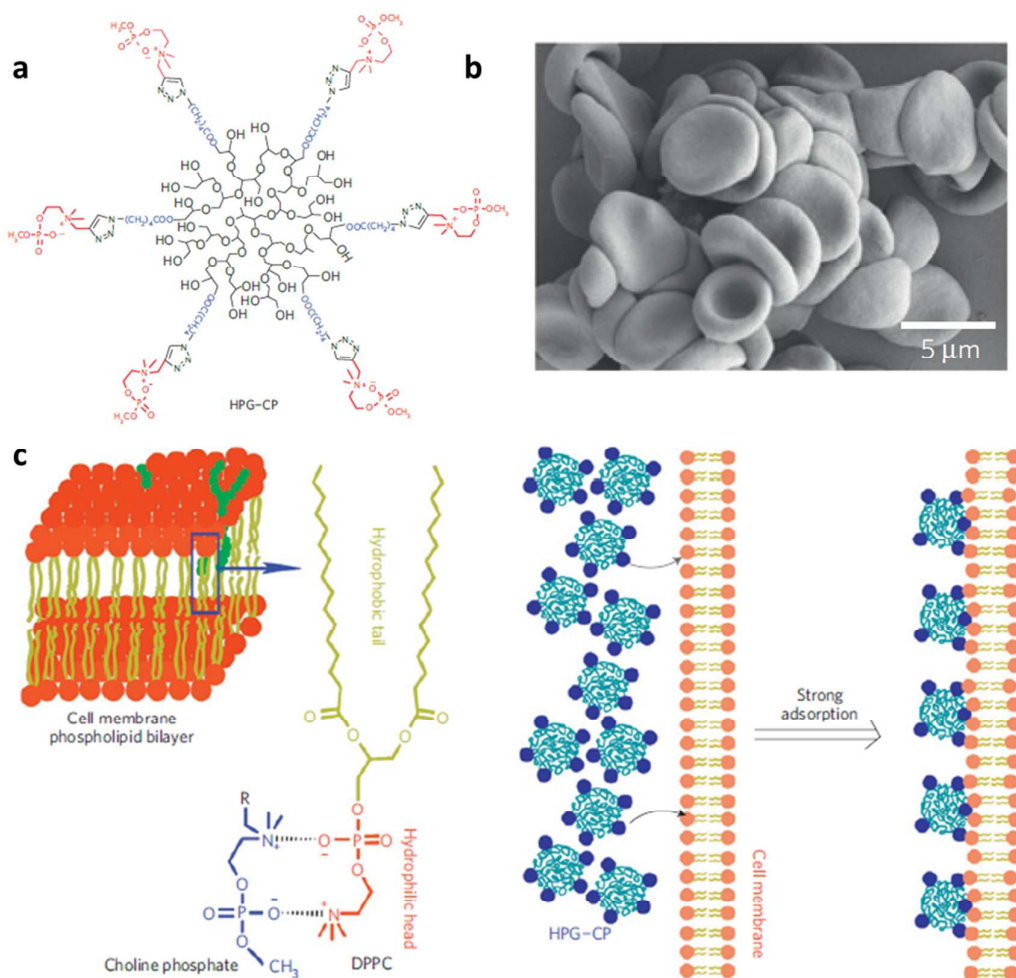


**Fig. 26** Chemical structure of HPG-CP: multivalent HPG structures (black) with CP end groups (red) linked by 1,2,3-triazol units (green) (a) and SEM images (5,000) of red blood cells forming aggregates in saline solution as a result of the cell adhesion (b) and the mechanism of the biomembrane adhesion interaction (c). Reprinted with permission from ref. 296. Copyright 2012, Macmillan.

The ideal tissue adhesive design should incorporate simplicity, safety (including being bactericidal), efficacy, tailored setting times for the application, commercial applicability and the use should be inexpensive, painless and cosmetic. Inspired by marine mussel adhesion that exhibits strong adhesion under wet conditions, Wang and coworkers designed a simple and scalable hyperbranched poly( $\beta$ -amino ester) polymer as strong wet tissue adhesive.<sup>297</sup> Dopamine, an amine-derivative of an amino acid abundantly present in mussel adhesive proteins, was copolymerized with a trifunctional vinyl monomer, to form a hyperbranched poly(dopamine-co-acrylate) (PDA). The tissue adhesive properties of PDA polymer could be adjusted by using

different curing agents ( $\text{FeCl}_3$ , horseradish peroxidase (HRP)- $\text{H}_2\text{O}_2$ , fibrinogen and  $\text{NaIO}_4$ ) when tested on porcine dermal skin surfaces after curing the adhesive for 15 min, 1 h and 1 day at room temperature. Fibrinogen was found to be the best agent for achieving a relatively high adhesion strength ( $37 \pm 5.6$  kPa) within 15 min and HRP was the best for achieving a high adhesion strength ( $76 \pm 13.4$  kPa) after a one day curing period. This poly( $\beta$ -amino ester) based polymer was also able to degrade under physiological conditions via hydrolysis of their backbone esters to yield small molecule by breaking the ester bond. The polymer adhesive degraded to  $58.5\% \pm 3.7\%$  of its original mass after one month's incubation in PBS buffer solution at body temperature. Reinforced with nanosized HA particles (a basic calcium phosphate  $\text{Ca}_{10}(\text{PO}_4)_6(\text{OH})_2$ ), this polymer was also used as a tunable bone adhesive for sternal closure (Fig. 27).<sup>298</sup> Whilst wire cerclage typically caused postoperative sternal wound complications and KRYPTONITE™ bone cement might delay the emergency operation in the critical post-operative time, the PDA nanocomposite adhesive showed excellent adhesion and mechanical properties for the sternal bone model, strong enough to resist sternal displacement and also facilitated re-entry after 1-2 days. In addition, the PDA adhesive degraded in a manner inversely proportional to the healing process and also exhibited low cytotoxicity with minimal heat development during curing.

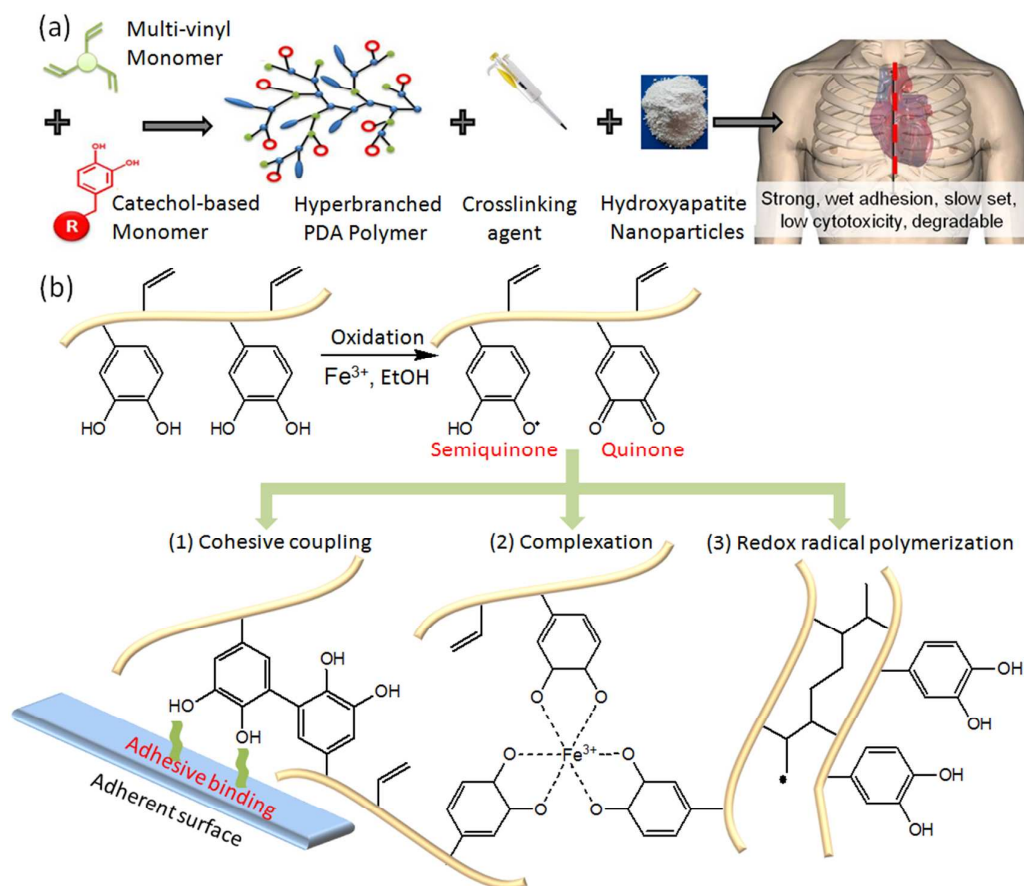


**Fig. 27** Strategy of using catechol-modified dendritic PDA polymer nanocomposite for sternal closure (a) and crosslinking mechanism of PDA with  $\text{Fe}^{3+}$  (b). Reproduced with permission from ref. 298. Copyright 2014, Royal Society of Chemistry.

## 7. HBPs for antimicrobial applications

Microbial infection has become one of the most serious complications in several areas, particularly in drug delivery, medical devices, health care and hygienic applications.<sup>299</sup> During the past few years, a variety of antimicrobial agents, including bactericides, disinfectants and antibiotics have already made a great achievement in antimicrobial treatment. However, these antimicrobial agents of low molecular weight still suffer from many disadvantages, such as environmental toxicity, short-term antimicrobial ability and antibacterial resistance.<sup>300,301</sup> Recently, polymer-based antimicrobial agents have raised intense interest due to their advantages of enhanced antimicrobial activity, low toxicity and decreased potential for resistance development.<sup>299,302,303</sup> Among them, antimicrobial agents based on HBPs are much more attractive because HBPs can be easily obtained in large scale by a one-step preparation and are even commercially available.<sup>14</sup>

Inorganic metallic nanoparticles, especially silver or gold nanoparticles (AgNPs or

AuNPs), are widely used antimicrobial agents in many biomedical fields. However, metallic nanoparticles often tend to congregate and separate from solutions, which lead to the decreased antimicrobial efficiency.<sup>14</sup> Therefore, many efforts have been made to find suitable polymeric matrices to prepare stable organic/inorganic hybrid nanocomposites with excellent antimicrobial activity. As a result, HBPs are proven to be the promising candidates for achieving this goal as they have better control over size, shape and structure of metal-nanoparticles than that of linear polymers. Zhu and coworkers prepared stable colloid AgNPs (or AuNPs) system in aqueous solution by utilizing the amine-terminated HPAMAM (HPAMAM-NH<sub>2</sub>) or dimethylamine-terminated HPAMAMs-N(CH<sub>3</sub>)<sub>2</sub> as both the reductant and stabilizer through a facile and green method.<sup>304,305</sup> These novel HBP/Ag(or Au) hybrid nanocomposites exhibited excellent antibacterial activity against Gram-positive and Gram-negative bacteria with the bacterial inhibition ratio up to 98% at a low silver or gold content of less than 3.0 µg mL<sup>-1</sup>. Later, the same authors further synthesized a series of cationic hyperbranched poly(sulfone-amine)s (PSAs) with different branched architectures and then used these PSAs as templates to prepare PSA/Ag nanocomposites through an in situ approach (Fig. 28).<sup>306</sup> The antimicrobial activity of PSAs and their polymer/silver (PSA/Ag) nanocomposites was investigated. As expected, the polymer DB had a great influence on the antimicrobial activity, which was quite different for PSAs and PSA/Ag nanocomposites. It was found that the antimicrobial activity of PSAs decreased with the DB due to the reduced zeta-potential and low toxicity of the HBPs. On the contrary, PSA/Ag nanocomposites showed an enhanced antimicrobial activity with an increasing DB owing to the high specific surface of small AgNPs. Besides these, several other research teams have also made important contributions to this area.<sup>307,308</sup> For example, Lin and coworkers prepared amino functional AgNPs with amino-terminated HBP (HBP-NH<sub>2</sub>) by one-step reaction and then grafted on the oxidized cotton fabric to obtain antibacterial cotton fabric with excellent antibacterial activity and laundering durability.<sup>307</sup> Furthermore, HBPs are also good matrices to produce metal oxide nanoparticles with antimicrobial activity, such as ZnO NPs and Fe<sub>3</sub>O<sub>4</sub> NPs.<sup>309,310</sup>

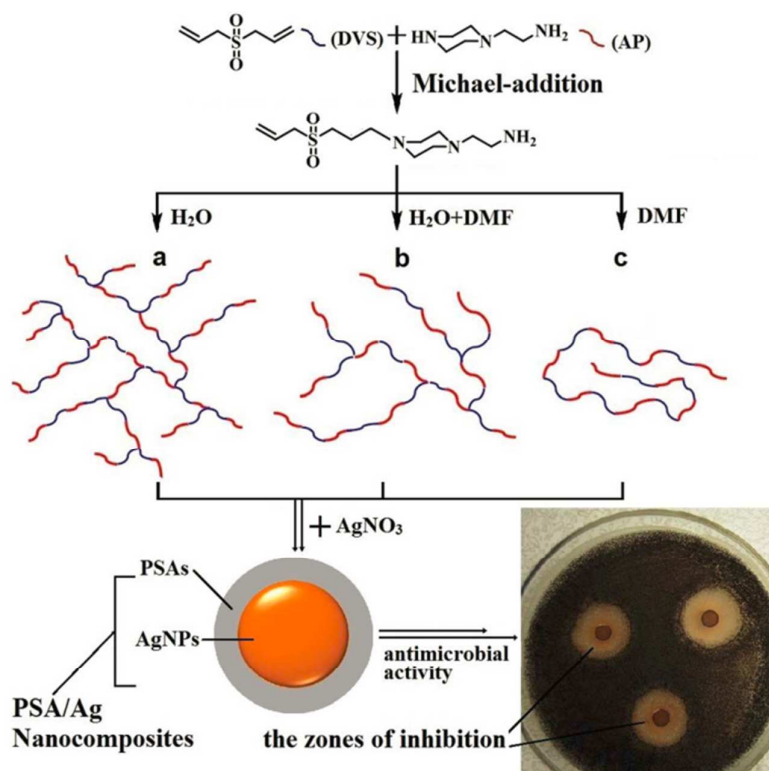


**Fig. 28** Synthesis route and antimicrobial evaluation of PSAs and PSA/Ag nanocomposites: (a) highly branched PSA was obtained in pure water; (b) slightly branched PSA obtained in a mixed solvent of water and DMF; (c) linear PSA was obtained in pure DMF. Reproduced with permission from ref. 306. Copyright 2012, Royal Society of Chemistry.

Besides the HBP/metal hybrid nanocomposites, cationic HBPs and antibiotics-containing HBPs are also promising candidates for future development of antimicrobial agents. Since quaternary ammonium compounds are the most useful antiseptics and disinfectants, they have been actively used in the preparation of antimicrobial polymers.<sup>301,311,312</sup> For instance, Kang and coworkers modified stainless steel (SS) surfaces with quaternary ammonium cations containing HBPs.<sup>312</sup> In comparison to the linear polymer-functionalized surfaces, the HBP-modified SS surfaces exhibited superior antibacterial efficacy. Besides, construction of antimicrobial HBPs by using small molecular antibiotics as a composition unit is also very appealing. Zhu and coworkers reported a kind of multifunctional hyperbranched glycoconjugated polymers prepared from natural aminoglycoside through Michael-addition polymerization.<sup>313</sup> By incorporating gentamicin into the polymer backbone, the resultant hyperbranched glycoconjugated polymers were facilitated with multiple advantages, such as good antibacterial and antitumor activities, high transfection and low cytotoxicity.

## 8. Antifouling materials based on HBPs

Biofouling marks a severe problem for polymeric materials applied as artificial devices, biosensors, immunoassays, drug delivery systems and others.<sup>314</sup> For example, protein adsorption that occurs after implantation of biomaterials can initiate a cascade of host responses, such as blood coagulation, platelet activation, thrombus formation, bacterial infection and other undesirable responses.<sup>315,316</sup> To overcome these problems, it is of crucial importance to explore novel antifouling materials.

In the past few years, linear polymers have been used to fabricate antifouling materials.<sup>317-319</sup> Especially, PEG, a flexible, hydrophilic and water soluble polyether, is the most useful and prominent example.<sup>320</sup> Nevertheless, it exhibits the disadvantage of thermal instability and rapid autooxidation to yield aldehydes and acids.<sup>321,322</sup> As a solution, Haag and coworkers prepared SAMs of HPG on gold surface which exhibited similar protein resistance as PEG SAMs but higher thermal and oxidative stability.<sup>322</sup> In the following years, a large number of HPG-based antifouling materials have been reported.<sup>323-325</sup> In a recent example, Kang and coworkers constructed novel HPG-grafted microporous membranes via simple alkyne-azide click reaction. The microporous membranes were fabricated from amphiphilic graft copolymer of poly(vinylidene fluoride) (PVDF-*g*-PDMAEMA) by phase inversion in an aqueous medium. After quaternization by propargyl bromide, azido-terminated HPG (HPG-N<sub>3</sub>) was further functionalized to the membrane surfaces by reacting with the pendant propargyl groups. The resulting membranes exhibited good resistance to protein adsorption and fouling.<sup>325</sup>

Besides the antifouling materials made with HPG, many other HBP-based materials are underway to realize optimized antifouling properties. Since PEI-coated surfaces can offer high resistance for protein adsorption due to the conformational flexibility and hydrophilicity,<sup>326,327</sup> polymeric thin films of its derivative, HPEI, were also intensively explored.<sup>328,329</sup> For instance, Nicholls and coworkers immobilized commercial available HPEI to gold surfaces using traditional carbodiimide chemistry. As expected, these HPEI films were capable of resisting the adsorption of a series of different proteins at a low concentration of 1 mg/mL, which was comparable to that of PEGylated surfaces under similar conditions. Especially, these polymeric films could hold the stability under aqueous media for at least 6 months.<sup>330</sup> Voit and coworkers made a series of hyperbranched polyesters films from hyperbranched polyesters with different DB, backbone structure, flexibility as well as the polarity. The film properties could be controlled from protein active to protein repelling by changing the backbone structure from aromatic, aromatic-aliphatic to aliphatic.<sup>330</sup> Recently, Zhu and coworkers reported a new methodology to optimize the protein resistant properties of polymeric film on a gold surface by adjusting the branched architecture

of hydrophilic polymer.<sup>331</sup> In this system, a series of poly(*S*-(4-vinyl) benzyl *S'*-propyltrithiocarbonate)-*co*-(poly(ethylene glycol) methacrylate)s (poly(VBPT-*co*-PEGMA)s) with different DB were synthesized by RAFT polymerization and then immobilized on the gold surface via thiols exposed after aminolysis reaction (Fig. 29). A uniform film with high stability and multifunctionality was obtained by an increased content of thiol groups caused by increasing the DB of poly(VBPT-*co*-PEGMA)s. These polymer-coated gold surfaces showed a good property of protein and cell resistance compared to the bare gold surface.

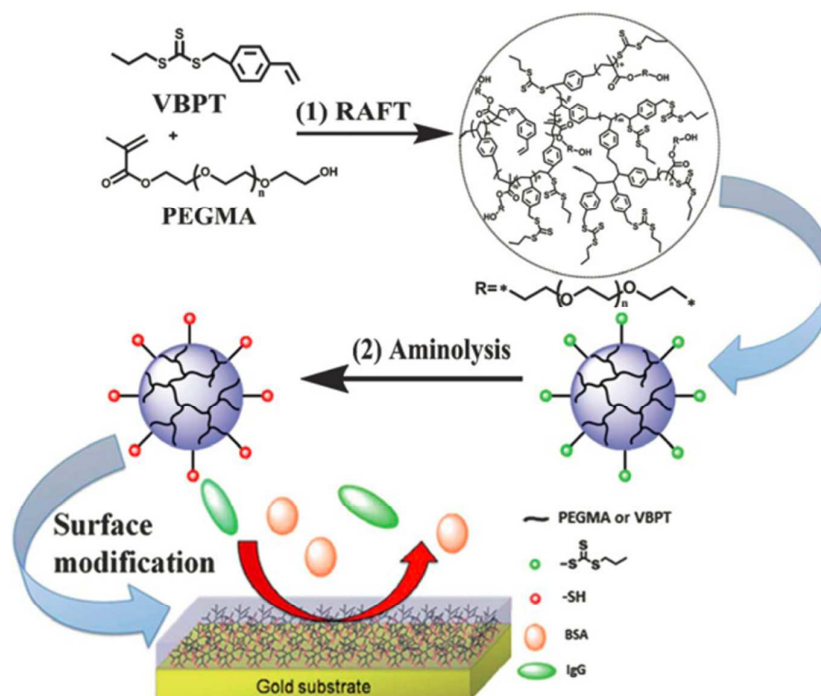


**Fig. 29** Synthesis route of branched poly(VBPT-*co*-PEGMA)s and preparation of branched poly(VBPT-*co*-PEGMA)s-coated gold surfaces. Reproduced with permission from ref. 331. Copyright 2012, Royal Society of Chemistry.

In addition, Wooley and coworkers have focusing their efforts on the construction of novel amphiphilic cross-linked polymer networks (HBFP-PEG) comprised of hyperbranched fluoropolymers (HBFP) and linear PEG as antifouling coatings.<sup>332-336</sup> In a recent example, they reported a dual-mode surface which combined both passive and active modes of antifouling for marine application.<sup>336</sup> Herein, a new generation of HBFP-*star*-PEG was obtained by crosslinking HBFP bearing ethylene glycol units with PEG. Followed by deposition and curing, the passive antifouling coatings were provided by the complex surface topography and chemical heterogeneity. HBFP-*star*-PEG was further decorated with an antifouling agent noradrenaline (NA) to form the active mode of fouling deterrence. This study demonstrated a new strategy

for combining actively antifouling moieties onto a passively antifouling network, leading to superior antifouling coatings.

### 9. Cytomimetic chemistry from HBPs

Using vesicles as model membranes to mimic cellular biological processes is emerging as an interesting and significant topic in recent years.<sup>337,338</sup> A variety of vesicles, such as lipid vesicles (liposomes), surfactant vesicles and block copolymer vesicles (polymersomes) have already been selected for this application.<sup>338-340</sup> The membrane fluidity of liposomes is excellent to ensure the deformability characteristics of biomembranes, however, their stability is not high enough due to the small molecular nature. On the contrary, polymersomes, which are stable and designable, show lower fluidity.<sup>13</sup> Fortunately, the HBP vesicles successfully combine good membrane fluidity with strong stability, offering a satisfying model membrane to mimic cellular morphologies and functions.

Recently, Zhou and Yan reported the real-time membrane fusion and fission of individual HBP vesicles to mimic biomembranes (Fig. 30).<sup>341,342</sup> The real-time membrane fusion process of two HBP vesicles was induced by ultrasonication as shown in Fig 30A, which included four successive stages: membrane contact, formation of a center wall, symmetric expanding of the fusion pore and complete fusion.<sup>341</sup> It was proposed that for very close apposition of membranes and small perturbations suffice to induce the fusion. The same authors also successfully observed a “cooperative fission” process of a mother vesicle with an inside daughter vesicle, which was triggered by adding glucose into the solution.<sup>342</sup> The fission event of daughter vesicle underwent five steps: suspension inside the mother vesicle (Fig. 30B a), coalescence with the mother vesicle membrane (Fig. 30B b and c), protrusion from the mother vesicle to form a pear structure (Fig. 30B d-i), fission (Fig. 30B m and n) and retraction into the mother vesicle (Fig. 30B o-s). The daughter vesicle suspended inside the mother vesicle for several minutes until the next cycle of fission. A total of three fission cycles of the daughter vesicle could be found and each one took longer time than the previous one.

Cell aggregation or cellular agglomeration through specific intracellular molecular recognition plays a critical role in various biological activities, including hemostasis, immune response, inflammation embryogenesis and the development of neuronal tissue. Since HBPs have a plenty of terminal functional groups, HBP vesicles have advantages in exerting multivalent intervesicular interactions to mimic the biomembranes. Very recently, Zhou and coworkers realized a large-scale vesicle aggregation process by using giant HBP vesicles as the building blocks and intervesicular host-guest interactions as the driving force.<sup>343,344</sup> In these cases,

controllable reversible driving force based on light-responsive host-guest interactions between  $\beta$ -CD and azobenzene (Azo) groups was firstly investigated.<sup>343</sup> The authors prepared two kinds of cell-size HBP vesicles by a co-assembly method and then mixed them to achieve large-scale macroscopic aggregation. This process was not only highly efficient, but also reversible under alternating irradiation with UV and visible light. Throughout the process, in real time vesicle fusion could be observed frequently and the aggregate dimension could be controlled by changing the vesicle concentration and composition. Soon after that, in another example of large-scale cytomimetic aggregation from HBP vesicles, a stronger intervesicular interaction, coming from  $\beta$ -CD/adamantane (AD) molecular recognition, was explored to trigger a more efficient vesicular aggregation.<sup>344</sup> Due to the stronger intervesicular  $\beta$ -CD/AD interaction, frequent fusion events and larger aggregates could be observed.

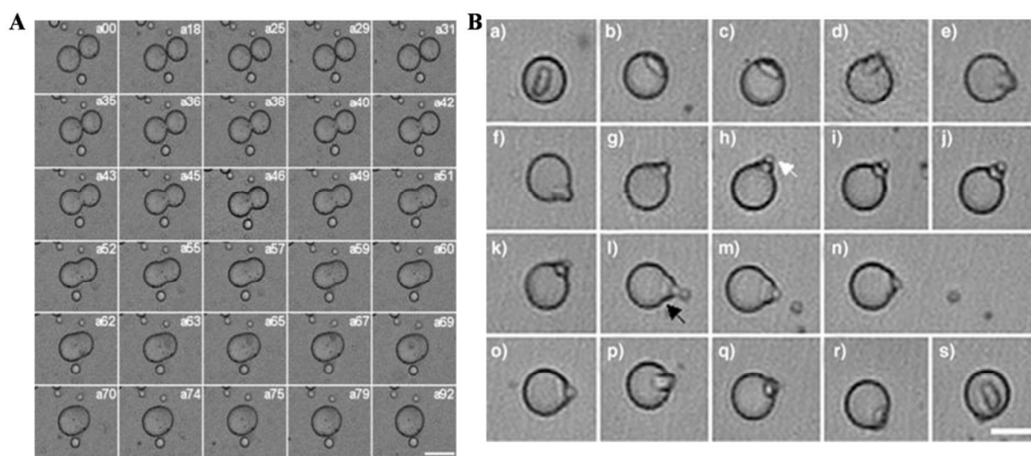


**Fig. 30** (A) Time sequence of fusion images of two giant polymer vesicles. The number in the symbol labeled on each images denotes the elapsed time (in seconds), and the time of first images is set as zero. The scale bar represents 50  $\mu\text{m}$ . (B) Cooperative fission of a daughter-vesicle inside a mother vesicle. The scale bar represents 25  $\mu\text{m}$ . The time of images (a) is set as 0, and the elapsed times for the images are 33 (b), 64 (c), 105 (d), 130 (e), 134 (f), 165 (g), 170 (h), 179 (i), 182 (j), 190 (k), 243 (l), 246 (m), 263 (n), 273 (o), 421 (p), 620 (q), 719 (r) and 920 s (s), respectively. Reprinted with permission from ref. 341 and 342. Copyright 2005, American Chemical Society and 2005, Wiley.

Besides the noncovalent driving force for cell-mimetic vesicle aggregation, some strong covalent bonds were proven to be promising driving forces, like those formed by a thiol-ene click-chemistry reaction or a copper-catalysed azide-alkyne cycloaddition click-chemistry reaction.<sup>345,346</sup> Therefore, Zhou and coworkers creatively applied the copper-catalyzed azide-alkyne cycloaddition click chemistry in the cytomimetic aggregation of HBP vesicles and the vesicle aggregation process was systematically investigated.<sup>347</sup> Alkynyl or azide groups containing HBPs were firstly

synthesized, followed by respectively preparing  $N_3$ -based and Alk-based HBP vesicles through a co-assembly strategy. When mixing these two kinds of HBP vesicles together at a ratio of azide to alkyne groups of about 1:1, macroscopic vesicle aggregates were obtained. In the aggregation process, both the vesicle fusion and lateral phase separation on the vesicle membrane happened. Interestingly, the fusion rate and phase separation degree were dependent on the content of azide and alkyne groups, whereas the vesicle fusion could be completely inhibited while using the micelles as desmosome mimics to connect HBP vesicles (Fig. 31). This work has extended the controllable cytomimetic vesicle aggregation process by using the covalent bonds as the driving force.

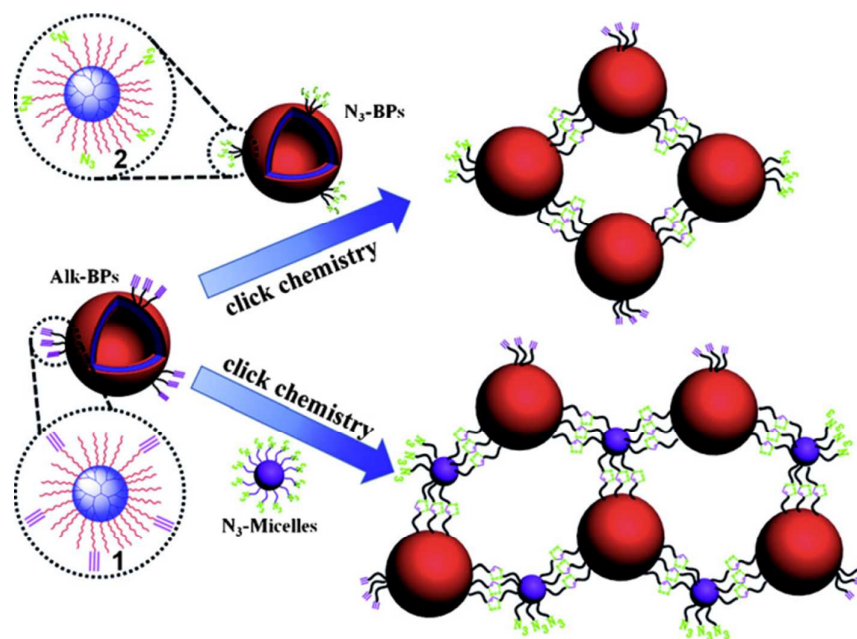


**Fig. 31** Schematic representation of aggregation of HBP vesicles triggered by click chemistry between alkyne and azide groups. Reproduced with permission from ref. 347. Copyright 2012, Wiley.

Besides the aforementioned potential fields, various new bioapplications of HBPs could be explored and extended in accordance with specific requirements based on the unique structure and properties of HBPs.

## 10. Conclusions and perspectives

In this review we have summarized recent research progress in bioapplications of HBPs. The potential for HBPs in biological and biomedical applications is clearly huge, and herein we have reviewed bioapplications in therapy (drug delivery, gene transfection, and protein delivery), bioimaging, biomineralization, tissue engineering,

antimicrobial, antifouling and cytomimetic chemistry. Obviously, during the past few years, the application of HBPs in biological systems has experienced rapid growth. Recent research has shown that HBPs are useful tools for solving fundamental problems in biological and biomedical fields. Their successful applications in many different biological realms confirm their high potential and hold great promise concerning the development of future biological and biomedical science. One apparent advantage of HBPs for bioapplications is their three-dimensional globular structure and multivalent character, which provides excellent platforms for designing and constructing multifunctional systems combining targeting, imaging, diagnostics and therapy. It will stimulate the continuously growing interest in this research field. Another attractive feature of HBPs is their simple preparation, which makes them accessible to a wide range of research groups. As the synthesis of HBPs is well known to occur by simple one-pot polymerization, it is likely to promote interdisciplinary collaborations between polymer groups and research teams focused on bioapplications within hospitals and medical research institutes. Such collaborations can promote the interdisciplinary researches among polymer chemistry, biology, biomedicine, nano-science and technology.

Despite tremendous progress has been made during the past decade, the development and bioapplications of HBPs is still in its infancy and a lot of discoveries still lie ahead. Firstly, the structure of HBPs still has some limitations for many of these potential bioapplications. Compared with perfect dendrimers, the less well-defined structure of HBPs is and will be an obvious drawback. The broad polydispersity can complicate the characterization of HBPs as well their studies for biomedical applications. Therefore, the controlled synthetic methodologies that yield well-defined HBPs with reasonable polydispersity are primarily required to translate this state-of-the-art macromolecule from the laboratory to clinic. Furthermore, a continuous effort is necessary to modify and tailor HBPs architectures to fit the future demands of biological and biomedical applications. So far, we still have only vague answers concerning what kind of structures satisfy the target applications and the relationship between structures and functions remain to be further explored.

On the base of the current development state of HBPs for bioapplications, it is expected that a great deal of potential for HBPs still remains to be explored. Especially, although a large amount of HBPs have been widely studied for drug/protein delivery, gene transfection, bioimaging and tissue engineering, they have not been applied in the clinic. One of the next big challenges is to transfer these HBPs presented herein to *in vivo* experiments, including on humans. Indeed, HBPs have made great progress in therapeutic and diagnostic applications and a larger number of excellent HBP systems have been applied in these fields. However, the *in vivo* studies, even in mice, are still rare. This may be mainly explained by some obstacles

encountered before clinical trials. First of all, the HBP formulation is difficult to scale-up while maintaining all the parameters that would govern *in vivo* behavior and therapeutic efficiency (e.g., the DB and molecular weight of the HBPs, drug loading and biological activity). Secondly, the commonly employed HBPs for biomedical applications perhaps do not possess perfect biocompatibility and biodegradability, which is indispensable in clinical application. Consequently, an urgent need to overcome these problem would be to develop more robust and reproducible, scalable synthesis methodologies to readily fulfill the needs of clinical trials. Moreover, bioapplications of HBPs such as antibiosis, antifouling and cytomimetic chemistry may definitely merit further investigation.

Finally, considering future advanced materials for bioapplications, the integration of functional HBPs and other topological polymers might be useful methods for creating new functional materials which would make up for the defects of each component. We believe that the progress of HBP research and development will spread much faster than predicted and HBPs may play an even more important role in biological and biomedical sciences than imagined as an increased number of commercialized HBPs are emerging in the future.

### Acknowledgements

We thank the National Basic Research Program (2012CB821500, 2013CB834506), National Natural Science Foundation of China (21374062, 21204048), the Open Project of State Key Laboratory of Chemical Engineering (SKL-ChE-12C04), and China National Funds for Distinguished Young Scientists (21025417) for financial support.

### Notes and references

- 1 P. J. Flory, *J. Am. Chem. Soc.*, 1952, **74**, 2718-2723.
- 2 Y. H. Kim and O. W. Webster, *Polym. Prepr. (Am. Chem. Soc. Div. Polym. Chem.)*, 1988, **29**, 310-311.
- 3 Y. H. Kim and O. W. Webster, *J. Am. Chem. Soc.*, 1990, **112**, 4592-4593.
- 4 D. A. Tomalia and J. M. J. Fréchet, *J. Polym. Sci., Part A: Polym. Chem.*, 2002, **40**, 2719-2728.
- 5 C. Gao and D. Y. Yan, *Prog. Polym. Sci.*, 2004, **29**, 183-275.
- 6 A. Carlmark, C. Hawker, A. Hult and M. Malkoch, *Chem. Soc. Rev.*, 2009, **38**, 352-362.
- 7 B. I. Voit and A. Lederer, *Chem. Rev.*, 2009, **109**, 5924-5973.
- 8 S. Peleshanko and V. V. Tsukruk, *Prog. Polym. Sci.*, 2008, **33**, 523-580.
- 9 D. Y. Yan, C. Gao and H. Frey, *Hyperbranched Polymers*, John Wiley & Sons,

- Inc., Hoboken, NJ, 2011.
- 10 C. R. Yates and W. Hayes, *Eur. Polym. J.*, 2004, **40**, 1257-1281.
  - 11 D. Konkolewicz, M. J. Monteiro and S. b. Perrier, *Macromolecules*, 2011, **44**, 7067-7087.
  - 12 M. Jikei and M. Kakimoto, *Prog. Polym. Sci.*, 2001, **26**, 1233-1285.
  - 13 Y. F. Zhou and D. Y. Yan, *Chem. Commun.*, 2009, 1172-1188.
  - 14 Y. F. Zhou, W. Huang, J. Y. Liu, X. Y. Zhu and D. Y. Yan, *Adv. Mater.*, 2010, **22**, 4567-4590.
  - 15 E. Žagar and M. Žigon, *Prog. Polym. Sci.*, 2011, **36**, 53-88.
  - 16 D. Wilms, S.-E. Stiriba and H. Frey, *Acc. Chem. Res.*, 2010, **43**, 129-141.
  - 17 R. J. Dong, Y. F. Zhou and X. Y. Zhu, *Acc. Chem. Res.*, 2014, ASAP.
  - 18 X. Y. Zhu, Y. F. Zhou and D. Y. Yan, *J. Polym. Sci., Part B: Polym. Phys.*, 2011, **49**, 1277-1286.
  - 19 J. Khandare, M. Calderon, N. M. Dagia and R. Haag, *Chem. Soc. Rev.*, 2012, **41**, 2824-2848.
  - 20 H. B. Jin, W. Huang, X. Y. Zhu, Y. F. Zhou and D. Y. Yan, *Chem. Soc. Rev.*, 2012, **41**, 5986-5997.
  - 21 M. Calderon, M. A. Quadir, S. K. Sharma and R. Haag, *Adv. Mater.*, 2010, **22**, 190-218.
  - 22 M. Irfan and M. Seiler, *Ind. Eng. Chem. Res.*, 2010, **49**, 1169-1196.
  - 23 Q. Zhu, F. Qiu, B. S. Zhu and X. Y. Zhu, *RSC Adv.*, 2013, **3**, 2071-2083.
  - 24 C. M Paleos, D. Tsiourvas, Z. Sideratou and L.-A. Tziveleka, *Expert Opin. Drug Deliv.*, 2010, **7**, 1387-1398.
  - 25 W. Yang, C.-Y. Pan, M.-D. Luo and H.-B. Zhang, *Biomacromolecules*, 2010, **11**, 1840-1846.
  - 26 C. Kojima, K. Yoshimura, A. Harada, Y. Sakanishi and K. Kono, *J. Polym. Sci., Part A: Polym. Chem.*, 2010, **48**, 4047-4054.
  - 27 Z. Guo, Y. W. Zhang, W. Huang, Y. F. Zhou and D. Y. Yan, *Macromol. Rapid Commun.*, 2008, **29**, 1746-1751.
  - 28 X. Meng, Q. G. He, H. M. Cao and J. G. Cheng, *Chinese Chem. Lett.*, 2011, **22**, 725-728.
  - 29 R. J. Dong, L. Z. Zhou, J. L. Wu, C. L. Tu, Y. Su, B. S. Zhu, H. C. Gu, D. Y. Yan and X. Y. Zhu, *Chem. Commun.*, 2011, **47**, 5473-5475.
  - 30 R. Barbey and S. Perrier, *ACS Macro Lett.*, 2013, **2**, 366-370.
  - 31 J. Y. Liu, Y. Pang, Z. Zhu, D. L. Wang, C. T. Li, W. Huang, X. Y. Zhu and D. Y. Yan, *Biomacromolecules*, 2013, **14**, 1627-1636.
  - 32 Z. F. Jia, H. Chen, X. Y. Zhu and D. Y. Yan, *J. Am. Chem. Soc.*, 2006, **128**, 8144-8145.
  - 33 C. Schüll and H. Frey, *Polymer*, 2013, **54**, 5443-5455.

- 34 J.-Y. Yin, H.-J. Liu, S. Jiang, Y. Chen and Y. Yao, *ACS Macro Lett.*, 2013, **2**, 1033-1037.
- 35 Y. F. Shi, C. L. Tu, R. B. Wang, J. Y. Wu, X. Y. Zhu and D. Y. Yan, *Langmuir*, 2008, **24**, 11955-11958.
- 36 H. W. Duan and S. M. Nie, *J. Am. Chem. Soc.*, 2007, **129**, 3333-3338.
- 37 G. S. Tong, T. Liu, S. M. Zhu, B. S. Zhu, D. Y. Yan, X. Y. Zhu and L. Zhao, *J. Mater. Chem.*, 2011, **21**, 12369-12374.
- 38 Y. F. Shi, L. B. Liu, C. L. Tu, L. J. Zhu, D. Y. Yan, G. L. Li, F. L. Guo and X. Y. Zhu, *J. Appl. Polym. Sci.*, 2011, **122**, 1077-1083.
- 39 D. L. Wang, Y. Su, C. Y. Jin, B. S. Zhu, Y. Pang, L. J. Zhu, J. Y. Liu, C. L. Tu, D. Y. Yan and X. Y. Zhu, *Biomacromolecules*, 2011, **12**, 1370-1379.
- 40 S. Lee, K. Saito, H. R. Lee, M. J. Lee, Y. Shibasaki, Y. Oishi and B. S. Kim, *Biomacromolecules*, 2012, **13**, 1190-1196.
- 41 W. Y. Dong, Y. F. Zhou, D. Y. Yan, H. Q. Li and Y. Liu, *Phys. Chem. Chem. Phys.*, 2007, **9**, 1255-1262.
- 42 Z. Q. Shi, Y. F. Zhou and D. Y. Yan, *Macromol. Rapid Commun.*, 2008, **29**, 412-418.
- 43 Y. M. Xia, Y. M. Wang, Y. P. Wang, C. L. Tu, F. Qiu, L. J. Zhu, Y. Su, D. Y. Yan, B. S. Zhu and X. Y. Zhu, *Colloids Surf., B*, 2011, **88**, 674-681.
- 44 L. J. Zhu, C. L. Tu, B. S. Zhu, Y. Su, Y. Pang, D. Y. Yan, J. L. Wu and X. Y. Zhu, *Polym. Chem.*, 2011, **2**, 1761-1768.
- 45 Y. Jin, L. Song, D. L. Wang, F. Qiu, D. Y. Yan, B. S. Zhu and X. Y. Zhu, *Soft Matter*, 2012, **8**, 10017-10025.
- 46 J. Zhang, H.-J. Liu, Y. Yuan, S. Jiang, Y. Yao and Y. Chen, *ACS Macro Lett.*, 2013, **2**, 67-71.
- 47 J. Xu, S. Luo, W. Shi, and S. Liu, *Langmuir*, 2006, **22**, 989-997.
- 48 Y.-Z. You, C.-Y. Hong, C.-Y. Pan and P.-H. Wang, *Adv. Mater.*, 2004, **16**, 1953-1957.
- 49 H. Y. Hong, Y. Y. Mai, Y. F. Zhou, D. Y. Yan and Y. Chen, *J. Polym. Sci., Part A: Polym. Chem.*, 2008, **46**, 668-681.
- 50 Z. F. Jia, G. L. Li, Q. Zhu, D. Y. Yan, X. Y. Zhu, H. Chen, J. L. Wu, C. L. Tu and J. Sun, *Chem. Eur. J.*, 2009, **15**, 7593-7600.
- 51 M. Schömer, J. Seiwert and H. Frey, *ACS Macro Lett.*, 2012, **1**, 888-891.
- 52 S. Son, E. Shin and B. S. Kim, *Biomacromolecules*, 2014, **15**, 628-634.
- 53 Y. Liu, C. R. Yu, H. B. Jin, B. B. Jiang, X. Y. Zhu, Y. F. Zhou, Z. Y. Lu and D. Y. Yan, *J. Am. Chem. Soc.*, 2013, **135**, 4765-4770.
- 54 C.-J. Chen, G.-Y. Liu, X.-S. Liu, D.-D. Li and J. Ji, *New J. Chem.*, 2012, **36**, 694-701.
- 55 E. Burakowska, S. C. Zimmerman and R. Haag, *Small*, 2009, **5**, 2199-2204.

- 56 R. J. Dong, Y. Liu, Y. F. Zhou, D. Y. Yan and X. Y. Zhu, *Polym. Chem.*, 2011, **2**, 2771-2774.
- 57 J. Y. Liu, Y. Pang, J. Chen, P. Huang, W. Huang, X. Y. Zhu and D. Y. Yan, *Biomaterials*, 2012, **33**, 7765-7774.
- 58 J. Y. Liu, Y. Pang, W. Huang, Z. Zhu, X. Y. Zhu, Y. F. Zhou and D. Y. Yan, *Biomacromolecules*, 2011, **12**, 2407-2415.
- 59 J. Y. Liu, Y. Pang, W. Huang, X. H. Huang, L. L. Meng, X. Y. Zhu, Y. F. Zhou and D. Y. Yan, *Biomacromolecules*, 2011, **12**, 1567-1577.
- 60 J. Y. Liu, W. Huang, Y. Pang, P. Huang, X. Y. Zhu, Y. F. Zhou and D. Y. Yan, *Angew. Chem. Int. Ed.*, 2011, **50**, 9162-9166.
- 61 J. Y. Liu, Y. Pang, Z. Zhu, D. L. Wang, C. T. Li, W. Huang, X. Y. Zhu and D. Y. Yan, *Biomacromolecules*, 2013, **14**, 1627-1636.
- 62 D. Y. Yan, Y. F. Zhou and J. Hou, *Science* 2004, **303**, 65-67.
- 63 Y. W. Zhang, W. Huang, Y. F. Zhou and D. Y. Yan, *Chem. Commun.* 2007, 2587-2589.
- 64 M. Ornatska, S. Peleshanko, K. L. Genson, B. Rybak, K. N. Bergman and V. V. Tsukruk, *J. Am. Chem. Soc.* 2004, **126**, 9675-9684.
- 65 Y. F. Zhou and D. Y. Yan, *Angew. Chem. Int. Ed. Engl.* 2004, **43**, 4896-4899.
- 66 Y. Y. Mai, Y. F. Zhou and D. Y. Yan, *Small* 2007, **3**, 1170-1173.
- 67 C. H. Liu, C. Gao and D. Y. Yan, *Angew. Chem. Int. Ed. Engl.* 2007, **46**, 4128-4131.
- 68 X. Y. Sun, W. Huang, Y. F. Zhou and D. Y. Yan, *Phys. Chem. Chem. Phys.* 2010, **12**, 11948-11953.
- 69 Y. Y. Mai, Y. F. Zhou and D. Y. Yan, *Macromolecules* 2005, **38**, 8679-8686.
- 70 J. Mao, P. H. Ni, Y. Y. Mai and D. Y. Yan, *Langmuir* 2007, **23**, 5127-5134.
- 71 Y. F. Zhou, D. Y. Yan, W. Y. Dong, and Y. Tian, *J. Phys. Chem. B*, 2007, **111**, 1262-1270.
- 72 A. Sunder, R. Hanselmann, H. Frey and R. Mülhaupt, *Macromolecules*, 1999, **32**, 4240-4246.
- 73 M. Hu, M. S. Chen, G. L. Li, Y. Pang, D. L. Wang, J. L. Wu, F. Qiu, X. Y. Zhu and J. Sun, *Biomacromolecules*, 2012, **13**, 3552-3561.
- 74 C. Tonhauser, C. Schüll, C. Dingels and H. Frey, *ACS Macro Lett.*, 2012, **1**, 1094-1097.
- 75 Y. Pang, J. Y. Liu, J. L. Wu, G. L. Li, R. B. Wang, Y. Su, P. He, X. Y. Zhu, D. Y. Yan and B. S. Zhu, *Bioconjugate Chem.*, 2010, **21**, 2093-2102.
- 76 D. Steinhilber, A. L. Sisson, D. Mangoldt, P. Welker, K. Licha and R. Haag, *Adv. Funct. Mater.*, 2010, **20**, 4133-4138.
- 77 R. A. Shenoi, J. K. Narayanannair, J. L. Hamilton, B. F. Lai, S. Horte, R. K. Kainthan, J. P. Varghese, K. G. Rajeev, M. Manoharan and J. N. Kizhakkedathu, *J.*

- Am. Chem. Soc.*, 2012, **134**, 14945-14957.
- 78 J. Y. Liu, W. Huang, Y. F. Zhou and D. Y. Yan, *Macromolecules*, 2009, **42**, 4394-4399.
- 79 J. Y. Liu, W. Huang, Y. Pang, X. Y. Zhu, Y. F. Zhou and D. Y. Yan, *Biomaterials*, 2010, **31**, 5643-5651.
- 80 J. Y. Liu, Y. Pang, W. Huang, X. Y. Zhu, Y. F. Zhou and D. Y. Yan, *Biomaterials*, 2010, **31**, 1334-1341.
- 81 J. Y. Liu, W. Huang, Y. Pang, X. Y. Zhu, Y. F. Zhou and D. Y. Yan, *Biomacromolecules*, 2010, **11**, 1564-1570.
- 82 X. Chang and C. M. Dong, *Biomacromolecules*, 2013, **14**, 3329-3337.
- 83 Z. Kadlecova, L. Baldi, D. Hacker, F. M. Wurm and H.-A. Klok, *Biomacromolecules*, 2012, **13**, 3127-3137.
- 84 M. Scholl, T. Q. Nguyen, B. Bruchmann and H.-A. Klok, *J. Polym. Sci., Part A: Polym. Chem.*, 2007, **45**, 5494-5508.
- 85 M. Ahmed, B. F. Lai, J. N. Kizhakkedathu and R. Narain, *Bioconjugate Chem.*, 2012, **23**, 1050-1058.
- 86 M. S. Chen, J. L. Wu, L. Z. Zhou, C. Y. Jin, C. L. Tu, B. S. Zhu, F. Wu, Q. Zhu, X. Y. Zhu and D. Y. Yan, *Polym. Chem.*, 2011, **2**, 2674-2682.
- 87 Y. Tao, L. Zhang, Fan Yan and X. Wu, *Biomacromolecules*, 2007, **8**, 2321-2328.
- 88 J. Hu, G. Zhang and S. Liu, *Chem. Soc. Rev.*, 2012, **41**, 5933-5949.
- 89 M. Calderon, R. Graeser, F. Kratz and R. Haag, *Bioorg. Med. Chem. Lett.*, 2009, **19**, 3725-3728.
- 90 K. Abu Ajaj, R. Graeser, I. Fichtner and F. Kratz, *Cancer Chemother Pharmacol.*, 2009, **64**, 413-418.
- 91 A. Warnecke, I. Fichtner, G. Sass and F. Kratz, *Arch. Pharm. Chem. Life Sci.*, 2007, **340**, 389-395.
- 92 M. R. Radowski, A. Shukla, H. von Berlepsch, C. Bottcher, G. Pickaert, H. Rehage and R. Haag, *Angew. Chem. Int. Ed.*, 2007, **46**, 1265-1269.
- 93 J. Zou, W. Shi, J. Wang and J. Bo, *Macromol. Biosci.*, 2005, **5**, 662-668.
- 94 L. Ye, K. Letchford, M. Heller, R. Liggins, D. Guan, J. N. Kizhakkedathu, D. E. Brooks, J. K. Jackson and H. M. Burt, *Biomacromolecules*, 2010, **12**, 145-155.
- 95 R. K. Kainthan, C. Mugabe, H. M. Burt and D. E. Brooks, *Biomacromolecules*, 2008, **9**, 886-895.
- 96 M. Krämer, M. Kopaczynska, S. Krause and R. Haag, *J. Polym. Sci., Part A: Polym. Chem.*, 2007, **45**, 2287-2303.
- 97 C. H. Liu, C. Gao and D. Y. Yan, *Macromolecules*, 2006, **39**, 8102-8111.
- 98 P. Kolhe, J. Khandare, O. Pillai, S. Kannan, M. Lieh-Lai and R. Kannan, *Pharm. Res.*, 2004, **21**, 2185-2195.
- 99 O. Perumal, J. Khandare, P. Kolhe, S. Kannan, M. Lieh-Lai, and R. Kannan,

- Bioconjugate Chem.*, 2009, **20**, 842-846.
- 100 G. L. Li, J. Y. Liu, Y. Pang, R. B. Wang, L. M. Mao, D. Y. Yan, X. Y. Zhu and J. Sun, *Biomacromolecules*, 2011, **12**, 2016-2026.
- 101 S. Lee, K. Saito, H. R. Lee, M. J. Lee, Y. Shibasaki, Y. Oishi and B. S. Kim, *Biomacromolecules*, 2012, **13**, 1190-1196.
- 102 Y. Y. Zhuang, Y. Su, Y. Peng, D. L. Wang, H. P. Deng, X. D. Xi, X. Y. Zhu and Y. F. Lu, *Biomacromolecules*, 2014, **15**, 1408-1418.
- 103 K. J. Haxton and H. M. Burt, *Dalton Trans.*, 2008, 5872-5875.
- 104 Y. Y. Zhou, Z. Guo, Y. W. Zhang, W. Huang, Y. F. Zhou and D. Y. Yan, *Macromol. Biosci.*, 2009, **9**, 1090-1097.
- 105 W. Saiyin, D. L. Wang, L. Li, L. J. Zhu, B. Liu, L. Sheng, Y. Li, B. S. Zhu, L. M. Mao, G. L. Li and X. Y. Zhu, *Mol. Pharmaceutics*, 2014, **11**, 1662-1675.
- 106 R. Haag, *Angew. Chem. Int. Ed.*, 2004, **43**, 278-282.
- 107 M. E. Fox, F. C. Szoka and J. M. J. Fréchet, *Acc. Chem. Res.*, 2009, **42**, 1141-1151.
- 108 D. L. Wang, H. Y. Chen, Y. Su, F. Qiu, L. J. Zhu, X. Y. Huan, B. S. Zhu, D. Y. Yan, F. L. Guo and X. Y. Zhu, *Polym. Chem.*, 2013, **4**, 85-94.
- 109 S. Chen, X. Z. Zhang, S. X. Cheng, R. X. Zhuo and Z. W. Gu, *Biomacromolecules*, 2008, **9**, 2578-2585.
- 110 M. Prabakaran, J. J. Grailer, S. Pilla, D. A. Steeber and S. Gong, *Biomaterials*, 2009, **30**, 5757-5766.
- 111 H. Y. Chen, G. L. Li, H. Chi, D. L. Wang, C. L. Tu, L. Pan, L. J. Zhu, F. Qiu, F. L. Guo and X. Y. Zhu, *Bioconjugate Chem.*, 2012, **23**, 1915-1924.
- 112 D. Groger, M. Kerschitzki, M. Weinhart, S. Reimann, T. Schneider, B. Kohl, W. Wagermaier, G. Schulze-Tanzil, P. Fratzl and R. Haag, *Adv. Healthcare Mater.*, 2014, **3**, 375-385.
- 113 J. Guo, H. Hong, G. Chen, S. Shi, Q. Zheng, Y. Zhang, C. P. Theuer, T. E. Barnhart, W. Cai and S. Gong, *Biomaterials*, 2013, **34**, 8323-8332.
- 114 L. A. Tziveleka, C. Kontoyianni, Z. Sideratou, D. Tsiourvas and C. M. Paleos, *Macromol. Biosci.*, 2006, **6**, 161-169.
- 115 X. Li, Y. Qian, T. Liu, X. Hu, G. Zhang, Y. You and S. Liu, *Biomaterials*, 2011, **32**, 6595-6605.
- 116 L. Sun, Y. Yang, C. M. Dong and Y. Wei, *Small*, 2011, **7**, 401-406.
- 117 Y. Wang, M. Zheng, F. Meng, J. Zhang, R. Peng and Z. Zhong, *Biomacromolecules*, 2011, **12**, 1032-1040.
- 118 M. Zheng, Y. Zhong, F. Meng, R. Peng and Z. Zhong, *Mol. Pharmaceutics*, 2011, **8**, 2434-2443.
- 119 S. Sajeesh, T. Y. Lee, S. W. Hong, P. Dua, J. Y. Choe, A. Kang, W. S. Yun, C. Song, S. H. Park, S. Kim, C. Li and D. K. Lee, *Mol. Pharmaceutics*, 2014, **11**,

- 872-884.
- 120 Z. Kadlecova, Y. Rajendra, M. Matasci, L. Baldi, D. L. Hacker, F. M. Wurm and H.-A. Klok, *J. Controlled Release*, 2013, **169**, 276-288.
- 121 D. Dey, M. Inayathullah, A. S. Lee, M. C. LeMieux, X. Zhang, Y. Wu, D. Nag, P. E. De Almeida, L. Han, J. Rajadas and J. C. Wu, *Biomaterials*, 2011, **32**, 4647-4658.
- 122 H. L. Jiang, Y. K. Kim, R. Arote, J. W. Nah, M. H. Cho, Y. J. Choi, T. Akaike and C. S. Cho, *J. Controlled Release*, 2007, **117**, 273-280.
- 123 M. A. Gosselin, W. Guo and R. J. Lee, *Bioconjugate Chem.*, 2001, **12**, 989-994.
- 124 S. Choi and K.-D. Lee, *J. Controlled Release*, 2008, **131**, 70-76.
- 125 Y. Wang, P. Chen and J. Shen, *Biomaterials*, 2006, **27**, 5292-5298.
- 126 J. Liu, X. Jiang, L. Xu, X. Wang, W. E. Hennink and R. Zhuo, *Bioconjugate Chem.*, 2010, **21**, 1827-1835.
- 127 W. Xia, P. Wang, C. Lin, Z. Li, X. Gao, G. Wang and X. Zhao, *J. Controlled Release*, 2012, **157**, 427-436.
- 128 M. Krämer, J. F. Stumbé, G. Grimm, B. Kaufmann, U. Krüger, M. Weber and R. Haag, *Chembiochem*, 2004, **5**, 1081-1087.
- 129 B. Zhang, X. Ma, W. Murdoch, M. Radosz, Y. Shen, *Biotechnol. Bioeng.*, 2013, **110**, 990-998.
- 130 F. Martello, M. Piest, J. F. Engbersen and P. Ferruti, *J. Controlled Release*, 2012, **164**, 372-379.
- 131 R. B. Wang, L. Z. Zhou, Y. F. Zhou, G. L. Li, X. Y. Zhu, H. C. Gu, X. L. Jiang, H. Q. Li, J. L. Wu, L. He, X. Q. Guo, B. S. Zhu, and D. Y. Yan, *Biomacromolecules*, 2010, **11**, 489-495.
- 132 X. Wang, Y. He, J. Wu, C. Gao and Y. Xu, *Biomacromolecules*, 2010, **11**, 245-251.
- 133 Y. Chen, L. Z. Zhou, Y. Pang, W. Huang, F. Qiu, X. L. Jiang, X. Y. Zhu, D. Y. Yan and Q. Chen, *Bioconjugate Chem.*, 2011, **22**, 1162-1170.
- 134 Y. Ping, D. Wu, J. N. Kumar, W. Cheng, C. L. Lay and Y. Liu, *Biomacromolecules*, 2013, **14**, 2083-2094.
- 135 J. Blacklock, Y. Z. You, Q. H. Zhou, G. Mao and D. Oupický, *Biomaterials*, 2009, **30**, 939-950.
- 136 J. Chen, C. Wu and D. Oupický, *Biomacromolecules*, 2009, **10**, 2921-2927.
- 137 Y. Lim, S.-M. Kim, Y. Lee, W. Lee, T. Yang, M. Lee, H. Suh and J. Park, *J. Am. Chem. Soc.*, 2001, **123**, 2460-2461.
- 138 Y. Lim, C. Kim, K. Kim, S. W. Kim, and J. Park, *J. Am. Chem. Soc.*, 2000, **122**, 6524-6525.
- 139 Y. Liu, D. Wu, Y. Ma, G. Tang, S. Wang, C. He, T. Chung and S. Goh, *Chem. Commun.*, 2003, 2630-2631.

- 140 Z. Zhong, Y. Song, J. F.J. Engbersen, M. C. Lok, W. E. Hennink and J. Feijen, *J. Controlled Release*, 2005, **109**, 317-329.
- 141 D. Wu, Y. Liu, X. Jiang, C. He, S. H. Goh, and K. W. Leong, *Biomacromolecules*, 2006, **7**, 1879-1883.
- 142 S. A. Chew, M. C. Hacker, A. Saraf, R. M. Raphael, F. K. Kasper and A. G. Mikos, *Biomacromolecules*, 2009, **10**, 2436-2445.
- 143 S. A. Chew, M. C. Hacker, A. Saraf, R. M. Raphael, F. K. Kasper and A. G. Mikos, *Biomacromolecules*, 2010, **11**, 600-609.
- 144 J. Y. Cherng, P. van de Wetering, H. Talsma, D. J. A. Crommelin and W. E. Hennink, *Pharm. Res.*, 1996, **13**, 1038-1042.
- 145 P. van de Wetering, J. Y. Cherng, H. Talsma and W. E. Hennink, *J. Controlled Release*, 1997, **49**, 59-69.
- 146 L. Tao, J. Liu, B. H. Tan and T. P. Davis, *Macromolecules*, 2009, **42**, 4960-4962.
- 147 A. Schallon, V. Jérôme, A. Walther, C. V. Synatschke, A. H. E. Müller and R. Freitag, *React. Funct. Polym.*, 2010, **70**, 1-10.
- 148 B. Newland, H. Tai, Y. Zheng, D. Velasco, A. D. Luca, S. M. Howdle, C. Alexander, W. Wang and A. Pandit, *Chem. Commun.*, 2010, **46**, 4698-4700.
- 149 J. H. Tan, N. A. J. McMillan, E. Payne, C. Alexander, F. Heath, A. K. Whittaker and K. J. Thurecht, *J. Polym. Sci., Part A: Polym. Chem.*, 2012, **50**, 2585-2595.
- 150 S. R. Yu, J. J. Chen, R. J. Dong, Y. Su, B. Ji, Y. F. Zhou, X. Y. Zhu and D. Y. Yan, *Polym. Chem.*, 2012, **3**, 3324-3329.
- 151 R. K. Kainthan, M. Gnanamani, M. Ganguli, T. Ghosh, D. E. Brooks, S. Maiti and J. N. Kizhakkedathu, *Biomaterials*, 2006, **27**, 5377-5390.
- 152 J. A. Khan, R. K. Kainthan, M. Ganguli, J. N. Kizhakkedathu, Y. Singh and S. Maiti, *Biomacromolecules*, 2006, **7**, 1386-1388.
- 153 L.-A. Tziveleka, A.-M. G. Psarra, D. Tsiourvas and C. M. Paleos, *Int. J. Pharm.*, 2008, **356**, 314-324.
- 154 W. J. Kim, A. C. Bonoio, T. Hayakawa, C. Xia, M. Kakimoto, H. E. Pudavar, K.-S. Lee and P. N. Prasada, *Int. J. Pharm.*, 2009, **376**, 141-152.
- 155 X. Guo and L. Huang, *Acc. Chem. Res.*, 2012, **45**, 971-979.
- 156 V. Sokolova and M. Epple, *Angew. Chem. Int. Ed.*, 2008, **47**, 1382-1395.
- 157 D. Pissuwan, T. Niidome and M. B. Cortie, *J. Controlled Release*, 2011, **149**, 65-71.
- 158 R. Namgung, Y. Zhang, Q. L. Fang, K. Singha, H. J. Lee, I. K. Kwon, Y. Y. Jeong, I. K. Park, S. J. Son and W. J. Kim, *Biomaterials*, 2011, **32**, 3042-3052.
- 159 M. Thomas and A. M. Klibanov, *Proc. Natl. Acad. Sci. USA*, 2003, **100**, 9138-9143.
- 160 Y. F. Shi, J. J. Du, L. Z. Zhou, X. Li, Y. Zhou, L. Li, X. Zang, X. Zhang, F. Pan, H. Zhang, Z. Wang and X. Y. Zhu, *J. Mater. Chem.*, 2012, **22**, 355-360.

- 161 A. I. Graul, B. Lupone, E. Cruces and M. Stringer, *Drugs Today*, 2013, **49**, 33-68.
- 162 S. Salmaso and P. Caliceti, *Int. J. Pharm.*, 2013, **440**, 111-123.
- 163 X. Gao, X. Zhang, X. Z. Wu, X. Zhang, Z. Wang and C. Li, *J. Control. Release*, 2009, **140**, 141-147.
- 164 X. Zhang, X. Zhang, Z. Wu, X. Gao, S. Shu, Z. Wang and C. Li, *Carbohydr. Polym.*, 2011, **84**, 1419-1425.
- 165 M. Jiang, Y. Wu, Y. Heb and J. Nie, *Polym. Int.*, 2009, **58**, 31-39.
- 166 F. Wurm, J. Klos, H. J. Räder and H. Frey, *J. Am. Chem. Soc.*, 2009, **131**, 7954-7955.
- 167 F. Wurm, C. Dingels, H. Frey and H.-A. Klok, *Biomacromolecules*, 2012, **13**, 1161-1171.
- 168 J.-H. Kim, K. Park, H. Y. Nam, S. Lee, K. Kim and I. C. Kwon, *Prog. Polym. Sci.*, 2007, **32**, 1031-1053.
- 169 Y. Yu, C. Feng, Y. N. Hong, J. Z. Liu, S. J. Chen, K. M. Ng, K. Q. Luo and B. Z. Tang, *Adv. Mater.*, 2011, **23**, 3298-3302.
- 170 J. Lippincott-Schwartz, E. Snapp and A. Kenworthy, *Nat. Rev. Mol. Cell Biol.*, 2001, **2**, 444-456.
- 171 S. Y. Chen, Z. H. Tan, N. Li, R. B. Wang, L. He, Y. F. Shi, L. Jiang, P. Y. Li and X. Y. Zhu, *Macromol. Biosci.*, 2011, **11**, 828-838.
- 172 S. Y. Chen, G. M. Sun, L. Jiang, N. Li, P.Y. Li and X. Y. Zhu, *Chem. J. Chinese Univer.*, 2009, **30**, 825-829.
- 173 S. R. Yu, R. J. Dong, J. J. Chen, F. Chen, W. Jiang, Y. F. Zhou, X. Y. Zhu and D. Y. Yan, *Biomacromolecules*, 2014, **15**, 1828-1836.
- 174 Y. Pang, Q. Zhu, J. Y. Liu, J. L. Wu, R. B. Wang, S. Y. Chen, X. Y. Zhu, D. Y. Yan, W. Huang and B. S. Zhu, *Biomacromolecules*, 2010, **11**, 575-582.
- 175 Y. Pang, J. Y. Liu, Y. Su, B. S. Zhu, W. Huang, Y. F. Zhou, X. Y. Zhu and D. Y. Yan, *Sci. China: Chem.*, 2010, **53**, 2497-2508.
- 176 K. Kim, M. Lee, H. Park, J. H. Kim, S. Kim, H. Chung, K. Choi, I. S. Kim, B. L. Seong and I. C. Kwon, *J. Am. Chem. Soc.*, 2006, **128**, 3490-3491.
- 177 W. Du, Z. Xu, A. M. Nyström, K. Zhang, J. R. Leonard and K. L. Wooley, *Bioconjugate Chem.*, 2008, **19**, 2492-2498.
- 178 C. L. Tu, L. J. Zhu, P. P. Li, Y. Chen, Y. Su, D. Y. Yan, X. Y. Zhu and G. Y. Zhou, *Chem. Commun.*, 2011, **47**, 6063-6065.
- 179 X. Michalet, F. F. Pinaud, L. A. Bentolila, J. M. Tsay, S. Doose, J. J. Li, G. Sundaresan, A. M. Wu, S. S. Gambhir and S. Weiss, *Science*, 2005, **307**, 538-544.
- 180 L. J. Zhu, Y. F. Shi, C. L. Tu, R. B. Wang, Y. Pang, F. Qiu, X. Y. Zhu, D. Y. Yan, L. He, C. Y. Jin and B. S. Zhu, *Langmuir*, 2010, **26**, 8875-8881.
- 181 P. Das and N. R. Jana, *ACS Appl. Mater. Interfaces*, 2014, **6**, 4301-4309.

- 182 L. Zhou, B. He, J. Huang, Z. Cheng, X. Xu and C. Wei, *ACS Appl. Mater. Interfaces*, 2014, **6**, 7719-7727.
- 183 F. Qiu, D. L. Wang, Q. Zhu, L. Z. Zhu, G. S. Tong, Y. F. Lu, D. Y. Yan and X. Y. Zhu, *Biomacromolecules*, 2014, **15**, 1355-1364.
- 184 W. Yang, C. Y. Pan, X. Q. Liu and J. Wang, *Biomacromolecules*, 2011, **12**, 1523-1531.
- 185 F. Qiu, D. L. Wang, R. B. Wang, X. Y. Huan, G. S. Tong, Q. Zhu, D. Y. Yan and X. Y. Zhu, *Biomacromolecules*, 2013, **14**, 1678-1686.
- 186 H. Shi, G. Wang, J. Liang and B. Liu, *Med. Chem. Commun.*, 2013, **4**, 554-558.
- 187 F. Qiu, C. L. Tu, R. B. Wang, L. J. Zhu, Y. Chen, G. S. Tong, B. S. Zhu, L. He, D. Y. Yan and X. Y. Zhu, *Chem. Commun.*, 2011, **47**, 9678-9680.
- 188 K. Li, K.-Y. Pu, L. Cai and B. Liu, *Chem. Mater.*, 2011, **23**, 2113-2119.
- 189 K. Y. Pu, J. B. Shi, L. P. Cai, K. Li and B. Liu, *Biomacromolecules*, 2011, **12**, 2966-2974.
- 190 K. Y. Pu and B. Liu, *Adv. Funct. Mater.*, 2011, **21**, 3408-3423.
- 191 M. Sun, C. Y. Hong and C. Y. Pan, *J. Am. Chem. Soc.*, 2012, **134**, 20581-20584.
- 192 W. J. M. Mulder, G. J. Strijkers, G. A. F. van Tilborg, A. W. Griffioen and K. Nicolay, *NMR Biomed.*, 2006, **19**, 142-164.
- 193 S. Langereis, A. Dirksen, T. M. Hackeng, M. H. P. van Genderen and E. W. Meijer, *New J. Chem.*, 2007, **31**, 1152-1160.
- 194 Y. Li, M. Beija, S. Laurent, L. vander Elst, R. N. Muller, H. T. T. Duong, A. B. Lowe, T. P. Davis and C. Boyer, *Macromolecules*, 2012, **45**, 4196-4204.
- 195 K. J. Chen, S. M. Wolahan, H. Wang, C. H. Hsu, H. W. Chang, A. Durazo, L. P. Hwang, M. A. Garcia, Z. K. Jiang, L. Wu, Y. Y. Lin and H. R. Tseng, *Biomaterials*, 2011, **32**, 2160-2165.
- 196 L. A. Wang, K. G. Neoh, E. T. Kang and B. Shuter, *Biomaterials*, 2011, **32**, 2166-2173.
- 197 L. Wang, K. G. Neoh, E. T. Kang, B. Shuter and S. C. Wang, *Adv. Funct. Mater.*, 2009, **19**, 2615-2622.
- 198 J. K. Oha and J. M. Park, *Prog. Polym. Sci.*, 2011, **36**, 168-189.
- 199 K. J. Thurecht, I. Blakey, H. Peng, O. Squires, S. Hsu, C. Alexander and A. K. Whittaker, *J. Am. Chem. Soc.*, 2010, **132**, 5336-5337.
- 200 K. Münnemann, M. Közer, I. Blakey, A. K. Whittaker and K. J. Thurecht, *Chem. Commun.*, 2012, **48**, 1583-1585.
- 201 Z. Sideratou, D. Tsiourvas, T. Theodossiou, M. Fardis and C. M. Paleos, *Bioorg. Med. Chem. Lett.*, 2010, **20**, 4177-4181.
- 202 N. Arsalani, H. Fattahi, S. Laurent, C. Burtea, L. Vander Elst and R. N. Muller, *Contrast Media Mol. Imaging*, 2012, **7**, 185-194.
- 203 W. J. Du, A. M. Nystrom, L. Zhang, K. T. Powell, Y. L. Li, C. Cheng, S. A.

- Wickline and K. L. Wooley, *Biomacromolecules*, 2008, **9**, 2826-2833.
- 204 N. R. B. Boase, I. Blakey and K. J. Thurecht, *Polym. Chem.*, 2012, **3**, 1384-1389.
- 205 N. Li, Y. Jin, L. Xue, P. Li, D. Yan and X. Zhu, *Chinese J. Polym. Sci.*, 2013, **31**, 530-540.
- 206 K. Saatchi, N. Gelder, P. Gershkovich, O. Sivak, K. M. Wasan, R. K. Kainthan, D. E. Brooks and U. O. Häfeli, *Int. J. Pharm.*, 2012, **422**, 418-427.
- 207 H. Wang, S. Wang, H. Su, K. J. Chen, A. L. Armijo, W. Y. Lin, Y. Wang, J. Sun, K. Kamei, J. Czernin, C. G. Radu and H. R. Tseng, *Angew. Chem., Int. Ed.*, 2009, **48**, 4344-4348.
- 208 Y. Xiao, H. Hong, A. Javadi, J. W. Engle, W. Xu, Y. Yang, Y. Zhang, T. E. Barnhart, W. Cai and S. Gong, *Biomaterials*, 2012, **33**, 3071-3082.
- 209 G. Sun, J. Xu, A. Hagooley, R. Rossin, Z. Li, D. A. Moore, C. J. Hawker, M. J. Welch and K. L. Wooley, *Adv. Mater.*, 2007, **19**, 3157-3162.
- 210 K. J. Thurecht, *Macromol. Chem. Phys.*, 2012, **213**, 2567-2572.
- 211 D. Ding, G. Wang, J. Liu, K. Li, K. Y. Pu, Y. Hu, J. C. Ng, B. Z. Tang and B. Liu, *Small*, 2012, **8**, 3523-3530.
- 212 B. E. Rolfe, I. Blakey, O. Squires, H. Peng, N. R. Boase, C. Alexander, P. G. Parsons, G. M. Boyle, A. K. Whittaker and K. J. Thurecht, *J. Am. Chem. Soc.*, 2014, **136**, 2413-2419.
- 213 N. R. B. Boase, I. Blakey, B. E. Rolfe, K. Mardon and K. J. Thurecht, *Polym. Chem.*, 2014, DOI: 10.1039/C4PY00513A.
- 214 K. Saatchi, P. Soema, N. Gelder, R. Misri, K. McPhee, J. H. Baker, S. A. Reinsberg, D. E. Brooks and U. O. Häfeli, *Bioconjugate Chem.*, 2012, **23**, 372-381.
- 215 S. Mann, *Angew. Chem. Int. Ed.*, 2000, **39**, 3393-3406.
- 216 J. R. Young, S. A. Davis, P. R. Bown and S. Mann, *J. Struct. Biol.*, 1999, **126**, 195-215.
- 217 H. Colfen, *Curr. Opin. Colloid Interface Sci.*, 2003, **8**, 23-31.
- 218 J. Donners, B. R. Heywood, E. W. Meijer, R. J. M. Nolte and N. Sommerdijk, *Chem. Eur. J.*, 2002, **8**, 2561-2567.
- 219 L. B. Gower, *Chem. Rev.*, 2008, **108**, 4551-4627.
- 220 J. T. Han, X. Xu and K. Cho, *J. Cryst. Growth*, 2007, **308**, 110-116.
- 221 X. R. Xu, J. T. Han and K. Cho, *Chem. Mater.*, 2004, **16**, 1740-1746.
- 222 G. Falini, S. Albeck, S. Weiner and L. Addadi, *Science*, 1996, **271**, 67-69.
- 223 G. He, T. Dahl, A. Veis and A. George, *Nat. Mater.*, 2003, **2**, 552-558.
- 224 L. Addadi, D. Joester, F. Nudelman and S. Weiner, *Chem. Eur. J.*, 2006, **12**, 981-987.
- 225 J. L. Arias and M. S. Fernandez, *Chem. Rev.*, 2008, **108**, 4475-4482.
- 226 G. Wang, L. Li, J. Lan, L. Chen and J. You, *J. Mater. Chem.*, 2008, **18**,

- 2789-2797.
- 227 E. J. Vandenberg, *J. Polym. Sci., Part A: Polym. Chem.*, 1985, **23**, 915-949.
- 228 M. Balz, E. Barriau, V. Istratov, H. Frey and W. Tremel, *Langmuir*, 2005, **21**, 3987-3991.
- 229 K. Naka, Y. Tanaka, Y. Chujo and Y. Ito, *Chem. Commun.*, 1999, 1931-1932.
- 230 K. Naka, Y. Tanaka and Y. Chujo, *Langmuir*, 2002, **18**, 3655-3658.
- 231 S. Albeck, S. Weiner and L. Addadi, *Chem. Eur. J.*, 1996, **2**, 278-284.
- 232 W. H. Dong, H. Cheng, Y. Yao, Y. F. Zhou, G. S. Tong, D. Y. Yan, Y. J. Lai and W. Li, *Langmuir*, 2011, **27**, 366-370.
- 233 R. Tokar, P. Kubisa, S. Penczek and A. Dworak, *Macromolecules*, 1994, **27**, 320-322.
- 234 W. Y. Dong, C. L. Tu, W. Tao, Y. F. Zhou, G. S. Tong, Y. L. Zheng, Y. Li and D. Y. Yan, *Cryst. Growth Des.*, 2012, **12**, 4053-4059.
- 235 J. W. Nielsen, K. K. Sand, C. S. Pedersen, L. Z. Lakshtanov, J. R. Winther, M. Willemoes and S. L. S. Stipp, *Cryst. Growth Des.*, 2012, **12**, 4906-4910.
- 236 S. V. Patwardhan, *Chem. Commun.*, 2011, **47**, 7567-7582.
- 237 H. A. Lowenstam and S. Weiner, *On biomineralization*, 1989.
- 238 S. Mann, J. Webb and R. J. P. Williams, *Biomineralization: chemical and biochemical processes*, 1989.
- 239 C. C. Lee, J. A. MacKay, J. M. J. Fréchet and F. C. Szoka, *Nat. Biotechnol.*, 2005, **23**, 1517-1526.
- 240 A. Harada, K. Nakanishi, S. Ichimura, C. Kojima and K. Kono, *J. Polym. Sci., Part A: Polym. Chem.*, 2009, **47**, 1217-1223.
- 241 M. Scholl, Z. Kadlecova and H.-A. Klok, *Prog. Polym. Sci.*, 2009, **34**, 24-61.
- 242 J. J. Yuan and R. H. Jin, *Langmuir*, 2005, **21**, 3136-3145.
- 243 R. H. Jin and J. J. Yuan, *Chem. Commun.*, 2005, 1399-1401.
- 244 R. H. Jin and J. J. Yuan, *Macromolecul. Chem. Phys.*, 2005, **206**, 2160-2170.
- 245 J.-J. Yuan, P.-X. Zhu, N. Fukazawa and R.-H. Jin, *Adv. Funct. Mater.*, 2006, **16**, 2205-2212.
- 246 J. J. Yuan and R. H. Jin, *Adv. Mater.*, 2005, **17**, 885-888.
- 247 R.-H. Jin and J.-J. Yuan, *Chem. Mater.*, 2006, **18**, 3390-3396.
- 248 H. Menzel, S. Horstmann, P. Behrens, B. Barnreuther, I. Krueger and M. Jahns, *Chem. Commun.*, 2003, 2994-2995.
- 249 O. Helmecke, A. Hirsch, P. Behrens and H. Menzel, *J. Colloid Interface Sci.*, 2008, **321**, 44-51.
- 250 Q. Wang, J. Yu, Y. Yan, S. Xu, F. Wang, Q. Li, J. Wang, X. Zhang and D. Liu, *Polym. Chem.*, 2012, **3**, 1284-1290.
- 251 M. A. Mintzer and M. W. Grinstaff, *Chem. Soc. Rev.*, 2011, **40**, 173-190.
- 252 T. M. Fillion, J. Xu, M. L. Prasad and J. Song, *Biomaterials*, 2011, **32**, 985-991.

- 253 Y.-M. Lin, W. Chrzanowski, J. Knowles, A. Bishop and A. Bismarck, *Adv. Eng. Mater.*, 2010, **12**, B101-B112.
- 254 Z. S. Akdemir, N. Kayaman-Apohan, M. V. Kahraman, S. E. Kuruca, A. Gungor and S. Karadenizli, *J. Biomater. Sci., Polym. Ed.*, 2011, **22**, 857-872.
- 255 D. Puppi, D. Dinucci, C. Bartoli, C. Mota, C. Migone, F. Dini, G. Barsotti, F. Carlucci and F. Chiellini, *J. Bioact. Compat. Polym.*, 2011, **26**, 478-492.
- 256 D. Puppi, N. Detta, A. M. Piras, F. Chiellini, D. A. Clarke, G. C. Reilly and E. Chiellini, *Macromol. Biosci.*, 2010, **10**, 887-897.
- 257 B. Das, P. Chattopadhyay, M. Mandal, B. Voit and N. Karak, *Macromol. Biosci.*, 2013, **13**, 126-139.
- 258 Y.-L. Luo, C.-H. Zhang, F. Xu and Y.-S. Chen, *Polym. Adv. Technol.*, 2012, **23**, 551-557.
- 259 B. Das, P. Chattopadhyay, D. Mishra, T. K. Maiti, S. Maji, R. Narayan and N. Karak, *J. Mater. Chem. B*, 2013, **1**, 4115-4126.
- 260 I. Frisman, R. Orbach, D. Seliktar and H. Bianco-Peled, *J. Mater. Sci. Mater. Med.*, 2010, **21**, 73-80.
- 261 F. P. Brandl, A. K. Seitz, J. K. V. Tessmar, T. Blunk and A. M. Göepferich, *Biomaterials*, 2010, **31**, 3957-3966.
- 262 M. A. Azagarsamy and K. S. Anseth, *ACS Macro Lett.*, 2013, **2**, 5-9.
- 263 Y. Dong, A. O. Saeed, W. Hassan, C. Keigher, Y. Zheng, H. Tai, A. Pandit and W. Wang, *Macromol. Rapid Commun.*, 2012, **33**, 120-126.
- 264 Y. Dong, W. Hassan, Y. Zheng, A. O. Saeed, H. Cao, H. Tai, A. Pandit and W. Wang, *J. Mater. Sci. Mater. Med.*, 2012, **23**, 25-35.
- 265 W. Hassan, Y. Dong and W. Wang, *Stem Cell Res. Ther.*, 2013, **4**.
- 266 Y. Dong, W. U. Hassan, R. Kennedy, U. Greiser, A. Pandit, Y. Garcia and W. Wang, *Acta Biomater.*, 2014, **10**, 2076-2085.
- 267 H. Tai, A. Tochwin and W. Wang, *J. Polym. Sci., Part A: Polym. Chem.*, 2013, **51**, 3751-3761.
- 268 H. Tai, W. Wang, C. Alexander, K. M. Shakesheff and S. M. Howdle, *J. Controlled Release*, 2008, **132**, E48-E50.
- 269 H. Tai, D. Howard, S. Takae, W. Wang, T. Vermonden, W. E. Hennink, P. S. Stayton, A. S. Hoffman, A. Endruweit, C. Alexander, S. M. Howdle and K. M. Shakesheff, *Biomacromolecules*, 2009, **10**, 2895-2903.
- 270 R. Kennedy, W. Ul Hassan, A. Tochwin, T. Zhao, Y. Dong, Q. Wang, H. Tai and W. Wang, *Polym. Chem.*, 2014, **5**, 1838-1842.
- 271 J. G. Zhang, O. B. Krajden, R. K. Kainthan, J. N. Kizhakkedathu, I. Constantinescu, D. E. Brooks and M. I. C. Gyongyossy-Issa, *Bioconjugate Chem.*, 2008, **19**, 1241-1247.
- 272 M. H. M. Oudshoorn, R. Rissmann, J. A. Bouwstra and W. E. Hennink,

- Biomaterials*, 2006, **27**, 5471-5479.
- 273 M. H. M. Oudshoorn, R. Penterman, R. Rissmann, J. A. Bouwstra, D. J. Broer and W. E. Hennink, *Langmuir*, 2007, **23**, 11819-11825.
- 274 N. E. Fedorovich, M. H. Oudshoorn, D. van Geemen, W. E. Hennink, J. Alblas and W. J. A. Dhert, *Biomaterials*, 2009, **30**, 344-353.
- 275 J. Shepherd, P. Sarker, S. Rimmer, L. Swanson, S. MacNeil and I. Douglas, *Biomaterials*, 2011, **32**, 258-267.
- 276 J. D. Thomas, G. Fussell, S. Sarkar, A. M. Lowman and M. Marcolongo, *Acta Biomater.*, 2010, **6**, 1319-1328.
- 277 J. Xu and J. Song, *Proc. Natl. Acad. Sci. U. S. A.*, 2010, **107**, 7652-7657.
- 278 S. Balakrishnan, M. Krishnan, R. Narayan and P. Dubois, *Polym. Eng. Sci.*, 2006, **46**, 235-240.
- 279 J.-F. Lutz, O. Akdemir and A. Hoth, *J. Am. Chem. Soc.*, 2006, **128**, 13046-13047.
- 280 J.-F. Lutz, K. Weichenhan, O. Akdemir and A. Hoth, *Macromolecules*, 2007, **40**, 2503-2508.
- 281 Y. Dong, P. Gunning, H. Cao, A. Mathew, B. Newland, A. O. Saeed, J. P. Magnusson, C. Alexander, H. Tai, A. Pandit and W. Wang, *Polym. Chem.*, 2010, **1**, 827-830.
- 282 J. Nikolovski and D. J. Mooney, *Biomaterials*, 2000, **21**, 2025-2032.
- 283 J. A. Burdick and K. S. Anseth, *Biomaterials*, 2002, **23**, 4315-4323.
- 284 F. Yang, C. G. Williams, D. A. Wang, H. Lee, P. N. Manson and J. Elisseeff, *Biomaterials*, 2005, **26**, 5991-5998.
- 285 C. R. Nuttelman, M. C. Tripodi and K. S. Anseth, *J. Biomed. Mater. Res. Part A*, 2004, **68A**, 773-782.
- 286 D. J. Menzies, A. Cameron, B. G. C. Maisonneuve, L. GrOndahl, E. Wolvetang and J. Cooper-White, *J. Tissue Eng. Regen. Med.*, 2012, **6**, 208-208.
- 287 R. Knischka, P. J. Lutz, A. Sunder and H. Frey, *Abstr. Pap. Am. Chem. Soc.*, 2001, **221**, U438-U438.
- 288 R. K. Kainthan, J. Janzen, E. Levin, D. V. Devine and D. E. Brooks, *Biomacromolecules*, 2006, **7**, 703-709.
- 289 R. K. Kainthan, E. B. Muliawan, S. G. Hatzikiriakos and D. E. Brooks, *Macromolecules*, 2006, **39**, 7708-7717.
- 290 R. K. Kainthan, S. R. Hester, E. Levin, D. V. Devine and D. E. Brooks, *Biomaterials*, 2007, **28**, 4581-4590.
- 291 R. K. Kainthan and D. E. Brooks, *Biomaterials*, 2007, **28**, 4779-4787.
- 292 R. K. Kainthan, J. Janzen, J. N. Kizhakkedathu, D. V. Devine and D. E. Brooks, *Biomaterials*, 2008, **29**, 1693-1704.
- 293 A. A. Alencar de Queiroz, J. C. Bressiani, A. H. Bressiani, O. Z. Higa and G. A. Abraham, in *Bioceramics 21*, eds. M. Prado and C. Zavaglia, 2009, vol. 396-398,

- pp. 633-636.
- 294 T. F. Yang, W. Chin, J. Cherng and M. Shau, *Biomacromolecules*, 2004, **5**, 1926-1932.
- 295 J. Y. Zhang, B. A. Doll, E. J. Beckman and J. O. Hollinger, *J. Biomed. Mater. Res. Part A*, 2003, **67A**, 389-400.
- 296 X. Yu, Z. Liu, J. Janzen, I. Chafeeva, S. Horte, W. Chen, R. K. Kainthan, J. N. Kizhakkedathu and D. E. Brooks, *Nat. Mater.*, 2012, **11**, 468-476.
- 297 H. Zhang, L. P. Bre, T. Zhao, Y. Zheng, B. Newland and W. Wang, *Biomaterials*, 2014, **35**, 711-719.
- 298 H. Zhang, L. P. Bre, T. Zhao, B. Newland, C. Mark Da and W. Wang, *J. Mater. Chem. B*, 2014, **2**, 4067-4071.
- 299 E.-R. Kenawy, S. D. Worley and R. Broughton, *Biomacromolecules*, 2007, **8**, 1359-1384.
- 300 G. Taubes, *Science*, 2008, **321**, 356-361.
- 301 P. Ortega, B. M. Cobaleda, J. M. Hernández-Ros, E. Fuentes-Paniagua, J. Sánchez-Nieves, M. P. Tarazona, J. L. Copa-patiño, J. Soliveri, F. J. de la Mata and R. Gómez, *Org. Biomol. Chem.*, 2011, **9**, 5238-5248.
- 302 E.-R., Kenawy, *J. Appl. Polym. Sci.*, 2001, **82**, 1364-1374.
- 303 A. M. Carmona-Ribeiro and L. D. de Melo Carrasco, *Int. J. Mol. Sci.*, 2013, **14**, 9906-9946.
- 304 Y. W. Zhang, H. S. Peng, W. Huang, Y. F. Zhou, X. H. Zhang and D. Y. Yan, *J. Phys. Chem. C*, 2008, **112**, 2330-2336.
- 305 Y. W. Zhang, H. S. Peng, W. Huang, Y. F. Zhou and D. Y. Yan, *J. Colloid Interface Sci.*, 2008, **325**, 371-376.
- 306 R. B. Wang, L. Wang, L. Z. Zhou, Y. Su, F. Qiu, D. L. Wang, J. L. Wu, X. Y. Zhu and D. Y. Yan, *J. Mater. Chem.*, 2012, **22**, 15227-15234.
- 307 D. S. Zhang, L. Chen, C. F. Zang, Y. Y. Chen and H. Lin, *Carbohydr. Polym.*, 2013, **92**, 2088-2094.
- 308 H. Deka, N. Karak, R. D. Kalita and A. K. Buragohain, *Polym. Degrad. Stab.*, 2010, **95**, 1509-1517.
- 309 D. S. Zhang, G. Y. Zhang, L. Chen, Y. F. Liao, Y. Y. Chen and H. Lin, *J. Appl. Polym. Sci.*, 2013, 3778-3784.
- 310 B. Das, M. Mandal, A. Upadhyay, P. Chattopadhyay and N. Karak, *Biomed. Mater.*, 2013, **8**, 035003.
- 311 K. Chanawanno, S. Chantrapromma, T. Anantapong, A. Kanjana-Opas and H. K. Fun, *Eur. J. Med. Chem.*, 2010, **45**, 4199-4208.
- 312 W. J. Yang, K-G, Neoh, E-T, Kang, S. L-M, Teo and D. Rittschof, *Polym. Chem.*, 2013, **4**, 3105-3115.
- 313 M. S. Chen, M. Hu, D. L. Wang, G. J. Wang, X. Y. Zhu, D. Y. Yan and J. Sun,

- Bioconjugate Chem.*, 2012, **23**, 1189-1199.
- 314 A. Sadana, *Chem. Rev.*, 1992, **92**, 1799-1818.
- 315 R. S. Kane, P. Deschatelets and G. M. Whitesides, *Langmuir*, 2003, **19**, 2388-2391.
- 316 L. D. Unsworth, H. Sheardown and J. L. Brash, *Langmuir*, 2005, **21**, 1036-1041.
- 317 R. A. Frazier, G. Matthijs, M. C. Davies, C. J. Roberts, E. Schacht and S. J. B. Tendler, *Biomaterials*, 2000, **21**, 957-966.
- 318 T. Lehmann and J. R  he, *Macromol. Symp.*, 1999, **142**, 1-12.
- 319 B. E. Rabinow, Y. S. Ding, C. Qin, M. L. McHalsky, J. H. Schneider, K. A. Ashline, T. L. Shelbourn and R. M. Albrecht, *J. Biomater. Sci. Polym. Ed.*, 1994, **6**, 91-109.
- 320 J. M. Harris and S. Zalipsky, *Poly(ethylene glycol): Chemistry and Biological Applications*, American Chemical Society, Washington, DC, 1997.
- 321 E. Ostuni, R. G. Chapman, R. E. Holmlin, S. Takayama and G. M. Whitesides, *Langmuir*, 2001, **17**, 5605-5620.
- 322 C. Siegers, M. Biesalski and R. Haag, *Chem. Eur. J.*, 2004, **10**, 2831-2838.
- 323 P.-Y. J. Yeh, R. K. Kainthan, Y. Q. Zou, M. Chiao and J. N. Kizhakkedathu, *Langmuir*, 2008, **24**, 4907-4916.
- 324 S. X. Wang, Y. Zhou, S. C. Yang and B. J. Ding, *Coll. Surf. B: Biointerface*, 2008, **67**, 122-126.
- 325 T. Cai, W. J. Yang, K.-G. Neoh and E.-T. Kang, *Ind. Eng. Chem. Res.*, 2012, **51**, 15962-15973.
- 326 J. Suh, S. H. Lee, S. M. Kim and S. S. Hah, *Bioorg. Chem.*, 1997, **25**, 221-231.
- 327 K. Holmberg, F. Tiberg, M. Malmsten and C. Brink, *Colloids Surf., A*, 1997, **123**, 297-306.
- 328 R. G. Chapman, E. Ostuni, M. N. Liang, G. Meluleni, E. Kim, L. Yan, G. Pier, H. S. Warren and G. M. Whitesides, *Langmuir*, 2001, **17**, 1225-1233.
- 329 S. Suriyanarayanan, H-H. Lee, B. Liedberg, T. Aastrup and I. A. Nicholls, *J. Colloid. Interface. Sci.*, 2013, **396**, 307-315.
- 330 S. Reichelt, K.-J. Eichhorn, D. Aulich, K. Hinrichs, N. Jain, D. Appelhans and B. Voit, *Coll. Surf. B: Biointerface*, 2009, **69**, 169-177.
- 331 Y. Y. Zhuang, Q. Zhu, C. L. Tu, D. L. Wang, J. L. Wu, Y. M. Xia, G. S. Tong, L. He, B. S. Zhu, D. Y. Yan and X. Y. Zhu, *J. Mater. Chem.*, 2012, **22**, 23852-23860.
- 332 C. S. Gudipati, J. A. Finlay, J. A. Callow, M. E. Callow and K. L. Wooley, *Langmuir*, 2005, **21**, 3044-3053.
- 333 J. W. Bartels, C. Cheng, K. T. Powell, J. Q. Xu and K. L. Wooley, *Macromol. Chem. Phys.*, 2007, **208**, 1676-1687.
- 334 P. M. Imbesi, C. Fidge, J. E. Raymond, S. I. Cau  t and K. L. Wooley, *ACS Macro Lett.*, 2012, **1**, 473-477.

- 335 P. M. Imbesi, J. A. Finlay, N. Aldred, M. J. Eller, S. E. Felder, K. A. Pollack, A. T. Lonnecker, J. E. Raymond, M. E. Mackay, E. A. Schweikert, A. S. Clare, J. A. Callow, M. E. Callow and K. L. Wooley, *Polym. Chem.*, 2012, **3**, 3121-3131.
- 336 P. M. Imbesi, N. V. Gohad, M. J. Eller, B. Orihuela, D. Rittschof, E. A. Schweikert, A. S. Mount and K. L. Wooley, *ACS Nano*, 2012, **6**, 1503-1512.
- 337 D. E. Discher and A. Eisenberg, *Science*, 2002, **297**, 967-973.
- 338 F. M. Menger and K. D. Gabrielson, *Angew. Chem., Int. Ed. Engl.*, 1995, **34**, 2091-2106.
- 339 J. W. Szostak, D. P. Bartel, P. L. Luisi, *Nature*, 2001, **409**, 387-390.
- 340 D. M. Vriezema, J. Hoogboom, K. Velonia, K. Takazawa, P. C. M. Christianen, J. C. Maan, A. E. Rowan, R. J. M. Nolte, *Angew. Chem., Int. Ed.*, 2003, **42**, 772-776.
- 341 Y. F. Zhou and D. Y. Yan, *J. Am. Chem. Soc.*, 2005, **127**, 10468-10469.
- 342 Y. F. Zhou and D. Y. Yan, *Angew. Chem., Int. Ed.*, 2005, **44**, 3223-3226.
- 343 H. B. Jin, Y. L. Zheng, Y. Liu, H. X. Cheng, Y. F. Zhou and D. Y. Yan, *Angew. Chem., Int. Ed.*, 2011, **50**, 10352-10356.
- 344 H. B. Jin, Y. Liu, Y. L. Zheng, W. Huang, Y. F. Zhou and D. Y. Yan, *Langmuir*, 2012, **28**, 2066-2072.
- 345 F. M. Menger, J. Bian, V. A. Seredyuk, *Angew. Chem., Int. Ed.*, 2004, **43**, 1265-1267.
- 346 F. Loosli, D. A. Doval, D. Grassi, P-L. Zaffalon, F. Favarger and A. Zumbuehl, *Chem. Commun.*, 2012, **48**, 1604-1606.
- 347 H. B. Jin, W. Huang, Y. L. Zhou, Y. F. Zhou and D. Y. Yan, *Chem. Eur. J.*, 2012, **18**, 8641-8646.

### Curriculum Vitae



Dali Wang received his BSc degree in Polymer Materials and Engineering from Donghua University in 2009. Then he pursued his PhD degree under the supervision of Prof. Xinyuan Zhu in School of Chemistry and Chemical Engineering at Shanghai Jiao Tong University. Currently, his current research interests are focused on the synthesis and biomedical application of functional polymers.



Tianyu Zhao received his BSc degree in Material Science and Engineering at Tianjin University in 2007 and obtained his MSc degree in Chemistry at Shanghai Jiao Tong University in 2011. He then pursued his PhD degree under the supervision of Dr. Wenxin Wang in School of Medicine and Medical Science at University College Dublin. Currently, his current research interests focus on hyperbranched polymer design for gene and cell therapy.



Xinyuan Zhu received his BSc and MSc in Materials Science at Donghua University, and obtained his PhD in Materials Science at Shanghai Jiao Tong University in 2001. Then, he joined the BASF research laboratory at ISIS in Strasbourg as a post-doctoral researcher. In 2005, he became a full professor for Chemistry at Shanghai Jiao Tong University in China. His current researches focus on the controlled preparation of functional polymers and their biomedical applications.



Deyue Yan received his BSc degree in Chemistry at Nankai University and MSc degree in Polymer Chemistry at Jilin University. In 2002, he got the PhD degree in Polymer Chemistry at Catholic University of Leuven, Belgium. He began his work at East China University of Science and Technology as a lecturer in 1966, and then moved to Tongji University in 1980 as an associate professor. From 1987 to now, he was a full professor at Shanghai Jiao Tong University. His current research interests

focus on the supramolecular self-assembly of functional polymers and their biomedical applications.



Wenxin Wang received his BSc degree at Si Chuan University in 1990, and obtained his PhD at Shanghai Jiao Tong University in 1999. He became a Research Fellow at University of Liege in Belgium in 2000 and a Senior Research Fellow at the University of Nottingham in UK in 2001. Then, he joined the National University of Ireland, Galway in Ireland as a Lecturer. In 2013, he joined the University College Dublin as Senior Lecturer. His current research focusses on functional polymeric materials via controlled/living polymerization techniques, therapeutic drugs/DNA/RNA delivery and stem cell therapy for wound healing.